A NOVEL APPROACH TO ANTIPLATELET THERAPY: TARGETING PROTEASE ACTIVATED RECEPTOR 4

By

MICHELE MARIE MUMAW

Submitted in partial fulfillment of the requirements

For the degree of Doctor of Philosophy

Dissertation Advisor: Marvin T. Nieman PhD

Department of Pharmacology

CASE WESTERN RESERVE UNIVERSITY

January 2016

CASE WESTERN RESERVE UNIVERSITY

SCHOOL OF GRADUATE STUDIES

We hereby approve the thesis/dissertation of

Michele Marie Mumaw

candidate for the degree of Doctor of Philosophy*.

Marvin T. Nieman (Dissertation Advisor)

Johannes von Lintig (Committee Chair)

Krzysztof Palczewski (Committee Member)

Anne Hamik (Committee Member)

Aaron Proweller (Committee Member)

Date of Defense

July 31, 2015

*We also certify that written approval has been obtained for any

proprietary material contained therein.

Dedication

To my parents, Thomas and Kathleen Mumaw, and my husband, Russell Jackson, for their never-ending support and encouragement.

Table of Contents

List of Tables

List of Figures

Acknowledgements

First and foremost, I would like to thank my advisor, Dr. Marvin Nieman, for giving me a second chance in graduate school and letting me join his lab. While not always happy at the time, I truly appreciated Marvin's support in improving my scientific weaknesses including my writing and presentation skills. Thank you for all the time, effort, advice, and support you gave me to help me grow and continue to grow as a scientist and as an individual.

Secondly, I would like to thank past and present members of the Nieman Lab, specifically, Amal Arachiche and Maria de la Fuente. Both Amal and Maria made being in lab enjoyable no matter how stressed I was about lab work. Amal was always willing to give up her time to help me learn a new laboratory still or just bounce off experimental ideas. Besides her continuous experimental help, Maria taught me how to have fun in lab while still being very productive. I will be forever grateful to Maria for her constant help, her crazy amount of chocolate burning energy, and her friendship.

I would also like to thank my thesis committee of Dr. Johannes von Lintig, Dr. Krzysztof Palczewski, Dr. Anne Hamik, and Dr. Aaron Proweller for all of their constructive guidance and support. I would also like to acknowledge the cardiovascular training grant for supporting my growth as a scientist.

Finally, I need to thank my family and friends for their unconditional love and support through my time in graduate school. Without it I am sure I would not have survived. My parents, Thomas and Kathleen, and my brothers, David and Brian, have always been encouraging of me to pursue my aspirations and always do everything they can to support me. Most importantly, my husband Russell who helped me survive my grad school rollercoaster by always being there for me whether hearing about how nothing worked, going to lab late at night with me, listening to my countless practice presentations, or helping me forget about lab and taking a break every once in a while.

It’s the small, simple moments of happiness that make the darker times fade, and I’m thankful to everyone that always brought a little bit of light.

List of Abbreviations

2D6: PAR4 monoclonal antibody, epitope amino acids 73-78

II: Coagulation Factor II, prothrombin

IIa: Activated Coagulation Factor II, thrombin

5F10: PAR4 monoclonal antibody, epitope amino acids 41-47

5-HT2A: 5-hydroxytrytamine (serotonin) receptor 2A, G protein-coupled

14H6: PAR4 monoclonal antibody, epitope amino acids 48-53

ACD: Acid citrate dextrose

ACS: Acute Coronary Syndromes

ADP: Adenosine diphosphate

AKT: Protein Kinase B, serine/threonine kinase

$\alpha_{IIb}\beta_3$: Glycoprotein IIb/IIIa, integrin $\alpha_{IIb}\beta_3$, integrin complex found on platelets, binds fibrinogen to mediate platelet-platelet interactions

$\alpha_2\beta_1$: Integrin $\alpha_2\beta_1$, integrin complex found on platelets, binds collagen to mediate platelet adhesion

APC: Activated Protein C

AT III: Antithrombin

ATP: Adenosine triphosphate

AYPGKF: PAR4 activating peptide

BiFC: Biomolecular fluorescence complementation

BRET: Bioluminescence resonance energy transfer

BSA: Bovine Serum Albumin

CAN12: PAR4 inhibitory goat polyclonal antibody targeted to the anionic cluster on PAR4, D^{57}, D^{59}, E^{62}, and D^{65}

CO-IP: Coimmunoprecipitation

COX-1: Cyclooxygenase-1

COX-2: Cyclooxygenase-2

CYP: Cytochrome P450

CYP2C19: Cytochrome P450 2C19

CYP3A4: Cytochrome P450 3A4

DVT: Deep vein thrombosis

DTS: Dense tubular system

EC_{50}: Half maximal effective concentration

FcγIIa: FC-gamma receptor IIa, CD32

FDA: Food and Drug Administration

FII: Coagulation Factor II, prothrombin

FIIa: Activated Coagulation Factor II, thrombin

FV: Coagulation Factor V

FVa: Activated Coagulation Factor V

FVII: Coagulation Factor VII

FVIIa: Activated Coagulation Factor VII

FVIII: Coagulation Factor VIII

FVIIIa: Activated Coagulation Factor VIII

FIX: Coagulation Factor IX

FIXa: Activated Coagulation Factor IX

FX: Coagulation Factor X

FXa: Activated Coagulation Factor X

FXI: Coagulation Factor XI

FXIa: Activated Coagulation Factor XI

FXII: Coagulation Factor XII

FXIIa: Activated Coagulation Factor XII

FXIII: Coagulation Factor XIII

FXIIIa: Activated Coagulation Factor XIII

GFP: Green Fluorescent Protein

Glut-3: Glucose transporter 3

GPCR: G protein coupled receptor

GPIb-V-IX: Glycoprotein Ib-glycoprotein V- glycoprotein IX complex (CD42), VWF receptor

GPVI: Glycoprotein VI, collagen receptor

HIT: Heparin-induced thrombocytopenia

hPAR4: Human Protease Activated Receptor 4

IL-10: Interleukin-10, human cytokine synthesis inhibitory factor

LDL: Low-density lipoprotein

MBP: Maltose Binding Protein

MLC: Myosin light chain

MMP1: Matrix metalloprotease-1

MMRRC: Mutant Mouse Regional Resource Center

mPAR4: Mouse Protease Activated Receptor 4

NO: Nitric oxide

OCS: Open canalicular system

P2X1: Purinergic receptor P2X, ligand gated ion channel, 1

P2Y1: Purinergic receptor P2Y, G-Protein Coupled, 1, G_q class of GPCR, ADP receptor

P2Y12: Purinergic receptor P2Y, G-Protein Coupled, 12, G_i class of GPCR, ADP receptor

PAR: Protease Activated Receptor

PAR1: Protease Activated Receptor 1

PAR2: Protease Activated Receptor 2

PAR3: Protease Activated Receptor 3

PAR4: Protease Activated Receptor 4

$PAR4^{-/-}$: F2RL3-/- mice, PAR4 knock-out mice

PBS: Phosphate Buffered Saline

PF4: Platelet factor 4

PGI_2: Prostaglandin I_2

PI3K: Phosphoinositide 3-kinase

PPP: Platelet poor plasma

PRP: Platelet rich plasma

RhoA: Ras homolog gene family, member A

rLUC: Renilla luciferase

SFLLRN: PAR1 activating peptide

TF: Tissue Factor

TFLLRN: PAR1 activating peptide

tPA: Tissue plasminogen activator

TXA2: Thromboxane A_2

TXA2/PGH2: Thromboxane receptor

uPA: Urokinase

VWF: Von Willebrand factor

A Novel Approach To Antiplatelet Therapy: Targeting Protease Activated Receptor 4

By

MICHELE MARIE MUMAW

Abstract

Protease activated receptors (PARs) are seven transmembrane G-protein coupled receptors that are activated by cleavage of their N-terminus by a protease. Upon cleavage of their N-terminus, the new N-terminus acts as a tethered ligand for the receptor. The ligand then binds to the corresponding receptor activating it. In the case of human platelets, which express PAR1 and PAR4, PAR cleavage by thrombin leads to signaling through G_q and $G_{12/13}$ which causes numerous downstream intracellular effects in platelet activation including shape change, intracellular calcium release, secretion, and aggregation. To date the majority of PAR studies on platelets have focused on PAR1; however, PAR1 and PAR4 have distinct and overlapping signaling functions and affect the activation of one another. To more clearly understand the roles of PAR4 and to better understand the interplay between the two receptors, three main studies were conducted. First, heterodimerization of PAR1 and PAR4 was examined in detail. Secondly, studies were performed to evaluate the viability of targeting the anionic cluster on the N-terminus of PAR4 as an antiplatelet therapy target. Finally, PAR4 monoclonal antibodies were developed which are able to detect PAR4 expression and activation on human platelets.

Chapter 1 : Introduction and Background

Acute coronary syndromes (ACS) are one of the leading causes of death worldwide. The current standard for treatment of ACS is a combination therapy of aspirin and a P2Y12 antagonist that decreases the risk of reoccurrence. However, the current treatment regimen has a number of limitations; most significantly, patients still experience cardiovascular events and additionally have an increased bleeding risk. This study examines protease activated receptor 4 (PAR4), a G-protein coupled receptor expressed on human platelets that has limited tissue distribution and is necessary for stable clot formation, as a new antiplatelet therapy target. Overall, this study identifies a novel target region on PAR4 (the anionic cluster on PAR4's exodomain), provides insight toward developing future PAR antagonists based on the mechanism of thrombin binding to PAR4, and demonstrates the attractiveness of PAR4 as an antiplatelet therapy target that prevents cardiovascular events while having limited effect on hemostasis.

1.1 Hemostasis

Hemostasis is the process essential for arresting bleeding from a damaged blood vessel. Through the tightly regulated components of the hemostatic system, blood is converted from a liquid state to a gel like state at the site of injury, damaged blood vessels are plugged, and blood clots are removed following repair. Hemostasis is a multicomponent process composed of coagulation, fibrinolysis, and platelet activation that is highly conserved through evolution [1].

1.1.1 Coagulation

The Coagulation Cascade

Following damage to the endothelial lining of a blood vessel the process of coagulation begins. The coagulation pathway was named the coagulation cascade since the sequential activation of each clotting factor converts the next factor in the process from a zymogen, an inactive enzyme precursor present in circulation, to their active form [2, 3]. The coagulation cascade consists of 1) the extrinsic pathway, activated following damage to the endothelium and the exposure of tissue factor (TF) on sub-endothelial cells, 2) the intrinsic pathway, in which all of the factors are present in the blood, and 3) the common pathway where the intrinsic and extrinsic pathways overlap (Figure 1.1A) [4]. The ultimate goal of the coagulation cascade is to generate thrombin that can both activate platelets and cleave fibrinogen to generate fibrin.

The extrinsic pathway, composing the initiation phase of coagulation, is activated following damage to the endothelium that exposes the subendothelial matrix and the transmembrane receptor TF [5]. TF acts as a cofactor and binds FVII promoting conversion to the active form FVIIa. Together the TF/FVIIa complex cleaves FX into active FXa. Following activation FXa interacts with FVa to form the prothombinase complex which converts II (prothrombin) into IIa (thrombin).

Also known as the contact pathway, the intrinsic pathway is essential for the propagation phase of coagulation [1]. The intrinsic pathway is initiated by FXII activation on a

charged surface. FXIIa then activates FXI to FXIa which subsequently converts FIX to FIXa. Thrombin generated from extrinsic pathway activates VIII, VIIIa. FIXa and VIIIa then form the tenase complex which converts FX to FXa and feeds into the common pathway.

Both the extrinsic and intrinsic pathways lead into the common pathway that starts with FX. In the common pathway, FXa and FVa convert prothrombin (Factor II) to thrombin (Factor IIa). Thrombin has a wide range of functions from converting fibrinogen to fibrin which with platelets forms a hemostatic plug, activates factors FV, FVIII, FXI and FXIII, and is a potent platelet activator. Ultimately, the large quantity of thrombin generated produces fibrin fibers that are crosslinked to one another by FXIIIa to form a fibrin clot together with activated platelets (Figure 1.1B) [6].

Fibrinolysis

Fibrinolysis removes excess fibrin from circulation to prevent unnecessary accumulation of fibrin and eventually, after healing of the blood vessel, lyses and degrades the formed thrombus [7]. Fibrinolysis is a tightly controlled multi-step process that converts the circulating zymogen plasminogen to the protease plasmin. Plasmin is the major protease responsible for degrading fibrin. Plasminogen is converted to plasmin by both tissue plasminogen activator (tPA) and urokinase (uPA) [8]. tPA is secreted from endothelial cells and uPA is secreted from monocytes, macrophages, and the urinary epithelium [7, 8]. Plasmin then degrades fibrin to generate fibrin degradation products (Figure 1.1C) [7].

In the specific situation wherein plasmin degrades fibrin cross-linked by FXIIIa, plasmin cleaves the C-terminal region of the α and β chains in the D-domain which is followed by proteolysis of the connecting region between the D and E domains. One of the resulting degradation products, a D-dimer, is formed composed of two D domains (Figure 1.1B) [9]. Since D-dimers are formed only when the fibrinolytic system is active, a D-dimer assay was developed to diagnose disease states such as deep vein thrombosis, pulmonary embolism, and cancer-associated thrombosis [10-13].

Figure 1.1: Coagulation and Fibrinolysis.

A) The coagulation cascade is a multistep process composed of the extrinsic pathway, the intrinsic pathway, and the common pathway. The extrinsic pathway is responsible for the initial burst of thrombin generation following trauma leading to exposure of tissue factor. The intrinsic pathway amplifies thrombin generation. Together the extrinsic and intrinsic pathways feed into the common pathway which ultimately results in thrombin generation. Thrombin cleaves fibrinogen to generate insoluble fibrin that is cross-linked to generate fibrin strands and forms a clot with platelets. B) Fibrinogen is cleaved by thrombin to release fibrinopeptide A and B generating fibrin. Fibrin then forms a fibrin polymer that is crosslinked by FXIIIa. Plasmin cleaves fibrin to generate fibrin degradation products including D-dimers. C) In fibrinolysis plasminogen is converted to its active form, plasmin, by tPA and uPA. Plasmin then cleaves fibrin to generate fibrin degradation products.

Figure 1.1: Coagulation and Fibrinolysis

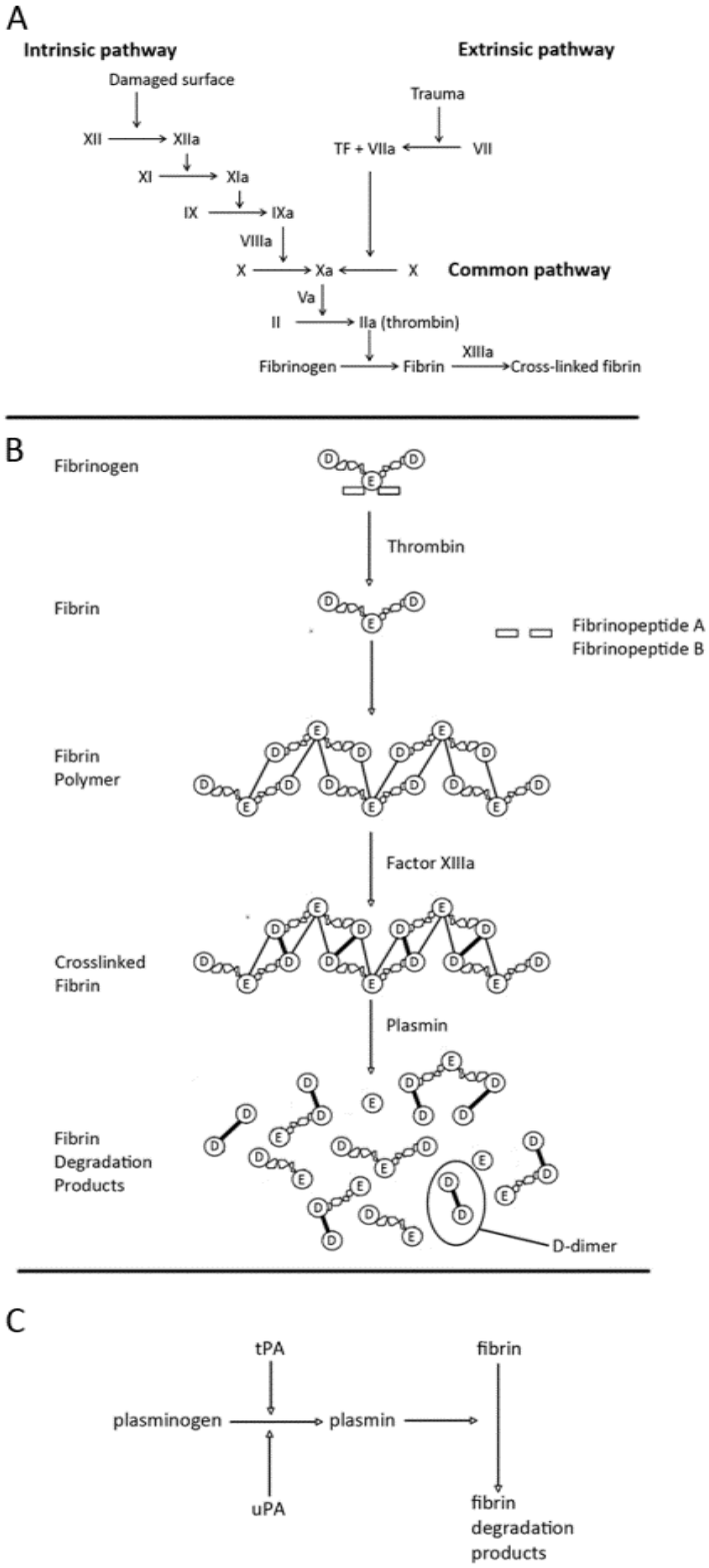

1.1.2 Platelets

Platelets are small anucleate discoid cells (~3.0 x 0.5 μm) produced from megakaryocytes which have a lifetime of approximately 7-10 days. The primary role of platelets is to maintain hemostasis; however, they have been shown to play a role in tumor growth and metastasis, inflammation, angiogenesis, antimicrobial host defense, and glomerular disease. Two-thirds of platelets in humans circulate in the blood while the other third remains sequestered in the spleen. Under normal conditions, platelets circulate in the blood in an inactive state and only become activated when they encounter damaged endothelium. At the site of a vascular injury, the subendothelial matrix is exposed which initiates platelet activation. Upon encountering damaged endothelium, platelets follow three steps to maintain hemostasis: adhesion, activation, and aggregation.

1.2 Platelets

1.2.1 Platelet Structure

The structure of platelets plays a crucial role in maintaining their discoid shape when in an inactivate state and controlling the dramatic morphologic changes that platelets undergo when activated. The platelet structure is composed of a number of structural elements: an open canalicular system, a dense tubular system, a spectrin and actin based cytoskeleton, a microtubule coil, and granules.

Open canalicular system

The open canalicular system (OCS) is a network of tunnels that start at the plasma membrane of the platelet and travel throughout the interior of the platelet. The OCS is

necessary for three different functions of platelets. First, it is a semi-selective conduit which allows small external molecules to enter into the platelet and the release of the content from granules. Second, the lipid content of the OCS serves as a reservoir of internal membrane that can be used for filipodia formation and platelet spreading. Third, the OCS is a storage location for plasma membrane glycoproteins in which the proteins are sequestered or released following platelet activation by agonists [14, 15].

Dense tubular system

The dense tubular system (DTS) is formed from the smooth endoplasmic reticulum of megakaryocytes [16]. It is the primary site of calcium storage in platelets. In the DTS calreticulin binds to Ca^{2+} and sequesters it to help maintain the resting platelet Ca^{2+} concentration at 100 nm/L [17]. Once platelets are activated by an agonist such as thrombin, cytoplasmic calcium levels rapidly rise as Ca^{2+} is released from the DTS into the cytoplasm [18]. The rapid rise in intracellular calcium levels causes granule release, cytoskeleton reorganization, and the association of $\alpha_{IIb}\beta_3$ [15].

Spectrin and actin based cytoskeleton

Together spectrin strands and actin filaments maintain plasma membrane integrity and provide structure that protects the disc shape of the resting platelet. Spectrin strands line the inside of the plasma membrane and connect to long actin filaments to form a singular continuous structure [19]. Actin, the most abundant protein in platelets, is formed into linear filaments or kept in storage as a non-filamental form in resting platelets [20]. The filaments are crosslinked by filamin and α-actinin to form a stiff cytoskeleton [21].

During platelet activation, the stored actin is converted to actin filaments which facilitate platelet spreading.

Microtubule coil

Located just below the plasma membrane, platelets contain a single microtubule of polymerized α-β tubulin dimers coiled 8-12 times [22]. The main function of the microtubule coil is to maintain the disc shape of resting platelets. Following platelet activation, the microtubule dissembles allowing spherical shape change.

Dense granules

The first secretory vesicles released in the process of platelet activation are dense granules. These small granules can be identified using electron microscopy by their electron-dense cores and are relatively low abundance granules, 3-8 dense granules per platelet [23, 24]. Dense granules contain small molecules such as ATP, ADP, serotonin, calcium, and catecholamines that are secreted following platelet activation and further enhance activation [25].

Alpha granules

The most abundant vesicle in platelets is the alpha granule. Alpha granules make up approximately 10% of the platelet volume and are responsible for storing both soluble and membrane bound proteins involved in platelet activation [26]. Following platelet activation, alpha granules fuse with the platelet plasma membrane to increase the overall

surface area of the platelet, transport membrane bound proteins to the plasma membrane, and release soluble proteins to further enhance platelet activation [27].

Under basal conditions the majority of the membrane bound proteins contained in alpha granules are expressed on the platelet plasma membrane (integrins, immunoglobulin family receptors, leucine-rich repeat family receptors, tetraspanins, CD36, Glut-3) [28-32]. Following fusion of alpha granules with the platelet membrane, the number of these receptors on the platelet membrane greatly increases enhancing their ability to aid in further platelet activation. Not all alpha granule membrane proteins are present on the surface of resting platelet surface; for example, P-selectin is only expressed on the platelet surface following alpha granule fusion with the platelet membrane [28].

Alpha granules also release soluble proteins following platelet activation which further propagate hemostasis. For example, platelet-platelet and platelet-subendothelial interactions are enhanced by the release of fibrinogen and VWF, respectively [33, 34]. Components of the coagulation system are also stored and released from alpha granules [28, 35].

1.2.2 Platelet Activation

Adhesion

Following vascular injury, platelets first adhere to the site of the damaged vessel. At the site of the damaged endothelium both von Willebrand factor (VWF) and collagen play a crucial role in platelet adhesion. VWF is released from endothelial cells into circulation

as well as exposed on the damaged endothelium. Under high shear conditions, GPIb-V-IX on the platelet surface binds to VWF linked by collagen to the subendothelial matrix of the vascular wall [36]. The transient GPIb-V-IX VWF interaction enables initial tethering to the damaged vessel wall and slows platelets which allows the second adhesion receptor, GPVI, to interact with collagen at the site of injury [37, 38]. Collagen bound GPVI activates downstream signaling events triggering platelet activation and more stable adhesion by collagen interacting with activated $\alpha_2\beta_1$ [39-42].

Activation

As platelets adhere to the damaged endothelium they are activated by a myriad of pathways. VWF binding to GPIb-V-IX activates downstream signaling causing integrin activation, calcium elevation, and eventually aggregation [43-46]. GPVI bound to collagen leads to integrin activation, granule secretion, and thromboxane A_2 synthesis [47, 48].

Platelets also express multiple receptors that are necessary for sustained platelet activation. Thrombin generated by the coagulation system is a potent platelet agonist which activates protease activated receptor 1 and 4 (PAR) on human platelets [49-55]. Thromboxane A2 is synthesized by activated platelets and binds to the thromboxane receptor (TXA2/PGH2) which further amplifies platelet activation [56]. Dense granules release ADP which binds to P2Y1 and P2Y12 that couple to G_q and G_i, respectively, to regulate mobilization of calcium and lead to a second wave of aggregation [57-60]. Secreted ATP binds to P2X1 to allow rapid influx of Ca^{2+} ions through the channel [61,

62]. Serotonin released from dense granules binds to the platelet serotonin receptor (5-HT2A) which couples to G_q to induce calcium mobilization [63]. Platelet activation also leads to the release of additional proteins from alpha-granules and the activation of integrins that is vital for platelet aggregation.

Aggregation

The next step in thrombus formation is aggregation which is mediated by the platelet integrin $\alpha_{IIb}\beta_3$. On resting platelets, $\alpha_{IIb}\beta_3$ is maintained in a low affinity, inactive state. The activation of platelet membrane receptors (e.g. PAR1, PAR4, TXA2, P2Y1, and P2Y12), induces intracellular signals that convert $\alpha_{IIb}\beta_3$ to an active ligand-binding state [64-67]. This process known as inside-out signaling enables platelet-platelet interactions. In an active state, $\alpha_{IIb}\beta_3$ is able to bind with high affinity to multiple extracellular ligands which enable platelet-platelet adhesion and thrombus formation [68]. Fibrinogen is the main $\alpha_{IIb}\beta_3$ ligand, but the receptor also binds to VWF and fibronectin that bridge platelets and activate them further [69-74]. Following ligand binding to the extracellular portion of $\alpha_{IIb}\beta_3$, the receptors cluster and conformational changes occur to the cytoplasmic portion of the integrin to initiate signaling inside the platelet, outside-in signaling [75-78]. The signaling events triggered by outside-in signaling are necessary for cytoskeletal reorganization, granule secretion, aggregation, platelet spreading, and stable platelet adherence [79-83].

Figure 1.2: Platelet Activation

Platelets initially adhere to the damaged endothelium through GPIb-V-IX interacting with VWF and GPVI and $\alpha_2\beta_1$ interacting with collagen. Platelets then secrete ATP, serotonin (5HT), and ADP from dense granules which activate P2X1, 5-HT2A, P2Y1, and P2Y12. TXA is generated, secreted, and activates the thromboxane receptor. Thrombin generated from the coagulation cascade activates PAR1 and PAR4. Together signaling from the receptors leads to platelet activation. $\alpha_{IIb}\beta_3$ is then converted to its active form, binds fibrinogen, and enables platelets to bind to one another and aggregate. Simultaneously, fibrinogen is cleaved to insoluble fibrin which forms a clot with aggregated platelets.

Figure 1.2: Platelet Activation

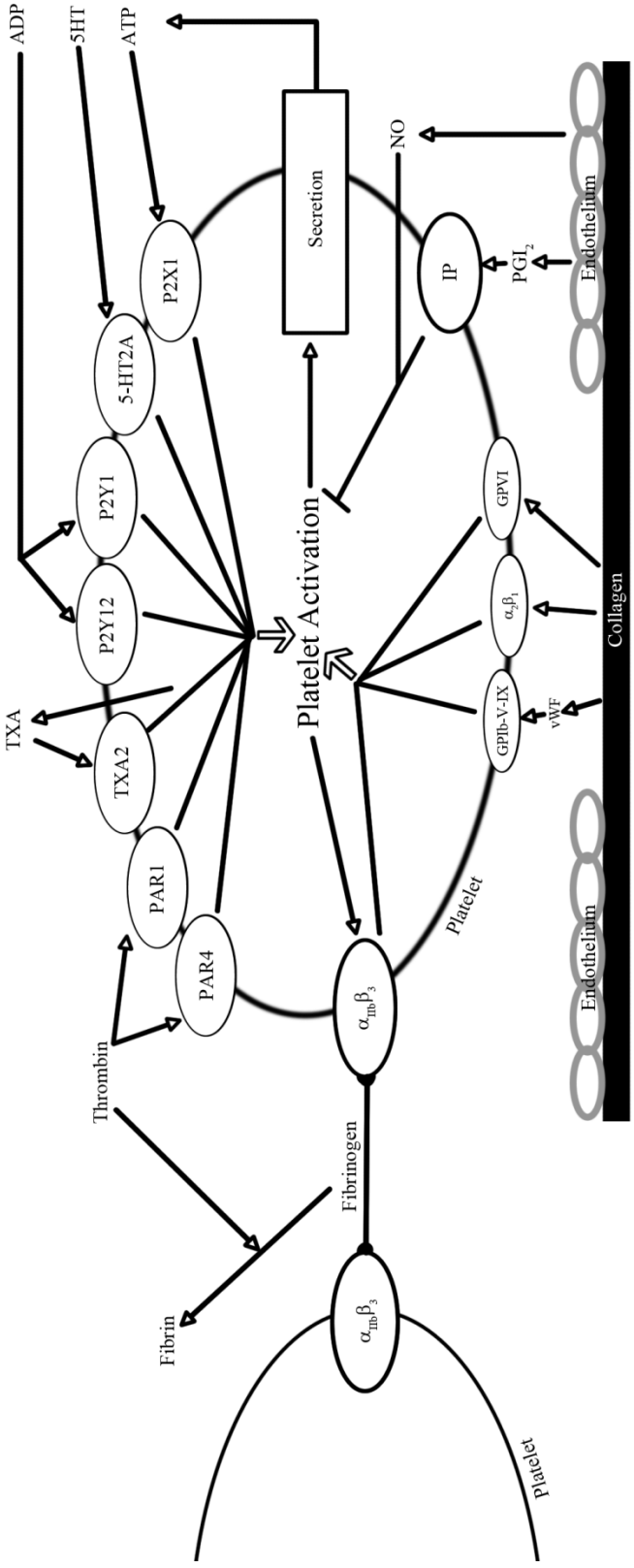

1.3 Thrombosis

Under normal healthy conditions the endothelium suppresses coagulation, platelet adhesion, platelet activation, and inflammation. This is accomplished through expression of tissue factor pathway inhibitor, production of tissue plasminogen activator and thrombomodulin, and secretion of NO, prostacyclin, and IL-10 [84]. However, under certain pathological circumstances the endothelium no longer adequately inhibits coagulation, platelet activation, and inflammation to suppress the formation of a localized thrombus. This results in the formation of a blood clot inside a blood vessel, known as thrombosis. Depending on the location and composition of the thrombus, it is defined as arterial thrombosis or venous thrombosis. Arterial thrombi are located in arterial blood vessels and are mainly composed of platelets ("white thrombus"). Venous thrombi are located in veins and are mainly composed of fibrin and red blood cells ("red thrombus"). The preferred method for preventing arterial thrombosis is antiplatelet therapy while venous thrombosis is normally treated with anticoagulant therapy.

Arterial Thrombosis

Arterial thrombosis is typically caused as a result of atherosclerosis [85]. Atherosclerosis is defined as the formation of an atherosclerotic plaque. The process of atherosclerosis is initiated by the accumulation of cholesterol-LDL in the intima of blood vessels. This leads to the activation of endothelial cells which recruit monocytes and T cells. The T cells enhance atherosclerosis activity and progression [86]. The monocytes differentiate into macrophages which engulf the LDL and form foam cells which can release growth factors and cytokines that cause vascular smooth muscle cells to migrate to the intima,

produce extracellular matrix components, and contribute to the fibrous cap formation [87, 88]. The macrophages with high lipid content undergo apoptosis and are removed by M2 macrophages which can be stressed to cause macrophage death [89]. The dead macrophages release pro-inflammatory compounds, lipids, metalloproteinases, and platelet activating molecules which are contained within the plaque (Figure 1.3A) [89-91].

Many different plaque characteristics contribute to rupture (plaque composition, location, sheer stress, vessel expansion). Following disruption of the plaque, pro-thrombotic molecules are exposed to blood triggering platelet adhesion, activation, and aggregation. Depending on the degree of stenosis and the size of the plaque, the newly formed clot can completely occlude the flow of blood at the site of rupture blocking blood from reaching downstream tissues and organs. For example, if a coronary vessel is occluded, a myocardial infarction (heart attack) results or if an artery to the brain is obstructed, a stroke occurs. Clots also can break off from the site of injury and travel in circulation to a smaller blood vessel to cause a thromboembolism.

Venous Thrombosis

In contrast to arterial thrombosis, venous thrombosis is the formation of a thrombus within the veins. Venous thrombosis occurs most often at sites where the vessel wall is altered, sheer stress is low, and there is hypercoagulability [92]. Depending on where the thrombus is located, it is associated with chronic diseases such as congestive heart

failure, respiratory insufficiency, cancer, recent surgery, or immobilization. If the thrombus dislocates and travels to the lungs, it can cause a life-threatening pulmonary embolism (Figure 1.3B).

Figure 1.3 Arterial and Venous Thrombosis

A) The primary cause of arterial thrombosis is the rupture of an atherosclerotic plaque. The multiple components involved in arterial thrombosis are illustrated. Arterial thrombi are mainly composed of platelets.

B) Venous thrombosis is triggered by abnormal blood flow, increased coagulability, and alterations in the vessel wall. Venous thrombi are mainly composed of red blood cells and fibrin.

Figure adapted from Mackman, N. Nature. 2008 Feb 21; 451(7181): 914–918.

Figure 1.3: Arterial and Venous Thrombosis

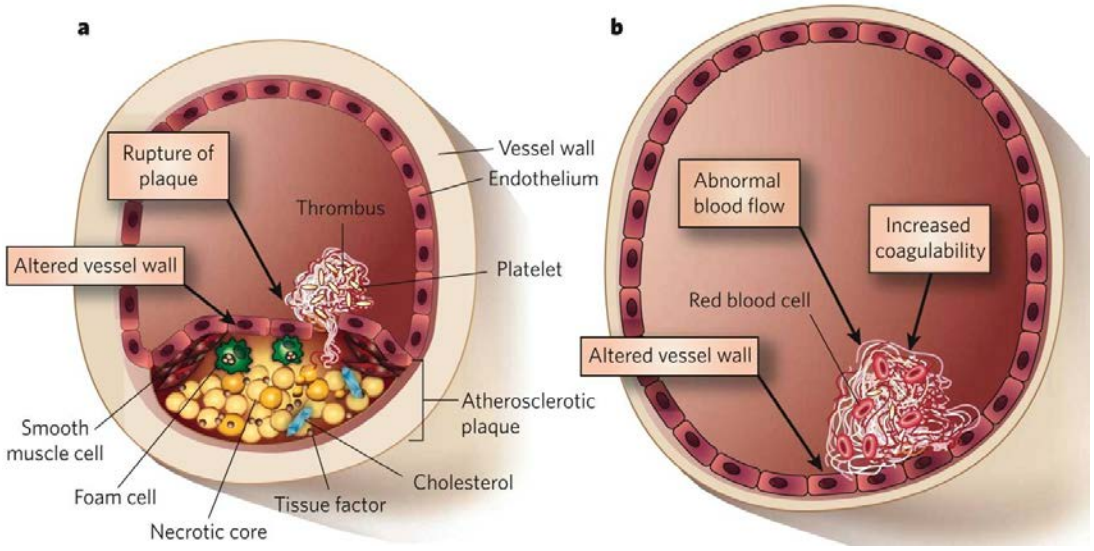

Mackman, N. Nature. 2008 Feb 21; 451(7181): 914–918.

1.4 Anti-thrombotic Therapies

1.4.1 Anticoagulant Therapies

Anticoagulants are a class of drugs that target different steps in the coagulation cascade to prevent the formation or activity of thrombin. They can be broken down into four groups: warfarin, heparin, factor Xa inhibitors, and direct thrombin inhibitors. Warfarin and heparin are the traditional anti-coagulants, but anticoagulants were expanded within the past few years to include newly developed anticoagulants, factor Xa inhibitors and direct thrombin inhibitors. The new anticoagulants are as good as or better than the traditional anticoagulants; however, they currently do not have a reversal agent in case of emergency bleeding situations. All of the anticoagulants are associated with an increased bleeding risk.

Warfarin

Warfarin's method of action is inhibition of the vitamin K-epoxide reductase, preventing the recycling of vitamin K and reduced vitamin K from vitamin K epoxide. Normally γ-carboxylation of factors II, VII, IX, and X, which enables binding of the coagulation factors to a phospholipidic surface, is coupled to the oxidation of the reduced form of vitamin K to vitamin K epoxide [93]. However, without the recycling of vitamin K epoxide to vitamin K and reduced vitamin K, γ- carboxylation of the vitamin K dependent clotting factors cannot occur. This ultimately prevents the formation of the active form of factors II, VII, IX, and X which causes an anti-thrombotic effect [94]. Since warfarin has a narrow therapeutic window, its effectiveness is influenced by

vitamin K consumption, and many commonly used drugs affect its metabolism, the internal normalized ratio (INR) needs to be closely monitored to maintain a safe dose of warfarin to prevent thrombosis while minimizing bleeding risk.

Heparin

Heparin is a glycosaminoglycan used for the treatment and prevention of thrombi formed from atrial fibrillation, venous thromboembolisms, and wide spread intravascular coagulation [94]. Following binding to antithrombin, heparin causes a conformational change which enhances the activity of antithrombin and increases the rate of inactivation of both Xa and IIa (thrombin) [95]. In some individuals, heparin-induced thrombocytopenia (HIT) occurs as a result of the formation of heparin antibodies against heparin bound platelet factor 4 (PF4). The heparin-PF4-IgG complex then activates platelets through their FcγIIa receptor which can cause thrombosis and thrombocytopenia [96]. In cases of HIT, alternate anticoagulant therapies need to be administered such as the new generation anticoagulants, FXa and direct thrombin inhibitors.

Factor Xa Inhibitors

Factor Xa inhibitors are part of the new group of anticoagulants developed to target a different point in the coagulation cascade. As the name indicates, factor Xa inhibitors target Xa, the first step in the common pathway. Three direct Xa inhibitors (apixaban, rivaroxiban, and edoxaban) have been developed that bind to the active site of Xa and inhibit its activity [97, 98]. Factor Xa inhibitors are available as an alternate anticoagulant

in the case of HIT, as well as for treatment of venous thromboembolism and thrombi formed as a result of atrial fibrillation [99].

Direct Thrombin Inhibitors

Direct thrombin inhibitors can be broken down into two groups, parenteral and oral. Two parenteral direct thrombin inhibitors (bivalirudin and argatroban) have been developed. Bivalirudin is a 20 amino acid polypeptide that binds to both the active site and exosite I of thrombin. Similar to bivalirudin, argatroban is also a polypeptide that binds to the active site of thrombin, however, it does not bind to exosite site I. Since administered intravenously, their onset of action is immediate, but they have short half-lives since they are polypeptides. Both bivalirudin and argatroban are alternatives to heparin [100].

The orally available direct thrombin inhibitor, dabigatran, is administered as a prodrug which is hydrolyzed to its active form that binds the active site of thrombin [100]. Since its onset is faster than warfarin and has a similar half-life but will not be affected by vitamin K intake, dabigatran is an alternate therapy for long-term treatment of venous thromboembolism.

Figure 1.4: Anticoagulant Therapies

There are 4 different types of anticoagulant therapies that target different factors in the coagulation cascade. Warfarin inhibits vitamin K-epoxide reductase preventing the formation of active vitamin K dependent clotting factors, II, VII, IX, and X. Heparin binds to antithrombin (AT III) and increases the inactivation of Xa and IIa. Apixaban, rivaroxiban, and edoxaban (factor Xa inhibitors) bind to the active site of Xa and inhibit it from activating II. The direct thrombin inhibitors bivalirudin, argatroban, and dabigatran bind to the active site of IIa and inhibit its enzymatic activity.

Figure 1.4: Anticoagulant Therapies

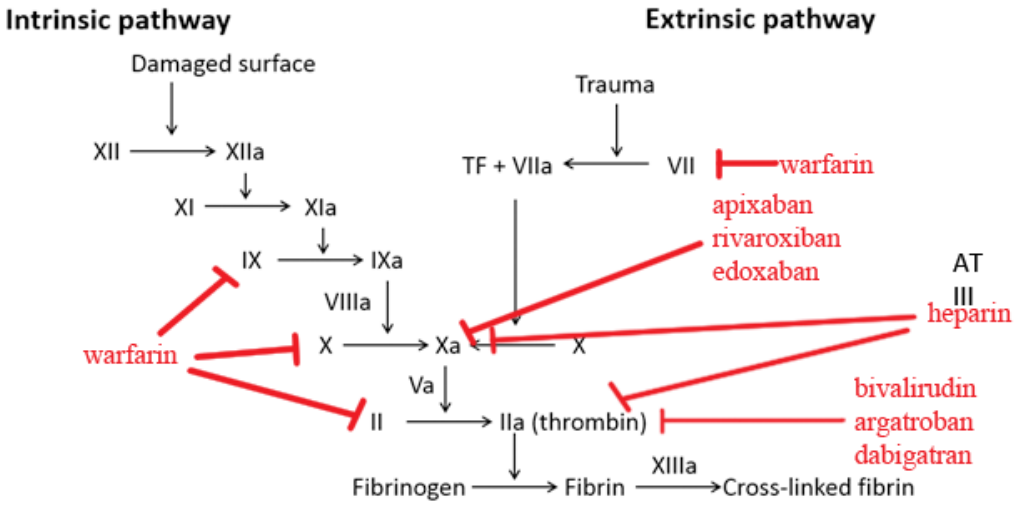

1.4.2 Antiplatelet Therapies

Antiplatelet therapies are a classification of drugs that target various pathways involved in platelet activation. Antiplatelet therapies are broken down into four groups based on the target of the therapy, aspirin, P2Y12 antagonists, $\alpha_{IIb}\beta_3$ antagonists, and PAR1 antagonists. The current standard of care for treating acute coronary syndromes is dual antiplatelet therapy of aspirin and a P2Y12 antagonist. However, a PAR1 antagonist, vorapaxar, just recently received FDA approval in 2014, and for a limited number of patients it is recommended as an addition to dual antiplatelet therapy to prevent cardiovascular death, myocardial infraction, and stroke. $\alpha_{IIb}\beta_3$ antagonists are only recommended for use in high risk patients who have low bleeding risk [101, 102]. Treatment with any of the antiplatelet therapies is associated with an increased bleeding risk.

Aspirin

Aspirin, acetylsalicylic acid, has become standard of care for treatment of cardiovascular disorders. Aspirin's mechanism of action is through inhibition of cyclooxygenase (COX) -1 and COX-2 [103, 104]. Aspirin irreversibly acetylates S529 on COX-1 changing the conformation of the active site so that it cannot bind arachidonic acid [103, 105, 106]. In the case of COX-2, aspirin acetylates S516 which results in the enzyme converting arachidonic acid to 15-R-hydroxyeicosateraenoc acid [106, 107]. Aspirin is able to irreversibly inhibit both enzymes preventing the synthesis of prostaglandins (Thromboxane A_2, Prostaglandin I_2, Prostaglandin E_2, Prostaglandin D_2, and Prostaglandin $F_{2\alpha}$) [108].

Of the prostaglandins produced from arachidonic acid, two have an effect on platelet aggregation, prostaglandin I_2 (PGI_2) and thromboxane A_2 (TXA_2). Prostacyclin I_2 is produced by the endothelium to inhibit platelet aggregation and maintain vasodilation [104]. In contrast thromboxane A_2 has a proaggregation effect. In response to platelet agonists, platelets increase production of TXA_2 which then amplifies aggregation further and stimulates vasoconstriction [109]. Since platelets express high levels of COX-1, the antiplatelet effect of aspirin occurs as a result of inhibiting COX-1 in platelets. In contrast, COX-2 is primarily responsible for PGI_2 synthesis by the endothelium [104, 110-112]. Since aspirin has a 170-fold greater inhibitory effect on COX-1 then COX-2, at low doses aspirin is able to irreversibly inhibit COX-1 on platelets preventing TXA_2 production for the lifetime of the platelet, but has a small temporary effect on PGI_2 production by COX-2 in the endothelium which ultimately provides the maximal effect for platelet inhibition [113-116].

P2Y12 Antagonists

Combination therapy of aspirin with a P2Y12 antagonist is the primary method of treating acute coronary syndrome (a decrease in blood flow to the heart). Currently, multiple P2Y12 inhibitors are available and approved by the FDA. Three of the inhibitors are thienopyridines, ticlopidine, clopidogrel, and prasugrel. Ticlopidine was the first generated thienopyridine P2Y12 inhibitor which received FDA approval in 1991,

however, due to its toxic side effects (neutropenia and thrombocytopenia) a new drug with a better safety profile was developed, clopidogrel [117-119].

Clopidogrel is the most widely prescribed antiplatelet therapy since it has relatively low cost, a generic form of the drug has been available since 2012, and is highly effective [120, 121]. Clopidogrel is orally administered as a prodrug, metabolized by numerous CYP isoenzymes including CYP2C19, and the active metabolite irreversibly binds to P2Y12 to cause inhibition of ADP-induced platelet activation and aggregation [122]. However, there are limitations to clopidogrel administration since only 15% of the drug is converted to an active metabolite and there are common loss-of-function variants to CYP2C19 preventing individuals from receiving clopidogrel treatment [123].

Prasugrel is a third generation P2Y12 inhibitor that was developed to overcome some of the limitations associated with clopidogrel. Similar to clopidogrel, prasugrel is orally administered as a prodrug which following metabolism irreversibly inhibits P2Y12 [15]. However, the majority of the prodrug is converted to the active metabolite and its metabolism does not appear to be affected by CYP variants [124, 125]. Since both prasugrel and clopidogrel irreversibly inhibit P2Y12, they are associated with a long half-life because the platelet population must be replaced.

Ticagrelor, the first non-thienopyridine inhibitor, is an orally active drug that reversibly binds P2Y12 [123]. Since the drug is administered in its active form, it overcomes the

metabolism issue associated with clopidogrel. In addition, Ticagrelor reversibly binds P2Y12 so it does not have a slow offset of action [126]. However, because ticagrelor is metabolized by CYP3A4 in the liver to be excreted, ticagrelor cannot be administered with other drugs that influence the activity of CYP3A4 [127]. Overall, treatment with any of the P2Y12 inhibitors is associated with increased bleeding risk.

$\alpha_{IIb}\beta_3$ Antagonists

Currently there are three FDA approved $\alpha_{IIb}\beta_3$ antagonists for treatment of acute cornonary syndromes, abciximab, tirofiban, and eptifibatide. Unlike aspirin and P2Y12 inhibitors which inhibit signal transduction leading to $\alpha_{IIb}\beta_3$ activation, $\alpha_{IIb}\beta_3$ antagonists directly block ligand binding to the receptor to prevent aggregation. While three different approaches have been used to develop $\alpha_{IIb}\beta_3$ antagonists (abciximab is a murine-human chimeric F_{ab} fragment, tirofiban is a nonpeptide small molecule designed after the RDG sequence, and eptifibatide is a KGD containing cyclic heptapeptide), they all bind reversibly to $\alpha_{IIb}\beta_3$ to prevent ligand binding [79, 128-131]. After the development of $\alpha_{IIb}\beta_3$ antagonists, P2Y12 antagonists were developed which have a better safety profile. As such, $\alpha_{IIb}\beta_3$ antagonists are only recommended for use in high risk patients who have low bleeding risk [101, 102].

Protease Activated Receptor 1 Antagonists

Even with dual antiplatelet therapy of aspirin and a P2Y12 antagonist, major cardiovascular events still occur in patients receiving treatment. Recent research has led

to the hypothesis that the residual risk may be due to thrombin-mediated platelet activation and two protease activated receptor 1 (PAR1) antagonists have been developed, vorapaxar and atopaxar.

Vorapaxar is a synthetic-tricyclic 3-phenylpyridine analog of himbacine (an antimuscarinic agent) that is highly selective for inhibiting PAR1 [132, 133]. Through interacting with transmembrane domains 3, 4, 5, 6, and 7 as well as extracellular loops 2 and 3 of PAR1, vorapaxar binds in a unique pocket of the receptor and the PAR1-vorapaxar complex cannot be easily reversed [134]. This most likely accounts for its long half-life (126-269 h) and prolonged effect [135]. Two phase III clinical trials were recently completed, TRA-CER and TRA 2P-TIMI 50. The TRA-CER trial evaluated the effect of vorapaxar vs placebo on patients with Non-ST segment elevation (partial occlusion of a coronary artery) acute coronary syndromes who were receiving standard of care therapy [136]. The trial found that vorapaxar had a modest effect on reducing thrombosis mediated coronary events, however, there was a significant increase in clinically important bleeding, including intracranial hemorrhage, and the trial was stopped after reaching a prespecified number of primary endpoints [136]. The TRA 2P-TIMI 50 trial investigated the addition of vorapaxar vs placebo onto standard of care therapy in the secondary prevention of atherothrombotic disease [137]. Based on the TRA-CER trial results and a 25 month follow-up of patients, patients who had previously had a stroke were removed from the trial and it continued with myocardial infarction and peripheral artery disease patients [136, 138]. At the end of the TRA 2P-TIMI 50 trial vorapaxar was found to significantly lower the risk of cardiovascular death or myocardial

infarction, but it did increase the risk of moderate or severe bleeding, including intracranial hemorrhage [137]. As a result, the FDA approved vorapaxar to reduce the risk of cardiovascular death, heart attack and stroke, but it carries a black box warning to not be used in patients with a history of stroke, transient ischemic attack, intracranial hemorrhage, or active pathological bleeding.

Atopaxar is another PAR1 antagonist that was under investigation as an antiplatelet agent. Similar to vorapaxar, atopaxar is orally available, potent, selective PAR1 antagonist, but it is more rapidly reversible and as a result a shorter half-life (22-26h) [139-141]. Two atopaxar phase II trials were recently completed, J-LANCELOT and LANCELOT ACS, that raised safety concerns (liver toxicity and malignant arrhythmias) and showed low efficacy resulting in suspension of further evaluation of atopaxar [139, 142].

Figure 1.5: Antiplatelet Therapies

There are currently 4 different classes of antiplatelet therapies that are available for treatment of acute coronary syndromes that each inhibits platelet activation by different agonists. Aspirin inhibits thromboxane and PGI2 production by inhibiting COX-1 and COX-2. P2Y12 antagonists (ticlopidine, clopidogrel, prasugrel, and ticagrelor) prevent activation of the P2Y12 receptor by ADP. $\alpha_{IIb}\beta_3$ antagonists (abciximab, tirofiban, and eptifibatide) prevent the receptor from binding fibrinogen. Vorapaxar and atopaxar are PAR1 selective antagonists.

Figure 1.5: Antiplatelet Therapies

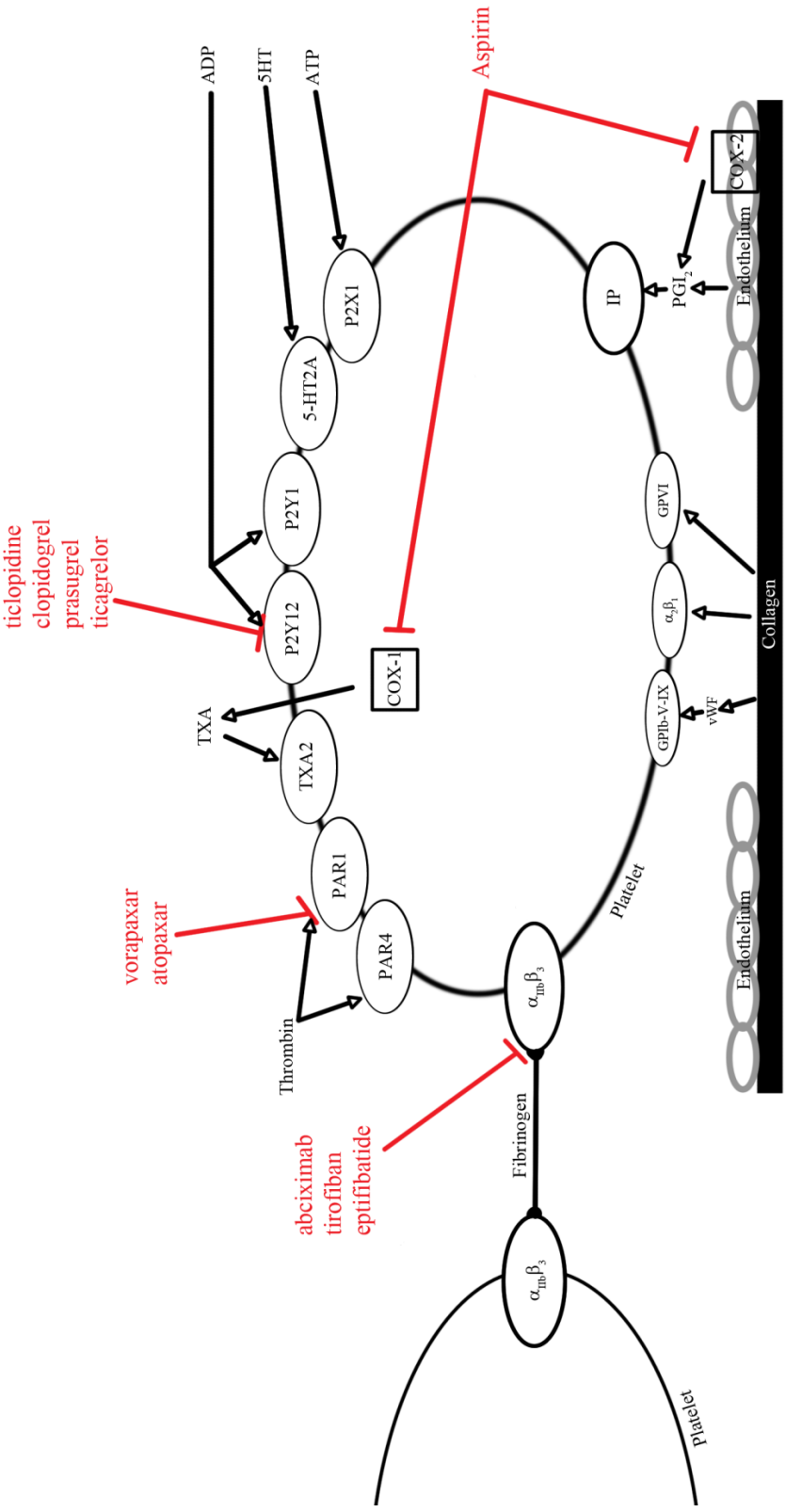

1.5 Protease Activated Receptors

Protease Activated Receptors (PARs) compose a unique family of seven-transmembrane G protein-coupled receptors that contain their own ligand sequence that is revealed following proteolytic cleavage [143]. The PAR family is composed of four members: PAR1, PAR2, PAR3, and PAR4 that are expressed in many cell types including platelets, endothelial cells, immune cells, smooth muscle cells, fibroblasts, neurons, astrocytes, and microglia [144, 145]. Following cleavage of their N-terminus by a protease, the newly exposed tethered ligand is able to intramolecularly bind to the receptor and trigger signaling [143]. Additionally, PARs can be activated by peptides which closely mimic their tethered ligand sequence. Depending on the receptor subtype, the cell type, and location within the plasma membrane, PARs couple to numerous G protein subtypes (G_q, G_i, $G_{12/13}$) [146] that activate various downstream signaling events (Figure 1.6).

Figure 1.6: Protease Activated Receptors

Protease activated receptors are G-protein coupled receptors that are activated by proteolytic cleavage of their N-terminus by a protease. Following cleavage, the new N-terminus acts as a tethered ligand which intramolecularly activates the PAR and leads to downstream signaling through G_q, G_i, and/or $G_{12/13}$.

Figure 1.6: Protease Activated Receptors

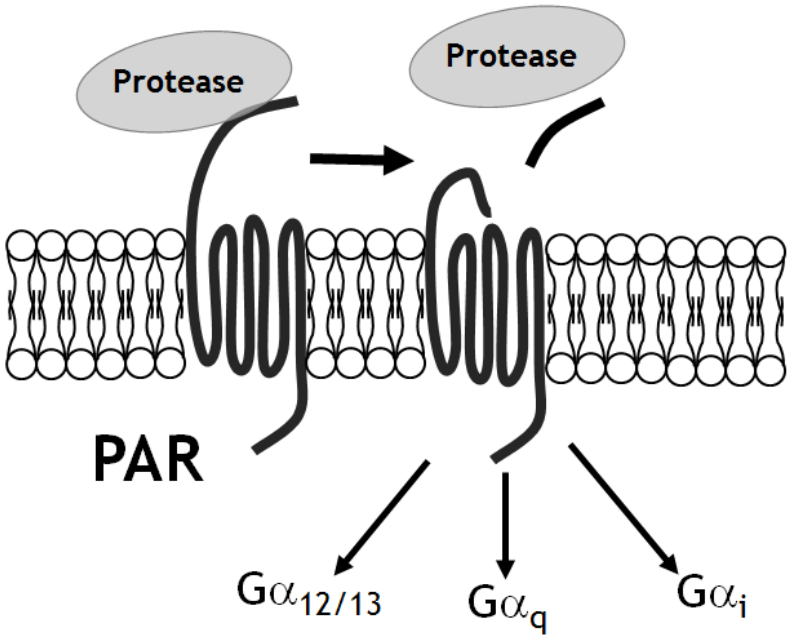

1.5.1 PAR1

PAR1 was originally discovered as a result of searching for the receptor that mediates the response to thrombin [54]. Since PAR1 was the first PAR to be discovered it is considered prototypic and has been studied in the most detail. PAR1 is widely expressed in human tissues, and in particular, is highly expressed in cells involved in hemostatic regulation [54, 147, 148]. PAR1 is predominantly activated by thrombin. Thrombin interacts with high affinity to two sites on PAR1 and low nanomolar concentrations of the enzyme are necessary to activate the receptor. The active site of thrombin binds to the cleavage site ($LPDR^{41}\downarrow SFLLRN$) on PAR1 and thrombin's anionic-binding exosite I interacts with the "hirudin-like" domain (residues 59-69) on PAR1 [149-151]. Following cleavage, the tethered ligand binds to PAR1 and triggers downstream signaling through G_q, G_i, and/or $G_{12/13}$ depending on the cell type [152]. In addition to cell type determining PAR1 signaling, the protease (thrombin, factor Xa, plasmin, kallikriens, activated protein C (APC), and matrix metalloprotease-1 (MMP1)) that cleaves PAR1 can regulate signaling [146, 153]. For example, activation of PAR1 by thrombin in endothelial cells is permeability-enhancing whereas activation of PAR1 by APC is barrier-protective, and the localization of PAR1 in the plasma membrane regulates this effect [154-156].

1.5.2 PAR2

PAR2 is widely expressed in human tissues and particularly in the liver, kidneys, pancreas, small intestine, and colon [157]. Unlike the other PARs, PAR2 is not activated by thrombin, but instead it is activated by trypsin, tryptase, membrane-anchored

matriptase, factor VIIa, and factor Xa [146]. The proteases cleave the receptor at $SKGR^{36}\downarrow SLIGK$, and similar to other PARs, the receptor activates G_q, G_i, and/or $G_{12/13}$ depending on the cell type. In addition, PAR1 can modulate the activation of PAR2 by PAR1's tethered ligand binding intermolecularly and transactivating PAR2 [158].

1.5.3 PAR3

In humans, PAR3 is less widely expressed than PAR1 and PAR2. It is only expressed in bone marrow and vascular endothelial cells [159]. Similar to PAR1, PAR3 contains a hirudin like sequence ($F^{48}EEFP$) that facilities cleavage of the N-terminus at $L^{35}PIK\downarrow TFRGAP$, however, PAR3 is only cleaved by thrombin and APC [160, 161]. PAR3 activates G_q to initiate signaling events [162].

1.5.4 PAR4

PAR4 is the most recently discovered PAR family member. PAR4 is highly expressed in the lung, pancreas, thyroid, testis, small intestine, and platelets [55]. Similar to PAR1 and PAR3, PAR4 is activated following proteolytic cleavage by thrombin but requires a higher concentration of thrombin (EC_{50} 5nM for PAR4 vs 0.2 nM for PAR1 and PAR3) to be activated [54, 55, 67, 159]. This is a result of the fact that PAR4 does not contain a hirudin like region, does not bind to exosite I, and therefore, cannot shift thrombin to a more active conformation through exosite I binding [163]. Instead, PAR4 contains an anionic cluster (D^{57}, D^{59}, E^{62}, and D^{65}) that interacts with thrombin's autolysis loop and slows the dissociation of thrombin from PAR4 prolonging the interaction time between

PAR4 and thrombin so cleavage can occur at the thrombin cleavage site P^{44}APR↓GYPGQV [55, 163-165]. In addition to being activated by thrombin, PAR4 can also be cleaved by trypsin or plasmin. Following activation, PAR4 signals through G_q, G_i, and/or $G_{12/13}$. While PAR4 has been mainly studied in the context on platelets, the receptor has also been shown to play a physiological role in other tissues and disease states such as myocardial ischemia/reperfusion injury, joint pain, inflammation, and diabetes [166-171].

1.6 Protease Activated Receptors on Platelets

1.6.1 Human Platelets

Of the 4 PAR family members human platelets express PAR1 and PAR4 with PAR1 more highly expressed than PAR4 [55]. In platelets, PAR1 and PAR4 have been shown to have unique and overlapping functions [172]. In the context of platelet activation, following cleavage of PAR1 or PAR4 by thrombin, both of the receptors signal through G_q and $G_{12/13}$. G_q signaling in platelets results in activation of phospholipase C-β which ultimately increases intramolecular calcium concentrations to cause granule secretion, integrin activation, and aggregation [173]. $G_{12/13}$ signaling ultimately leads to platelet shape change and granule secretion through activation of RhoA that activates Rho kinase that phosphorylates and inhibits myosin light chain phosphatase leading to enhanced myosin light chain phosphorylation and MLC-dependent contraction [174-177]. However, following thrombin activation in platelets, the two receptors have been shown to have differing roles on calcium release. Initially, thrombin stimulation of PAR1

results in a rapid increase in intracellular calcium which is followed by a sustained calcium response controlled by PAR4 [66, 178]. The prolonged signal from PAR4 activation has been shown to be necessary for stable clot formation [179, 180].

In addition to PAR1 and PAR4 signaling independently as monomers or homodimers, the receptors have been shown to form PAR1-PAR4 heterodimers [181-185]. Using bioluminescence resonance energy transfer (BRET), PAR1 was demonstrated to form constitutive homodimers [182]. Utilizing a similar approach of BRET and biomolecular fluorescence complementation (BiFC), PAR4 was shown to also form constitutive homodimers and this interaction is mediated through transmembrane helix 4 [183]. PAR1 and PAR4 also form heterodimers and this allows PAR1 to act as a cofactor for thrombin-induced PAR4 activation [184, 185]. Coexpression of PAR1 with PAR4 results in a ten-fold decrease in the EC_{50} for thrombin activation of PAR4 [165, 184]. The current proposed model for PAR1 acting as a cofactor is that following PAR1 cleavage by thrombin, the hirudin like region remains bound to exosite I of thrombin keeping it in the protease conformation [151, 186, 187]. An adjacent PAR4 is then able to interact with thrombin through its anionic region and the thrombin cleavage site can be more efficiently activated [165, 184, 188].

Furthermore, PAR4 has direct and indirect effects on P2Y12 signaling in platelets. Following activation, PAR4 and P2Y12 heterodimerize and recruit arrestin-2 to mediate PI3K-dependent AKT activation that affects platelet activation and stabilizes thrombi

[189, 190]. It has also previously been shown that PAR4 signals synergistically with P2Y12 to induce platelet activation [172].

Recently, it was determined that PAR4 contains polymorphisms at positions 120 (Ala/Thr) and 296 (Phe/Val) [191-193]. The polymorphism at amino acid 120 is more common and is distributed by race. PAR4-120A is more often found in white individuals and is less reactive compared to PAR4-120T that is hyper reactive to agonists, resistant to a PAR4 antagonist, and found primarily in self-identified black individuals [191]. This correlates with a heritable interindividual variation in platelet reactivity observed to be higher in black individuals than white individuals [194-196]. The polymorphism at 296 (Phe/Val) significantly decreases the activity of PAR4 which most likely accounts for valine at 296 being very uncommon.

1.6.2 Mouse Platelets

Mouse platelets express PAR3 and PAR4, however, PAR3 does not signal [67, 162, 197]. PAR activation of mouse platelets occurs only following PAR4 cleavage. On mouse platelets PAR4 signals through G_q and $G_{12/13}$ which leads to platelet shape change, granule secretion, integrin activation, and aggregation. Similar to human PAR4, mouse PAR4 is not an efficient thrombin substrate and requires high concentrations of thrombin to induced platelet activation [162, 165, 198]. At low thrombin concentrations (< 10 nM), mouse PAR3 acts as a cofactor for PAR4 activation, but at high thrombin concentrations (≥ 30 nM) PAR3 negatively regulates PAR4 G_q signaling without

affecting the $G_{12/13}$ pathway [162, 199]. The formation of PAR3 homodimers, PAR4 homodimers, and PAR3-PAR4 heterodimers may play a role in regulating the effect of PAR3 on PAR4 activation [199].

1.7 Statement of Purpose

Arterial thrombosis is responsible for the most deaths in the western world, yet there is an unmet need in decreasing major cardiovascular events while preventing clinically important bleeding. Platelets are a key component of pathological thrombosis. As such, the current standard of care for acute coronary syndromes targets platelets with a combination of aspirin and a P2Y12 inhibitor. While the current standard of care is effective at decreasing major cardiovascular events, they still occur and not all patients respond to combination therapy. As a result, antiplatelet therapy development shifted towards inhibiting thrombin activation of platelets.

To date, protease activated receptor 1 (PAR1) is thought of as the primary thrombin receptor on platelets that is activated by lower thrombin concentrations. PAR4 is dismissed as the low-affinity, redundant, back-up thrombin receptor to PAR1. As a result PAR1 has been the focus for drug therapy development. This has led to a detailed understanding of PAR1 activation resulting in a new antiplatelet therapy Zontivity (vorapaxar). Therapy with Zontivity is limited by the fact that treatment is associated with an increase in clinically important bleeding, specifically intracranial hemorrhage.

PAR1 and PAR4 have both overlapping and distinct properties. Thrombin stimulation of platelets causes an initial rapid increase in intracellular calcium through PAR1 that is followed by a sustained calcium response controlled by PAR4. The sustained calcium response initiated by PAR4 activation is necessary for stable clot formation. In addition,

it has been determined that the two receptors influence the activation and signaling of one another. Specifically, PAR1 and PAR4 form a heterodimer. Additionally, PAR1 lowers the EC50 of PAR4 activation ~10 fold. The exact mechanisms of how PAR1 and PAR4 heterodimerize and how PAR1 is able to influence PAR4 activation are still unknown.

The studies herein aim to 1) determine how the interaction between PAR1 and PAR4 influences receptor activation, 2) examine the feasibility of PAR4 as an antiplatelet therapeutic target, and 3) develop PAR4 monoclonal antibodies to monitor or inhibit PAR4 activation in endogenous cells.

(1) To define the functional relationship between PAR1 and PAR4, my thesis aimed to (a) map the heterodimer interface between PAR1 and PAR4, (b) determine if receptor cleavage is necessary for dimerization, and (c) examine if PAR1 assisted PAR4 activation is dependent on heterodimer formation.

(2) PAR4 is necessary for stable clot formation, has limited tissue distribution, and affects both thrombin and ADP signaling in platelets. My thesis aimed to determine if targeting a thrombin binding site on PAR4 (the anionic cluster) was a viable antiplatelet strategy. More specifically, I aimed to (a) develop a polyclonal antibody that interacted with PAR4's anionic cluster, (b) determine its ability to inhibit human platelet aggregation, (c) and evaluate its effect on thrombosis and hemostasis.

(3) Currently, there are a limited number of reliable reagents for studying PAR4. My thesis aimed to (a) develop PAR4 monoclonal antibodies (b) determine if they are sensitive to PAR4 activation, and (c) evaluate their ability to inhibit PAR4 activation.

In total, my thesis expands on the current understanding of how PAR1 and PAR4 interact and influence the activation of one another. It also demonstrates that PAR4 is a new viable target for antiplatelet therapy by preventing thrombosis without affecting hemostasis. In addition, these studies include the development of new tools that will enable studies that determine the role and function of PAR4 in endogenous cells and tissues.

Chapter 2 [*†]

Protease-activated Receptor 1 (PAR1) and PAR4 Heterodimers Are Required for PAR1-enhanced Cleavage of PAR4 by α-Thrombin

2.1 Abstract

Thrombin is a potent platelet agonist that activates platelets and other cells of the cardiovascular system by cleaving its G-protein-coupled receptors, protease-activated receptor 1 (PAR1), PAR4, or both. We now show that cleaving PAR1 and PAR4 with α-thrombin induces heterodimer formation. PAR1-PAR4 heterodimers were not detected when unstimulated; however, when the cells were stimulated with 10 nM α-thrombin, we were able to detect a strong interaction between PAR1 and PAR4 by bioluminescence resonance energy transfer. In contrast, activating the receptors without cleavage using PAR1 and PAR4 agonist peptides (TFLLRN and AYPGKF, respectively) did not enhance heterodimer formation. Preventing PAR1 or PAR4 cleavage with point mutations or hirugen also prevented the induction of heterodimers. To further characterize the PAR1-PAR4 interactions, we mapped the heterodimer interface by introducing point mutations in transmembrane helix 4 of PAR1 or PAR4 that prevented heterodimer formation. Finally, we show that mutations in PAR1 or PAR4 at the heterodimer interface prevented PAR1-assisted cleavage of PAR4. These data demonstrate that PAR1 and PAR4 require allosteric changes induced via receptor

[*] A version of this chapter was accepted for publication in the November 8, 2013 issue of *The Journal of Biological Chemistry*.

[†] I was a secondary author on this manuscript and my effort is detailed at the end of this chapter in 2.6 Effort.

cleavage by α-thrombin to mediate heterodimer formation, and we have determined the PAR1-PAR4 heterodimer interface. Our findings show that PAR1 and PAR4 have dynamic interactions on the cell surface that should be taken into account when developing and characterizing PAR antagonists.

2.2 Introduction

Protease-activated receptors (PARs) are a unique class of G-protein-coupled receptors that are activated by proteolytic cleavage of the N terminus by serine proteases [144]. There are four members of this family (PAR1-4). In the cardiovascular system, PARs are expressed in platelets, leukocytes, endothelial cells, and smooth muscle cells where they play an important role in hemostasis, thrombosis, inflammation, proliferation, and cell permeability [144, 200].

PAR1 has multiple roles on many cell types. One example of its diverse signaling is on endothelial cells where it can have barrier protective or barrier disruptive roles depending on the agonist and co-receptors present on the cell [154, 155, 201, 202]. The majority of research on PAR1 has been conducted in the context of human platelet activation by thrombin. A Phase III clinical trial with a PAR1 antagonist, vorapaxar, as an antiplatelet agent did not meet its primary end point due to bleeding complications [136]. Recently, a crystal structure of PAR1 bound to vorapaxar was solved [134]. Vorapaxar bound deep within the transmembrane helices explaining the essentially irreversible nature of its

interaction with PAR1. However, the physical changes in PAR1 that occur after activation by thrombin have not been studied in detail.

PAR4 is the primary signaling receptor on platelets of many species. In human platelets, PAR1 and PAR4 have both overlapping and unique signaling functions [172, 203]. For example, PAR4 activation produces a prolonged signal that is required for stable clot formation [66, 178-180]. Our laboratory has recently mapped the PAR4 homodimer interface to transmembrane helix 4 [183]. Mutations that disrupt PAR4 homodimers also disrupt Ca2+ signaling. On human platelets, PAR4 also interacts with PAR1 to enhance PAR4 activation [165, 184]. The details of this interaction are not known.

The activation of PAR1 and PAR4 requires the receptors to be cleaved by thrombin. PAR1 is an excellent thrombin substrate [188, 204]. PAR1 has a hirudin-like sequence that binds tightly to thrombin exosite I [151]. Based on biochemical and structural data from other tight exosite I binders, the PAR1 hirudin-like sequence likely induces thrombin into the protease conformation [186, 187]. In contrast, PAR4 does not bind to exosite I and is a poor thrombin substrate when it is expressed on cells alone [163, 165]. The inefficient activation of PAR4 is overcome by co-expression of PAR1 on human platelets and PAR3 on mouse platelets [67, 184]. The proposed model for PAR1 or PAR3 enhancing PAR4 activation is that after cleavage of PAR1 or PAR3, thrombin remains bound to the hirudin-like sequence via exosite I and cleaves an adjacent PAR4. In addition to recruiting thrombin to the surface of cells, the exosite I interaction is likely

holding thrombin in the protease conformation for efficient cleavage of PAR4 [162, 165, 184]. The functional significance of PAR1 or PAR3 co-expression with PAR4 is a 10-fold reduction in the EC50 of thrombin activation of PAR4 [162, 165, 184].

In addition to PAR1 and PAR4 having important independent roles in platelet signaling, the two receptors act synergistically by PAR1 enhancing PAR4 activation. To fully understand the relationship between PAR1 and PAR4, it is essential to have a complete understanding of the molecular arrangement and dynamics of their interactions. The present study demonstrates that α-thrombin promotes efficient heterodimerization between PAR1 and PAR4. The individual activating peptides for PAR1 and PAR4, TFLLRN and AYPGKF, respectively, and mutating the cleavage site of PAR1 or PAR4 does not induce PAR1-PAR4 heterodimerization. The current study also defines the heterodimer interface and maps it to transmembrane helix 4 of both PAR1 and PAR4. Finally, mutations that disrupt PAR1-PAR4 heterodimerization also disrupt PAR1-assisted cleavage of PAR4 by α-thrombin. Taken together, the current study defines the PAR1-PAR4 interaction and demonstrates a functional significance of the PAR1-PAR4 heterodimer.

2.3 Experimental Procedures

Reagents

Unless otherwise stated, all of the reagents were from Sigma. α-Thrombin was from Hematological Technologies (Essex Junction, VT).

Cell Culture

HEK293, HeLa, and COS-7 cells were from American Type Culture Collections and were cultured in DMEM supplemented with 10% bovine serum albumin (Hyclone, Logan, UT) and 1% penicillin/streptomycin (Invitrogen). Cells were transfected with Lipofectamine 2000 (Invitrogen) according to the manufacturer's instructions.

Molecular Cloning

The human PAR4 and the PAR4 transmembrane helix 4 mutants have been described (see Table 2.1) [183]. PAR4 with a mutation at the P1 residue of the thrombin cleavage site (PAR4-R47Q) was generated with overlapping PCR as previously described [188]. The nomenclature is that of Schechter and Berger [205] where the residue preceding the scissile bond is designated as P1. Human PAR1 in pLK-neo has been described and was the starting material for subsequent PCR reactions [165]. The HA tag (YPYDVPDYA) was added to the N terminus of the luciferase constructs, or V5 tag (GKPIPNPLLGLDST) was added to the N terminus of the GFP constructs at amino acid 26 such that the PAR1 signal sequence was removed. Alanine substitution mutants of PAR1 were generated with overlapping PCR using primers that mutated the relevant codon(s) to change Arg-41 (PAR1-R41A), Phe-2214.44, Leu-2244.47, Trp-2274.50, and Ile-2314.54 (PAR1-TM4-4A), Trp-2274.50 and Ile-2314.54 (PAR1-W227A/I231A), or Val-2354.58 and Leu-2394.62 (PAR1-V235A/L239A) (Table 2.1). The numbering system is that of Ballesteros and Weinstein. For co-immunoprecipitation studies, a T7 tag

(MASMTGGQQMG) was added to the C terminus of wild type PAR4 using pcDNA3.1. HA-PAR1 wild type and HA-PAR1-W227A/I231A were expressed using pEF1α-IRES-neo (Addgene), referred to as pEF1. For cleavage assays, V5-PAR4-wt or V5-PAR4-TM4-4A was expressed using pIRES-puro (Addgene), referred to as pIRES. A detailed list of primers used for all cloning is available upon request.

Bioluminescence Resonance Energy Transfer (BRET)

Initial experiments determined the optimal expression of PAR1 for BRET experiments as previously described for PAR4 (15). HEK293 cells (1 × 105) were transfected with PAR1-GFP (0–1 μg) or PAR1-rLuc (0–0.5 μg) to determine the minimal amount of plasmid for sufficient GFP and luciferase signal. GFP was determined by excitation at 495 nm and emission at 515 nm. Luciferase activity was determined using coelenterazine H (5 μM) and measuring total light emission without a filter in a PerkinElmer Life Sciences Victor 3 plate reader. The conditions that gave optimal expression for BRET studies were used in subsequent experiments. BRET experiments were performed as previously described [183]. To account for lower expression of PAR1, all PAR1-rLuc constructs were adjusted to 0.5 μg/transfection. PAR4-rLuc was used at 0.03 μg/transfection as previously described [183]. The PAR4-GFP constructs were used at 0–0.25 μg/transfection, and the PAR1-GFP constructs were used at 0–5 μg/transfection. The BRET data from three or four independent experiments were pooled and analyzed by global fit to all of the data using Prism software (GraphPad). The best model (hyperbolic versus linear) for each data set was also determined using Prism. The BRET50 values

were compared with an F test of the globally fit data with Prism; $p < 0.05$ was considered significant.

Co-immunoprecipitation and Western Blot Analysis

COS-7 cells in 10-cm plates were transiently transfected with PAR1-pEF1 (5 μg) and PAR4-T7-pcDNA3.1 (2 μg) or PAR1-pEF1 (5 μg) and PAR4-pcDNA3.1 (2 μg, no T7 tag). Transfected cells were removed from plates 48 h post-transfection and washed twice with PBS. Cells were stimulated with 10 nM α-thrombin for 20 min at 37 °C and lysed with lysis buffer (1% Triton X-100, 50 mM Tris, pH 7.4, 100 mM NaCl, 5 mM EDTA) containing protease inhibitors mixture (Roche Applied Science) rotating 30 min at 4 °C. Proteins were extracted by centrifugation of lysed cells at 12,000 × g for 30 min at 4 °C. The supernatant-containing 300 μg of protein was immediately incubated with T7 antibody-agarose (25 μl/sample, Novagen) and rotated at 4 °C overnight. Agarose beads were washed with 0.5× immunoprecipitation buffer three times, and the immunoprecipitated proteins were eluted with 0.1 M glycine, pH 2.6. Eluates were neutralized with Tris-HCl, pH 8.0, before adding 5× Laemmli reducing buffer. The samples were resolved by SDS-PAGE and transferred onto polyvinylidene difluoride membranes. Membranes were incubated with anti-PAR1 (1: 333 dilution; WEDE15 clone; Beckman Coulter) or anti-PAR4. Detection was performed with HRP-conjugated anti-mouse secondary antibody and an enhanced chemiluminescence system (Pierce).

Cleavage Assays

To determine the influence of PAR1 mutations on the rate of PAR4 cleavage, COS-7 cells in 10-cm plates were transiently transfected with HA-PAR1-pEF1 (0.5 μg) and V5-PAR4-pIRES (2 μg), HA-PAR1-W227A/I231A-pEF1 (5 μg) and V5-PAR4-pIRES (2 μg), or V5-PAR4-pIRES alone (2 μg). To determine the influence of PAR4 mutations, cells were transfected with HA-PAR1-pEF1 (5 μg) and V5-PAR4-TM4-4A-pIRES (2 μg) or V5-PAR4-TM4-4A-pIRES alone (2 μg). Transfected cells were removed from plates 24 h post-transfection with versene, washed twice with PBS, and resuspended at concentration of 106 cells/ml in PBS. Reactions were initiated at 37 °C by adding 10 nM α-thrombin or 100 nM α-thrombin. Reactions were stopped at different time points with hirudin (0.5 units/ml), washed once with PBS, and incubated with V5 tag antibody conjugated to Alexa Fluor 647 (AbD Serotec) with a 1:50 dilution. The decrease of mean fluorescence as a result of the loss of the V5 epitope was determined by flow cytometry on a BD LSRFortessa (Center for Aids Research, Immune Function Core, Case Western Reserve University). The mean fluorescence data were fit to an exponential decay with the equation fl = fl0e−kt to compare the rate of PAR4 cleavage. The initial cell surface expression of HA-PAR1 and V5-PAR4 was determined by quantitative flow cytometry before adding thrombin using HA (Cell Signaling Technology Inc) or V5 antibodies conjugated to Alexa Fluor 647 with a 1:50 dilution and performed essentially as described [183].

Calcium Mobilization Assays

HeLa cells were transfected with HA-PAR1-pEF1, HA-PAR1-W227A/I231A-pEF1, V5-PAR4-pIRES, or V5-PAR4-TM4-4A-pIRES, and stable clones were selected with

puromycin (1 μg/ml) or Geneticin (1 mg/ml). Calcium mobilization was measured with Fura-2 as previously described [183, 199]. Briefly, cells were removed from plates with versene, washed, and loaded with 5 μM Fura2-AM (Invitrogen) in Hepes-Tyrodes buffer supplemented with magnesium and calcium. Cells (2.5 × 105) were placed into 96-well plates, stimulated with α-thrombin, and read in a NOVOstar plate reader (BMG Labtech, Durham, NC). Fluorescence measurements were converted to intracellular calcium concentration by the formula of Grynkiewicz et al. [206].

2.4 Results

Previously, we determined the optimal conditions to analyze PAR4 homodimers by BRET using the minimal expression levels necessary to avoid overexpression artifacts [183]. Initial studies determined the minimal amount of plasmid to give sufficient PAR1-rLuc expression was 0.5 μg (data not shown) compared with 0.03 μg for PAR4 [183]. The interaction between PAR1 and PAR4 was examined by BRET experiments that were designed to achieve similar levels of PAR1 and PAR4 expression. The initial experiments examined the PAR1-PAR4 heterodimer with BRET in unstimulated cells, which did not show a specific interaction, indicated by a linear relationship (Fig. 2.1A and Table 2.2). However, upon stimulation with 10 nM α-thrombin for 10 min there was a robust increase in the formation of PAR1-PAR4 heterodimers indicated by a hyperbolic curve (Fig. 2.1A and Table 2.2). The α-thrombin-induced interaction of PAR1 and PAR4 did not change when rLuc was fused to PAR1 and GFP was fused to PAR4 (Fig. 2.1B); the BRET50 (0.126 ± 0.08 versus 0.077 ± 0.03, p = 0.16) and BRETmax (0.17 ± 0.04 versus 0.26 ± 0.03, p = 0.26) were both unchanged (Table 2.2). The specificity of the BRET

interaction was shown using the non-interacting GPCR rhodopsin (Fig. 2.1C). Similar to our previous studies with PAR4 [183], rhodopsin did not interact with PAR1. These data suggested that stimulation of the receptors with α-thrombin induced PAR1 and PAR4 to efficiently form heterodimers.

Studies next determined if the induction of PAR1-PAR4 heterodimers was due to activation or cleavage of the receptor using PAR-activating peptides, PAR mutants, or the thrombin inhibitor hirugen. PAR1 and PAR4 activation peptides, TFLLRN or AYPGKF, respectively, can be used to activate the receptors in the absence of cleavage. Cells were prepared for BRET and stimulated with 50 μM TFLLRN and 500 μM AYPGKF simultaneously for 10 min. The PAR activation peptides did not induce PAR1-PAR4 heterodimers (Fig. 2.2A). Stimulation of the cells with TFLLRN or AYPGKF individually also did not induce PAR1-PAR4 heterodimer formation (data not shown). To examine the requirement of PAR1 and PAR4 cleavage for the induction of heterodimers, the Arg in the P1 position of PAR1 or PAR4 was mutated and tested for its ability to form heterodimers. PAR1-R41A did not interact with PAR4 wild type after stimulation with 10 nM α-thrombin for 10 min (Fig. 2.2B). Similarly, the cleavage-deficient PAR4, PAR4-R47Q, did not interact with wild type PAR1 (Fig. 2.2C). Furthermore, blocking thrombin exosite I with hirugen also inhibited the induction of PAR1-PAR4 heterodimers (Fig. 2.2D). Flow cytometry with antibodies to the N-terminal tags HA or V5 on PAR1 or PAR4, respectively, confirmed that hirugen blocked the cleavage of PAR1 and PAR4 by thrombin (Fig. 2.2E).

PAR1 and PAR4 also form homodimers [182, 183]. In contrast to the PAR1-PAR4 heterodimers, thrombin did not influence the BRET50 or BRETmax for PAR1 or PAR4 homodimers (Fig. 2.3, A and B; Table 2). The BRET50 values were used to compare the relative affinities of α-thrombin-stimulated PAR1 homodimers, PAR4 homodimers, and PAR1-PAR4 heterodimers (Table 2.2). PAR4 homodimers had a lower BRET50 (higher relative affinity) (0.013 ± 0.01) compared with PAR1-PAR4 heterodimers regardless if the rLuc was fused to PAR4 (0.077 ± 0.026, p = 0.02) or PAR1 (0.126 ± 0.08, p = 0.01). PAR4 homodimers also had a lower BRET50 compared with PAR1 homodimers (0.159 ± 0.077, p = 0.01). Finally, the BRET50 for PAR1 homodimers and PAR1-PAR4 heterodimers were not statistically different regardless if the pLuc was fused to PAR1 or PAR4 (p = 0.80 or 0.14, respectively).

We next wanted to determine the PAR1-PAR4 heterodimer interface. We previously showed that the PAR4 homodimer interface is in transmembrane helix 4 (TM4) [183]. Therefore, we tested our panel of PAR4-TM4 alanine substitution mutants (Table 2.1) for the ability to associate with PAR1. The location of the mutations is shown in the molecular model of PAR4 that was generated by Swiss Modeler (Fig. 2.4A) [207-209]. Initial studies examined the surface expression with quantitative flow cytometry to ensure that each of the PAR4 mutants was expressed on the cell surface to the same degree as PAR4-wt (Fig. 2.4B). HEK293 cells were prepared for BRET assays and stimulated with 10 nM α-thrombin for 10 min. PAR4-TM4-2A (PAR4-L209A/L213A) was able to interact with PAR1 similar to PAR4 wild type with a BRET50 of 0.057 ± 0.023, p = 0.30 (Fig. 2.4C, Table 2.2). In contrast, PAR4-TM4-4A (PAR4-

L192A/L194A/M198A/L202A) did not interact with PAR1, indicated by the linear relationship (Fig. 2.4D, Table 2.2). Residues in TM1 have also been reported to mediate GPCR dimers/oligomers [210, 211]. Therefore, we mutated four conserved residues in TM1 of PAR4 (Table 2.1) and tested their role in mediating the PAR1 interaction. PAR4-TM1-4A (PAR4-L79A/V80A/L83A/L86A) interacted with PAR1 with the same BRET50 as PAR4 wild type (0.045 ± 0.040, p = 0.40) (Fig. 2.4E, Table 2.2).

Next, we wanted to determine the interface on PAR1 for the PAR1-PAR4 heterodimer. We generated a model of PAR1 using Swiss Modeler to guide our mutagenesis studies [183, 207-209]. This PAR1 model revealed residues in TM4 that were directed away from the body of the receptor (Fig. 2.5A). A series of alanine substitution mutants in TM4 of PAR1 were generated to determine their association with PAR4 (Table 2.1). The surface expression of each of the PAR1 mutants was verified by quantitative flow cytometry (Fig. 2.5B). The PAR1 mutants were tested in BRET assays for their ability to interact with PAR4 wild type. Similar to PAR4, mutations in residues near the outer membrane, PAR1-V235A/L239A, did not disrupt the ability of α-thrombin to mediate PAR1-PAR4 heterodimerization; the BRET50 (0.034 ± 0.024) was not statistically different from PAR1-wt (p = 0.16) (Fig. 2.5C, Table 2.2). However, mutating two residues near the center of TM4, PAR1-W227A/I231A, disrupted the interaction with PAR4 indicated by the linear BRET curve (Fig. 2.5D). Mutating two additional residues also disrupted PAR1-PAR4 heterodimers (Fig. 2.5E). These data suggest that, like PAR4 homodimers, several residues in TM4 of both receptors mediate the interaction between PAR1 and PAR4. Importantly, the residues in TM4 that mediate the PAR1-PAR4

interactions on both receptors (shown in orange in Figs. 2.4A and 2.5A) are in the same region along TM4 and align in a manner that would be capable of forming the interface.

We next examined the ability of PAR1 and PAR4 mutants to induce intracellular signaling by measuring the calcium mobilization in response to α-thrombin (Fig. 2.6). Consistent with our previous results, HeLa cells do not respond to α-thrombin in calcium mobilization (Fig. 2.6C) [165]. When expressed on HeLa cells, PAR4-TM4-4A retained the ability to respond to 30 nM α-thrombin, however, with reduced efficiency compared with PAR4 (Fig. 2.6A). These data are consistent with our previous results [183]. Similarly, PAR1-W227A/I231A also retained the ability to induce intracellular calcium mobilization but at a reduced level compared with the PAR1 (Fig. 2.6C). We verified by flow cytometry that HA-PAR1-W227A/I231A and V5-PAR4-TM4-4A PAR4 mutants were expressed to the same level as HA-PAR1-wt and V5-PAR4-wt, respectively, on the surface of HeLa cells (Fig. 2.6, B and D). These data show that the PAR1 and PAR4 mutants that disrupt the PAR1-PAR4 interface are expressed on the cell surface and have partial activity.

To examine the PAR1-PAR4 interaction with a second technique, we co-expressed PAR1 and PAR4 in COS-7 cells for co-immunoprecipitation studies. A T7 epitope was added to the C terminus of PAR4 to facilitate co-immunoprecipitation with anti-T7 agarose beads. PAR4 without a T7-epitope was used as a negative control. Cells expressing PAR1 and PAR4-cT7 were unstimulated or stimulated with 10 nM α-thrombin before lysis. We

were able to detect a specific interaction by co-immunoprecipitation with and without stimulation by α-thrombin (Fig. 2.7). To reliably detect the interaction with the co-immunoprecipitation experiments, a 10-fold higher expression of PAR1 and PAR4 was required than for the BRET experiments. This may have contributed to the interactions in the unstimulated cells. Finally, the PAR4 lacking the T7 epitope also failed to co-immunoprecipitate PAR1, indicating that PAR1 was not binding to the T7-agarose non-specifically.

In human platelets PAR1 serves as a cofactor for cleavage and activation of PAR4 at low thrombin concentrations (≤10 nM) (16, 17). In the previous studies we showed that PAR1 lowered the EC50 of PAR4 cleavage by α-thrombin 6-fold when coexpressed on HeLa cells [165]. Therefore, we wanted to determine if PAR1-PAR4 heterodimers were required for PAR1-assisted PAR4 cleavage. To mimic the conditions that were used in the BRET assays, COS-7 cells expressing PAR4 alone or with PAR1 were treated with 10 nM α-thrombin. Consistent with previous studies, PAR4 was not efficiently cleaved with 10 nM α-thrombin when expressed on cells alone (Fig. 2.8A, open circles). Coexpression of PAR1 increased the rate of cleavage (Fig. 2.8A, black circles). The rate constant (k) for PAR4 alone (0.006 ± 0.001) was 2.3-fold greater in the presence of PAR1 (0.014 ± 0.007 $p = 0.03$) (Table 2.3). Mutations in transmembrane helix 4 of PAR1 that disrupt PAR1-PAR4 heterodimers did not enhance PAR4 cleavage (Fig. 2.8A, gray circles and Table 2.3). Quantitative flow cytometry was used to ensure that the initial PAR4 expression was the same in each of the experiments (Fig. 2.8E, black bars). The initial expression of PAR1 and PAR1-W227A/I231A was also verified by flow

cytometry (Fig. 2.8D, black bars). Disrupting PAR1-PAR4 heterodimers with PAR4 mutations also abolished PAR1-assisted PAR4 cleavage (Fig. 2.8B). Coexpression of PAR1 did not influence the expression of PAR4-TM4-4A (Fig. 2.8E, dark gray bars). PAR1 was deliberately expressed at higher levels to confirm that the failure to increase the rate of PAR4 cleavage was not due to low expression of PAR1 (Fig. 2.8E, gray bars). Finally, we verified that PAR4-TM4-4A did not have intrinsic properties that made it less efficiently cleaved than PAR4 by increasing the α-thrombin concentration to 100 nM (Fig. 2.8C and Table 2.3). The disappearance of the V5 epitope was not due to internalization as PAR4-R47Q remained on the surface after stimulation with 100 nM α-thrombin (data no shown). Taken together, these data suggest that PAR1-PAR4 heterodimers are required for PAR1-assisted cleavage of PAR4.

2.5 Discussion

The current report shows that PAR1 and PAR4 form heterodimers that are modulated by α-thrombin. In contrast, the PAR1 and PAR4 activation peptides, TFLLRN and AYPGKP, respectively, were unable to induce heterodimers. We also show that cleavage-deficient mutants of PAR1 or PAR4 do not form heterodimers when stimulated with α-thrombin, confirming the requirement of receptor cleavage for heterodimerization. Additional experiments mapped the PAR1-PAR4 heterodimer interface to four residues in TM4 of both PAR1 and PAR4. Finally, mutations that disrupt PAR1-PAR4 heterodimers also disrupt PAR1-assisted cleavage of PAR4 by α-thrombin. Taken together, our studies have defined the PAR1-PAR4 heterodimer and have linked these physical interactions to enhanced PAR4 cleavage by PAR1.

Our studies show that thrombin induces PAR1-PAR4 heterodimers with BRET. We have focused on BRET because it allows us to examine the PAR1-PAR4 interactions in living cells at near physiologic levels of expression (Figs. 2.4 and 2.5). Importantly, the levels of expression required for the BRET studies were sufficient to detect an enhanced rate of cleavage of PAR4 by PAR1 (Fig. 2.8). We were also able to show the PAR1-PAR4 interactions with co-immunoprecipitation experiments (Fig. 2.7), which agree with Leger et al. [184]. However, we interpret our co-immunoprecipitation experiments with caution because the level of expression required for us to reliably detect PAR1 and PAR4 interactions with this technique was 10-fold higher than required for the BRET and cleavage studies. Our interpretation is that at high expression levels, PAR1 and PAR4 can specifically interact in a thrombin-independent manner. Leger et al. [184] also showed PAR1 and PAR4 co-immunoprecipitation from human platelets that were stimulated with thrombin, which are in agreement with our BRET studies. However, we have not been able to co-immunoprecipitate PAR1 and PAR4 from human platelets using the antibodies available to us.

The heterodimerization is specific to α-thrombin. This suggests that PAR1 and PAR4 undergo specific allosteric rearrangement when stimulated with thrombin that is distinct from the activation peptides. This may be due to the conformational changes that must occur for the tethered ligand to activate the receptor after cleavage. The movement of the N terminus likely causes long-range conformational changes through the receptor that would not be required when the receptors are stimulated by the peptides that activate

PAR1 and PAR4 independently of receptor cleavage. An alternative explanation is that PAR1 and PAR4 form constitutive heterodimers and cleavage of the receptors results in the rearrangement of the C termini, which facilitates the detection of the BRET signal. The evidence against this interpretation is mutations that disrupt dimerization also disrupt PAR-1-assisted PAR4 cleavage. This will best be addressed by high resolution time-resolved imaging techniques that are currently being developed [212]. A third possibility is that α-thrombin mediated the interaction by forming a trimolecular complex with PAR1 and PAR4. Our data in which α-thrombin pretreated with hirugen does not induce PAR1-PAR4 heterodimers suggests that the induction of PAR1-PAR4 heterodimers may be an exosite I-driven process (Fig. 2.2D). However, blocking exosite I also prevented cleavage of PAR1 and PAR4, which makes it difficult to separate the role of thrombin exosite I in efficient PAR1 cleavage and the potential cross-linking of PAR1 and PAR4. Finally, PAR1 and PAR4 may be differentially localized in the plasma membrane regions such as lipid rafts. Activation of the receptors may alter the interactions that PAR1 and PAR4 have with the membrane such that they are then able to interact with one another. Future studies will need to focus on the lipid environment and how it influences the protein-protein interactions.

There are many studies that have examined the arrangement of GPCRs in the membranes of cells and synthetic membranes [213-216]. From these studies there is compelling evidence for both monomeric and dimeric/oligomeric receptors having functional significance. Recent studies using a minimal system of purified proteins and high density lipoprotein discs show that rhodopsin and β2-adrenergic receptors can functional as

monomers [213, 214]. For example, Whorton et al. [213] demonstrated that the monomeric β2-adrenergic receptor was able to mediate agonist-dependent nucleotide exchange from the Gs heterotrimeric G-protein. However, recent studies by Jastrzebska et al. [217, 218] demonstrated that bovine rhodopsin purified from native tissues is functional as a heteropentamer existing of two receptors in complex with a heterotrimeric G-protein. There is also structural evidence for GPCRs existing as dimers [219, 220]. Recently, a crystal structure of PAR1 bound to vorapaxar was solved [134]. The structure provides key details of the vorapaxar binding site on PAR1. However, the structural changes that occur upon PAR1 cleavage by thrombin are still unknown. Furthermore, the influence of other membrane proteins, such as PAR4, are also unknown.

Many GPCR dimers are noncovalent, and the receptors are in equilibrium between monomers and dimers. An elegant study by Kasai et al. [221] has determined the two-dimensional KD of the monomer to dimer transition for the N-formyl peptide receptor. In this study using single molecule fluorescence the authors determined that N-formyl peptide receptor monomers convert to dimers every 150 ms and the dimers dissociate to monomers every 91 ms with an overall average of 41% of the receptors in a dimer at any given time. These studies highlight the dynamic nature of membrane receptor dimers. Our results show that PAR1-PAR4 heterodimers are also dynamic in nature and can be induced by α-thrombin (Fig. 2.1). In contrast, PAR1 and PAR4 homodimers were not affected by stimulation with α-thrombin (Fig. 2.3). The question remains whether PAR1 and PAR4 form dimers or oligomers. Our studies map the heterodimer interface to TM4; the same region that we have determined as the PAR4 homodimer interface [183].

Therefore, our data suggest that PAR1 and PAR4 are in equilibrium between monomers and homodimers, and stimulating with α-thrombin induces the PAR1 and PAR4 monomers to form heterodimers. The current study describes the conditions in which PAR1-PAR4 heterodimers efficiently form the interaction interface. These data will be essential for the development of quantitative studies to examine the stability of the homodimers compared with the heterodimers. An alternative hypothesis is that PAR1 homodimers may interact with PAR4 homodimers to form higher order oligomers as has been described for other GPCRs [212].

The molecular arrangement of GPCRs on the cell surface has been studied for several receptors [216, 222]. The specific region that is involved in the dimer interface varies, but there are common themes that emerge. TM4 is a common interface for GPCRs to interact with one another [183, 211, 223, 224]. Our recent studies have mapped the homodimer interface for PAR4 to a region on TM4 [183]. Mutating Leu-2094.58 and Leu-2134.62 to alanine reduced PAR4 homodimer formation. Furthermore, mutating Leu-1924.41, Leu-1944.43, Met-1984.47, and Leu-2024.51 to alanine completely disrupted the formation of PAR4 homodimers. In these studies, mutating single amino acids was not sufficient to disrupt PAR4 homodimers. A molecular model of PAR4 has this series of residues directed away from the body of the receptor and potentially available to mediate receptor dimers. We examined if these residues with outward facing side chains in TM4 of PAR4 had a role in mediating PAR1-PAR4 heterodimers (Fig. 2.4A). In contrast to PAR4 homodimers, mutating Leu-2094.54 and Leu-2134.62 did not disrupt PAR1-PAR4 heterodimer formation in response to 10 nM α-thrombin (Fig. 2.4C). However, mutating

Leu-1924.41, Leu-1944.43, Met-1984.47, and Leu-2024.51 to alanine dramatically reduced the ability of PAR1 and PAR4 to interact in response to α-thrombin (Fig. 2.4D). These four residues are located near the cytoplasmic side to TM4 (Fig. 2.4A) and are also at the PAR4 homodimer interface [183]. Importantly, each of our mutants that disrupts heterodimer formation is expressed on the cell surface (Figs. 2.4B and 2.5B) and is capable of mediated Ca2+ mobilization (Fig. 2.6). The dopamine D2 receptor and α1β-adrenoreceptor have been reported to form dimers/oligomers using residues in TM1 and TM4 [210, 211]. In our studies, mutating conserved residues in TM1 of PAR4 did not disrupt the formation of PAR1-PAR4 heterodimers (Fig. 2.4E). The residues in PAR1 that mediate the PAR1-PAR4 heterodimer are also in TM4 (Fig. 2.5). These residues are also found near the cytoplasmic side of TM4 and align with the critical residues identified in TM4 of PAR4. In summary, our data suggest that PAR1-PAR4 heterodimer are arranged in the membrane at a TM4-TM4 interface.

There are several GPCRs that have important signaling functions in platelets. We have described the dynamics of PAR1 and PAR4 heterodimers and have mapped the region for the interactions. Importantly, we have linked heterodimerization to PAR1-assisted PAR4 cleavage. These data are in agreement with earlier studies by Nakanishi-Matsui et al. [162] that demonstrated that the exodomain of PAR1 was not able to enhance PAR4 cleavage when fused to CD8 as it is unlikely that the PAR1-CD8 chimera is interacting with PAR4. PAR3 is well known to be a required cofactor of PAR4 activation on mouse platelets. We have recently shown that mouse PAR3 and mouse PAR4 form constitutive heterodimers and PAR3 negatively influences PAR4 signaling [199]. Previous studies by

Covic et al. [178] demonstrated that sequential activation of PAR1 and PAR4 on human platelets results in an increase in ADP response, which is dependent on PAR4. The sequential activation of PAR1 and PAR4 by thrombin may allow the receptors to rearrange in the platelet membrane and alter the signaling response. A recent study by Li et al. [189] described how PAR4 cooperates with the ADP receptor, P2Y12. In these studies platelets from arrestin-2-deficient mice had a reduction in Akt phosphorylation and fibrinogen binding in response to PAR4 activation. Li et al. [189] also showed that PAR4 physically interacts with the P2Y12 receptor in an agonist-dependent manner and may recruit arrestin-2 to PAR4. There is a complex arrangement of receptors and signaling molecules at the platelet surface in which PAR4 appears to be a common player. Future studies will need to examine how these and other GPCRs interact on platelets to mediate their full range of signaling in vivo.

The current data show that the induction of heterodimers is specific to α-thrombin. PAR1 and PAR4 both have distinct roles in platelet signaling. A recent Phase III clinical trial with the PAR1 antagonist vorapaxar that did not meet its primary end point underscores the need to fully understand the interactions between platelet receptors and how these interactions influence receptor function [136]. Future studies will need to generate models that can differentiate between heterodimer and homodimer signaling in platelets. The current work provides a framework for building platelet-specific models to examine the dynamics and signaling consequences of these interactions. In addition, understanding the molecular arrangement of PAR1 and PAR4 will provide insight for the development of antiplatelet therapies.

2.6 Effort

As a secondary author on this paper, "Protease-activated receptor 1 (PAR1) and PAR4 heterodimers are required for PAR1-enhanced cleavage of PAR4 by α-thrombin", published in JBC on November 2013, I contributed to the completion of this manuscript. HA-PAR1 wild type, HA-PAR1-W227A/I231A, V5-PAR4-wt, and V5-PAR4-TM4-4A were cloned and inserted into pEF1α-IRES-neo or pIRES-puro for the co-immunopreciptation, immunoblotting, cleavage assay, and calcium mobilization studies. HeLa cells were transfected with HA-PAR1-pEF1, HA-PAR1-W227A/I231A-pEF1, V5-PAR4-pIRES, or V5-PAR4-TM4-4A-pIRES, to generate stable clones used for the calcium mobilization studies. I performed the calcium mobilization studies and analyzed the data to determine the concentrations of calcium mobilized over time which were vital to answering reviewer comments and were included in the manuscript (Fig. 2.6). I also determined the surface expression of HA-PAR1, HA-PAR1-W227A/I231, V5-PAR4, and V5-PAR4-TM4-4A on the HeLa cells used for the calcium mobilization studies (Fig. 2.6). In addition, I contributed to writing a section of the manuscript, aided in answering reviewer comments, and helped with editing the document.

Table 2.1: PAR1 and PAR4 transmembrane point mutations. Sequences are shown with standard one-letter abbreviations. Wild type sequences are shown in plain font. Mutated residues are shown in bold font and underlined.

Table 2.1: PAR1 and PAR4 transmembrane point mutations.

Mutant	Sequence
	TM4
PAR1-wt	…GRASFTCLAIWALAIAGVVPLLL…
PAR1-V235A/L239A	…GRASFTCLAIWALAIAGV**A**PLL**A**…
PAR1-W227A/I231A	…GRASFTCLAI**A**ALA**A**AGVVPLLL…
PAR1-TM4-4A	…GRAS**A**TC**A**AI**A**ALA**A**AGVVPLLL…
	TM4
PAR4-wt	…RLALGLCMAAWLMAAALALPLTL…
PAR4-TM4-2A*	…RLALGLCMAAWLMAAALA**A**PLT**A**…
PAR4-TM4-4A*	…R**A**A**A**GLC**A**AAW**A**MAAALALPLTL…
	TM1
PAR4-wt	…RLVPALYGLVLVVGLPANGLALWVLAT…
PAR4-TM1-4A	…R**AA**PA**A**YG**A**VLVVGLPANGLALWVLAT…

Table 2.2: $BRET_{50}$ and $BRET_{max}$ values for PAR1-PAR4 heterodimers. PAR4-GFP and PAR1-Luc were stimulated with the indicated agonist for 10 min and examined in BRET assays. The data were fit to a hyperbolic curve, and the BRET50 and BRETmax for each pair were calculated. Nonspecific interactions are indicated as linear. Values are compared to PAR1-rLuc/PAR4-GFP and PAR4-rLuc/PAR1-GFP interactions with an F-test as described under "Experimental Procedures."

Table 2.2: $BRET_{50}$ and $BRET_{max}$ values for PAR1-PAR4 heterodimers.

rLuc (donor)	GFP (acceptor)	10 nM IIa	$BRET_{50}$	$BRET_{max}$
Heterodimers				
PAR4	PAR1	−	Linear	Linear
PAR4	PAR1	+	0.077 ± 0.03	0.17 ± 0.01
PAR1	PAR4	−	Linear	Linear
PAR1	PAR4	+	0.126 ± 0.08	0.20 ± 0.04
Homodimers				
PAR1	PAR1	−	0.118 ± 0.07	0.57 ± 0.10
PAR1	PAR1	+	0.159 ± 0.07	0.52 ± 0.15
PAR4	PAR4	−	0.021 ± 0.01[a]	0.26 ± 0.04
PAR4	PAR4	+	0.013 ± 0.01[a]	0.29 ± 0.06
PAR4 mutants				
PAR1	PAR4-TM4-2A	+	0.057 ± 0.023	0.21 ± 0.02
PAR1	PAR4-TM4-4A	+	Linear	Linear
PAR1	PAR4-TM1-4A	+	0.045 ± 0.040	0.17 ± 0.03
PAR1 mutants				
PAR1-227/231	PAR4	+	Linear	Linear
PAR1-235/239	PAR4	+	0.034 ± 0.024	0.42 ± 0.10
PAR1-TM4-4A	PAR4	+	Linear	Linear

[a] Statistically different values are indicated ($p \leq 0.05$).

Table 2.3: Rate of PAR4 cleavage on cells. The rate of PAR4 cleavage by 10 or 100 nM α-thrombin was determined with COS7 cells expressing V5-PAR4 or V5-PAR4-TM4-4A by measuring the disappearance of an N-terminal V5 epitope. The influence of PAR1 was determined by co-expressing PAR1 or PAR1-W227A/I231A.

Table 2.3: Rate of PAR4 cleavage on cells.

		Rate constant	
		10 nM IIa	100 nM IIa
		k	
PAR4		0.006 ± 0.001	1.07 ± 0.71
PAR4	PAR1	0.014 ± 0.007[a]	
PAR4	PAR1-W227A/I231A	0.006 ± 0.005	
PAR4-TM4-4A		0.007 ± 0.003	1.04 ± 0.41
PAR4-TM4-4A	PAR1	0.007 ± 0.0003	

[a] The rates constants were compared using a t test and were considered statistically different from PAR4 alone at $p < 0.05$.

Figure 2.1: Thrombin modulates PAR1-PAR4 heterodimer formation. HEK293 cells were transfected with HA-PAR4-rLuc (0.03 μg) and V5-PAR1-GFP (0–2.5 μg) (A), HA-PAR1-rLuc (0.5 μg) and V5-PAR4-GFP (0–0.25 μg) (B), or HA-PAR1-rLuc (0.5 μg) and rhodopsin-GFP (0–1.5 μg) (C). Forty-eight hours post-transfection, the cells were unstimulated (solid circles) or treated with α-thrombin (10 nM) for 10 min (open circles). The cells were analyzed for GFP expression, luciferase activity, and BRET. The data are from three independent experiments in which all points were analyzed by global fit to hyperbolic or linear curve.

Figure 2.1: Thrombin modulates PAR1-PAR4 heterodimer formation.

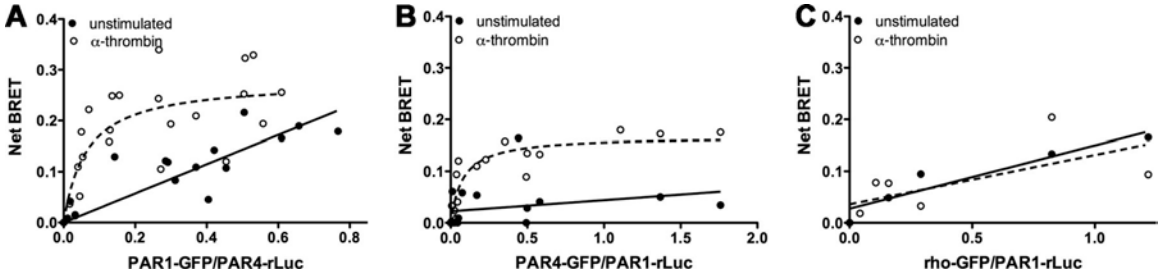

Figure 2.2: PAR1 and PAR4 cleavage by thrombin is required to modulate dimerization. (A) BRET assays were performed in HEK293 cells expressing HA-PAR1-rLuc (0.5 μg) and V5-PAR4-GFP (0–0.25 μg) after stimulation with TFLLRN (50 μM) and AYPGKF (500 μM) simultaneously for 10 min. HA-PAR4-rLuc (0.03 μg) and V5-PAR1-R41A-GFP (0–2.5 μg) (B) and HA-PAR4-R47Q-Luc (0.03 μg) and V5-PAR1-GFP (0–0.5 μg) (C) were analyzed by BRET assays after treatment with α-thrombin (10 nM) for 10 min. (D) BRET assays were performed in cells expressing HA-PAR1-rLuc and V5-PAR4-GFP stimulated with α-thrombin (10 nM) pretreated with hirugen (10 μM). For all BRET assays, GFP expression and luciferase activity were determined to calculate the GFP/rLuc ratio. The data are from three independent experiments in which all points were analyzed by global fit to hyperbolic or linear curve. E, the cleavage of HA-PAR1-rLuc or V5-PAR4-GFP by 10 nM α-thrombin pretreated with hirugen was analyzed by flow cytometry; error bars indicate S.D. of three independent experiments.

Figure 2.2: PAR1 and PAR4 cleavage by thrombin is required to modulate dimerization.

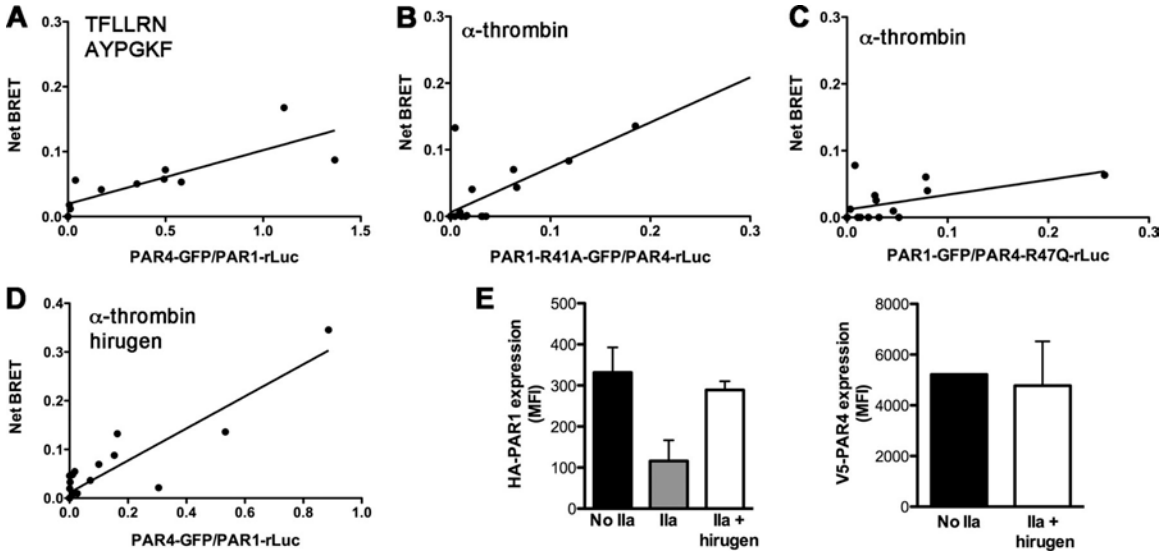

Figure 2.3: Thrombin does not modulate PAR1 or PAR4 homodimers. HEK293 cells were transfected with HA-PAR1-Luc (0.5 μg) and V5-PAR1-GFP (0–2.5 μg) (A) or HA-PAR4-Luc (0.03 μg) and V5-PAR4-GFP (0–0.24 μg) (B). Forty-eight hours post-transfection, the cells were unstimulated or treated with α-thrombin (10 nM) and analyzed for GFP expression, luciferase activity, and BRET. The data are from three independent experiments in which all points were analyzed by global fit to hyperbolic or linear curve.

Figure 2.3: Thrombin does not modulate PAR1 or PAR4 homodimers.

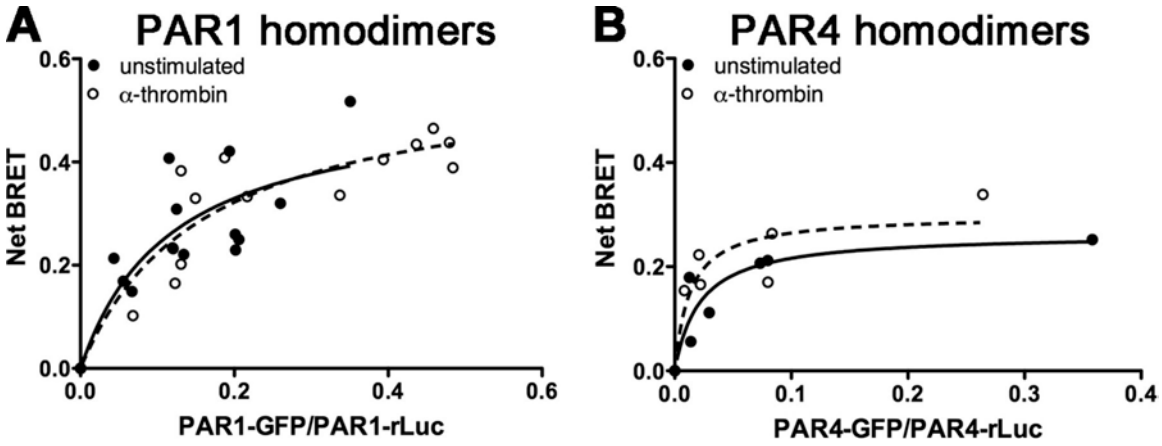

Figure 2.4: Residues in transmembrane helix 4 of PAR4 mediate interaction with PAR1. (A) Structural model of PAR4 based on rhodopsin generated with Swiss Modeler. TM1 is indicated in red, and TM4 is in blue. Residues that were analyzed in this study are shown as sticks. The residues in which alanine substitution disrupted α-thrombin-induced heterodimerization are shown in orange. The nomenclature is that of Ballesteros and Weinstein (27). (B) The expression of PAR4 wild type and mutants in HEK293 was analyzed by flow cytometry with an anti-V5 antibody. (C–E) BRET assays were performed in HEK293 cells expressing HA-PAR1-rLuc (0.5 μg) and V5-PAR4-TM4-2A-GFP (C), V5-PAR4-TM4-4A -GFP (D), or V5-PAR4-TM1-4M-GFP (0–0.25 μg) (E). Forty-eight hours post-transfection, the cells were treated with α-thrombin (10 nM) for 10 min and analyzed for GFP expression, luciferase activity, and BRET. The data are from three independent experiments in which all points were analyzed by global fit to hyperbolic or linear curve.

Figure 2.4: Residues in transmembrane helix 4 of PAR4 mediate interaction with PAR1.

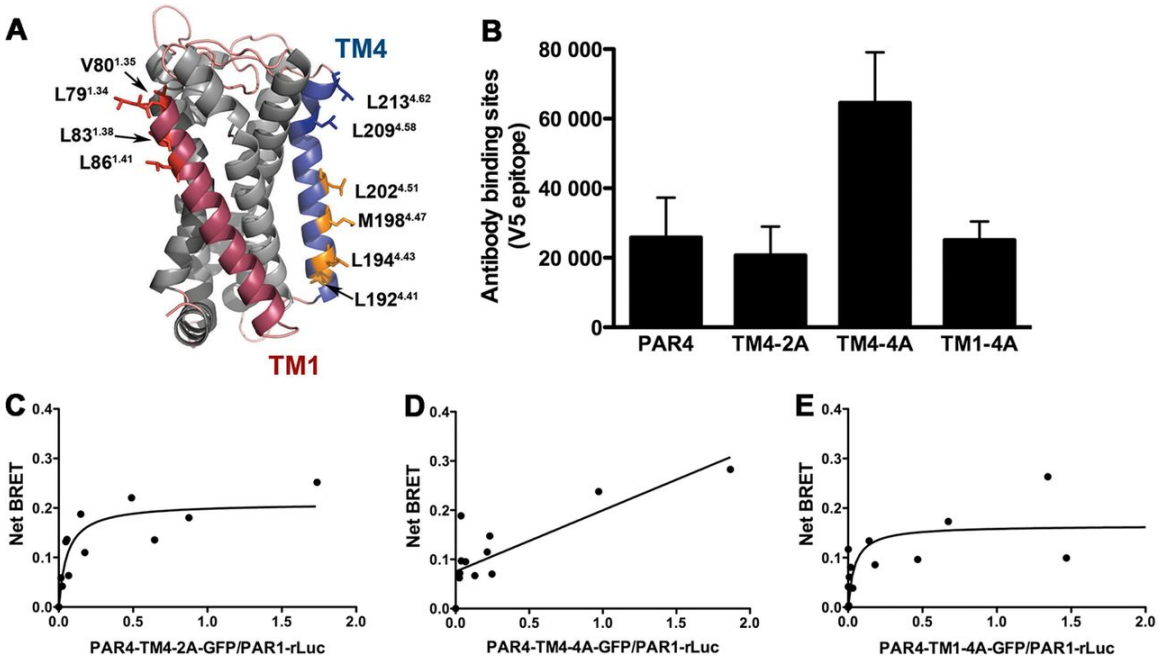

Figure 2.5: Residues in transmembrane helix 4 of PAR1 mediate interaction with PAR4. (A) Structural model of PAR1 based on rhodopsin generated with Swiss Modeler. TM1 is indicated in red, and TM4 is in blue. Residues that were analyzed in this study are shown as sticks. The residues in which alanine substitution disrupted α-thrombin-induced heterodimerization are shown in orange. The nomenclature is that of Ballesteros and Weinstein (27). (B) The expression of PAR1 wild type and mutants in HEK293 was analyzed by flow cytometry with an anti-HA antibody. (C–E) BRET assays were performed in HEK293 cells expressing V5-PAR4-GFP (0-.24 μg) and HA-PAR1-V235A/L239A-rLuc (C), HA-PAR1-W227A/I231A-rLuc (D), or HA-PAR1-TM4-4A-rLuc (0.5 μg) (E). Forty-eight hours post-transfection the cells were treated with α-thrombin (10 nM) for 10 min and analyzed for GFP expression, luciferase activity, and BRET. The data are from two or three independent experiments in which all points were analyzed by global fit to hyperbolic or linear curve.

Figure 2.5: Residues in transmembrane helix 4 of PAR1 mediate interaction with PAR4.

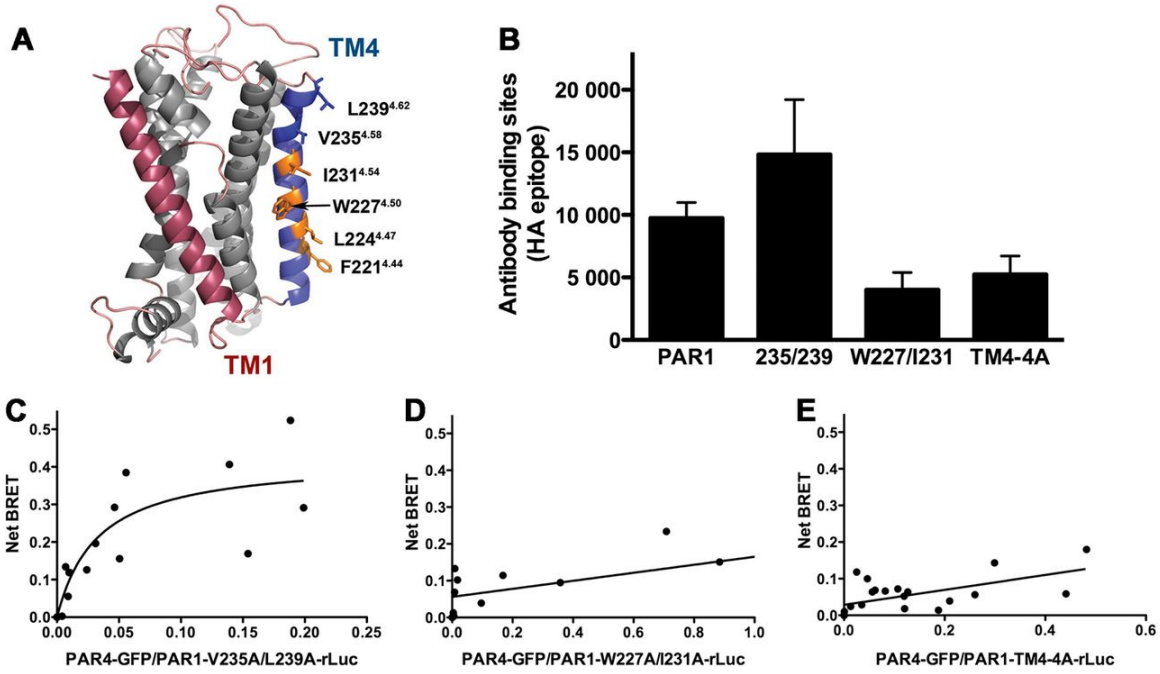

Figure 2.6: Thrombin-mediated intracellular calcium mobilization. HeLa cells expressing V5-PAR4 (black line) or V5-PAR4-TM4-4A (gray line) were loaded with Fura-2 in HEPES-Tyrode buffer, pH 7.4, containing 2 mM CaCl2 (A). Calcium mobilization was measured over time in response to 30 nM α-thrombin (indicated by the arrow) (A). The surface expression of V5-PAR4 or V5-PAR4-TM4-4A in the HeLa cells was determined by flow cytometry with a V5 tag antibody conjugated to AlexaFluor 647 (B). Calcium mobilization was determined in HeLa cells expressing HA-PAR1 (black line), HA-PAR1-W227A/I231A (gray line), or parental HeLa cells (dashed line) as in panel A (C). MFI, mean fluorescence intensity. The surface expression of HA-PAR1 or HA-PAR1-W227A/I231A was determined by flow cytometry with an HA antibody conjugated to AlexaFluor 647 (D).

Figure 2.6: Thrombin-mediated intracellular calcium mobilization.

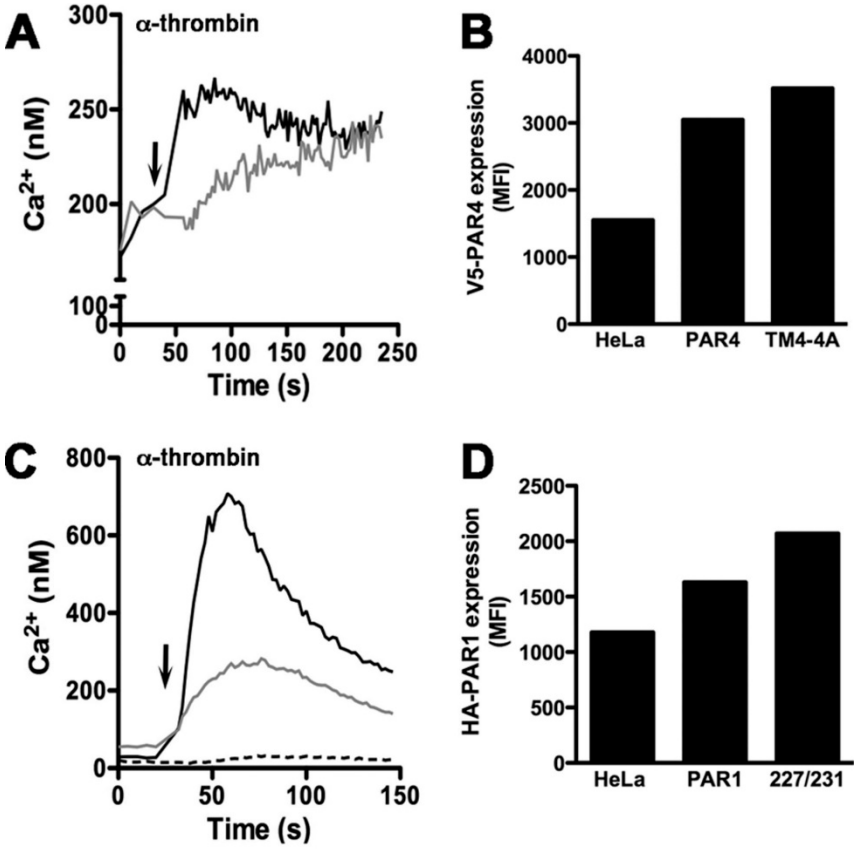

Figure 2.7: PAR1 and PAR4 co-immunoprecipitation studies. COS-7 cells were co-transfected with PAR1 (5 μg) and PAR4-cT7 (2 μg) or with PAR4 (no cT7, 2 μg); cT7 is a C-terminal T7 epitope. Forty-eight hours post transfection, cells were harvested, stimulated with α-thrombin (10 nM), lysed, and incubated with T7-agarose overnight at 4 °C. Co-immunoprecipitations (IP) were separated on SDS-PAGE and immunoblotted with anti-PAR1 or anti-PAR4. The space between lanes indicates samples run on the same gel in non-contiguous lanes, NS is nonstimulated.

Figure 2.7: PAR1 and PAR4 co-immunoprecipitation studies.

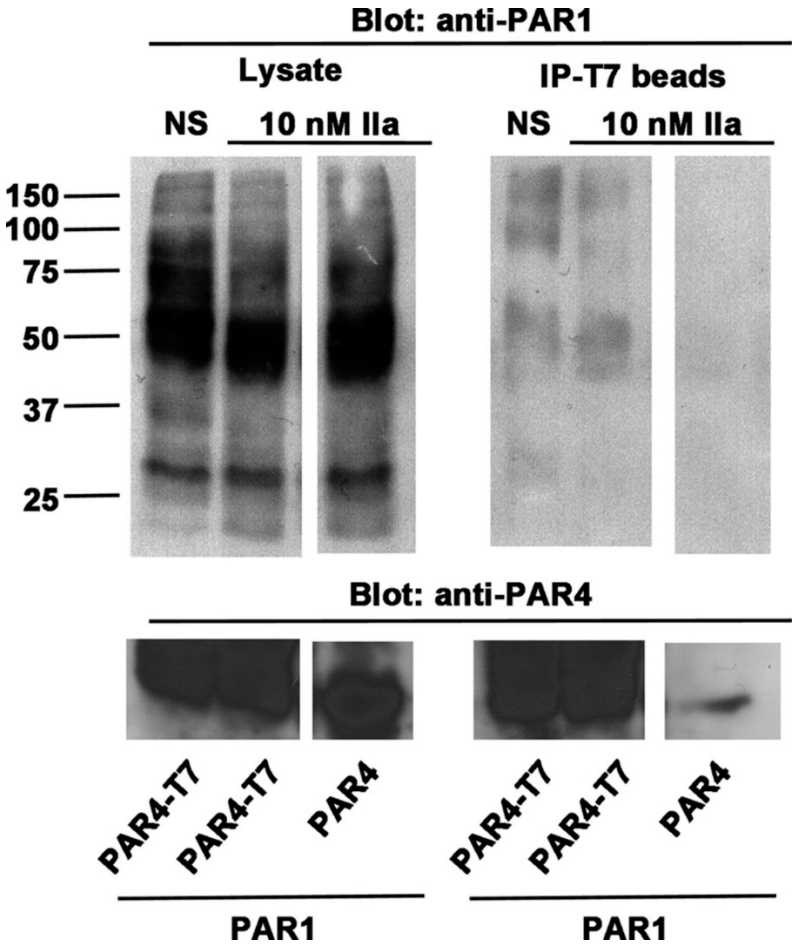

Figure 2.8: Dimerization is required for PAR1-assisted PAR4 cleavage by α-thrombin. V5-PAR4 was expressed on COS-7 cells alone (open circles), with PAR1 (black circles), or with PAR1-W227A/I231A (gray circles). PAR4 cleavage by 10 nM α-thrombin was determined by measuring the loss of the V5 epitope over time by flow cytometry (A). V5-PAR4-TM4-4A was expressed on COS-7 cells alone (open circles) or with PAR1 (black circles), and the loss of the V5-epitope in response to 10 nM α-thrombin was measured over time (B). V5-PAR4 (black circles) or V5-PAR4-TM4-4A (open circles) were expressed on COS-7 cells and treated with 100 nM α-thrombin (C). Quantitative flow cytometry was used to determine the expression of HA-PAR1 (black bar) or HA-PAR1-W227A/I231A (227/231) (dark gray bar) in the presence of V5-PAR4 and HA-PAR1 expression in the presence of V5-PAR4-TM4-4A (P4-4A) (light gray bar) (D). Quantitative flow cytometry to determine V5-PAR4 expression in the absence or presence of PAR1 or PAR1-W227A/I231A (227/231) (black bars) and V5-PAR4-TM4-4A (P4-4A) expression in the absence or presence of PAR1 (gray bars) (E).

Figure 2.8: Dimerization is required for PAR1-assisted PAR4 cleavage by α-thrombin.

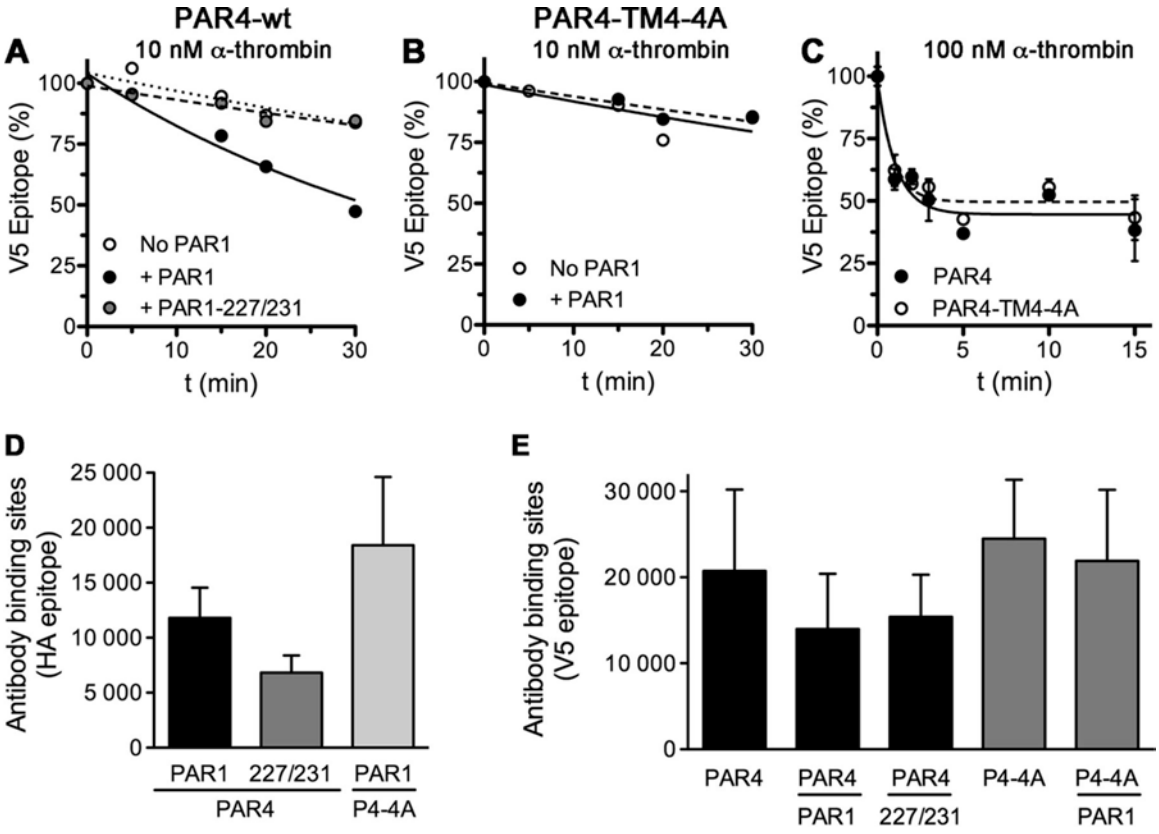

Chapter 3 ‡

Targeting the Anionic Region of Human Protease Activated Receptor 4 (PAR4) Inhibits Platelet Aggregation and Thrombosis without Interfering with Hemostasis.

3.1 Abstract

Background - Human platelet activation and aggregation is a complex process. To date, many therapies have been developed targeting proteins that mediate this process to prevent unwanted activation. However, the current standard of care for acute coronary syndromes still has limitations including bleeding risk.

Objective - The aim of the current study is to evaluate the PAR4 anionic cluster as a viable antiplatelet target using a polyclonal antibody (CAN12).

Methods - We used western blotting, aggregation, and secretion *ex vivo* to evaluate the ability of CAN12 to interact with PAR4 and inhibit platelet activation. The effects of CAN12 *in vivo* were evaluated with the Rose Bengal arterial thrombosis model and two models of hemostasis.

Results - We show that CAN12 is able to interact with human PAR4 and delay PAR4 cleavage. In addition, CAN12 inhibits thrombin induced human platelet aggregation and secretion in a dose dependent manner. We next determined that the specificity of CAN12 is agonist dependent. *In vivo*, we determined that CAN12 is able to inhibit arterial thrombosis and using two independent methods, we found that CAN12 does not influence hemostasis.

‡ A version of this chapter was accepted for publication in the August 2014 issue of the *Journal of Thrombosis and Haemostasis*.

Conclusion - Targeting the extracellular anionic cluster on PAR4 is a viable novel strategy as an antiplatelet therapy.

3.2 Introduction

Protease activated receptors (PARs) are G-protein coupled receptors activated by cleavage of their N-terminus by serine proteases. There are four members of the PAR family: PAR1-4 [225]. PAR1, PAR3, and PAR4 are activated by thrombin, but PAR2 is activated by trypsin [226]. Upon cleavage of the N-terminus, the new N-terminus acts as a tethered ligand for the receptor [54, 227]. PAR activation initiates multiple downstream signaling events in platelets including activation of the small GTPase RhoA, intracellular calcium release, secretion, and a decrease in accumulation of cAMP through G_q, $G_{12/13}$, and G_i [228-232]. The culmination of these events leads to platelet aggregation, and if uncontrollably activated, thrombosis.

The current standard for the treatment of acute coronary syndromes by antiplatelet therapy is dual treatment with aspirin and a thienopyridine [233]. However, the current standard for treatment still has a number of limitations, most significantly, increased bleeding risk [234]. This has led to a need for better antiplatelet therapies. Additional therapies, such as glycoprotein IIb/IIIa and PAR1 inhibitors have been investigated as alternate antiplatelet therapies, but have had limited success [136, 235, 236].

One innovative approach to antiplatelet therapies is targeting PAR4. Specifically, near the anionic cluster on PAR4, D^{57}, D^{59}, E^{62}, and D^{65}, which is C-terminal of the thrombin

cleavage site at R^{47} [164]. The anionic cluster of PAR4 is crucial for thrombin interacting with the purified PAR4 exodomain and PAR4 expressed on cells [165, 204, 237]. The anionic cluster slows the dissociation of PAR4 from thrombin in a way that cleavage can occur [164, 165]. We propose that if this region is blocked so that thrombin cannot as easily bind and cleave PAR4, human platelet aggregation can be delayed. Therefore, the anionic region on PAR4 could be a potential therapeutic target.

The current study examined a novel approach for antiplatelet therapy by targeting PAR4. We developed a goat polyclonal antibody that specifically targets the anionic cluster on PAR4. The antibody dose dependently inhibited thrombin induced human platelet aggregation and secretion. In addition, we demonstrated that the antibody is able to prevent carotid artery thrombosis when administered before or after initiation of an injury. Interestingly, using two independent methods, we demonstrated that treatment with the antibody does not influence hemostasis in mice. This study provides a new antiplatelet therapy target, the anionic region of PAR4, which could be a more efficacious approach for the treatment of acute coronary syndromes without the commonly associated increased bleeding risk.

3.3 Material and Methods

Reagents and Antibodies

All cell culture reagents were purchased from Invitrogen. Human α-thrombin was purchased from Haematological Technologies (specific activity 3200-3400 U/mg) (Essex Junction, VT). PAR4 activating peptide (AYPGKF-NH2) and PAR1 activating peptide

(SFLLRN-NH2) were synthesized at PolyPeptide Laboratories (San Diego, CA). Convulxin was purchased from Enzo Life Sciences Inc. (Farmingdale, NY). Collagen, ADP, and CHRONO-LUME were purchased from Chrono-log Corporation (Havertown, PA). Protease inhibitor cocktail tablets were purchases from Roche. Rose-Bengal sodium salt, fibrinogen from human plasma, red blood cell lysing buffer, and sepharose 2B were purchased from Sigma-Aldrich. The CAN12 antibody was prepared against the human PAR4 sequence (CANDSDTLELPD) by Bethyl Laboratories as a custom synthesis using a goat as the host. The antibody was affinity purified using a CANDSDTLTLPD peptide-specific immunosorbent. For control experiments, ChromPure goat IgG, whole molecule was purchased from Jackson ImmunoResearch Laboratories, Inc. (West Grove, PA). The secondary antibodies IRDYE 800CW donkey anti-mouse IgG, IRDYE 680RD donkey anti-goat IgG, and IR 680RD goat anti-rabbit IgG were purchased from LI-COR Biosciences (Lincoln, NE).

Animals

C57BL/6 mice were purchased from The Jackson Laboratory (Bar Harbor, Maine). F2RL3$^{-/-}$ mice (referred to as PAR4$^{-/-}$) were obtained from the Mutant Mouse Regional Resource Center (MMRRC) (Chapel Hill, NC). All animal studies were approved by the Institutional Animal Care and Use Committee at Case Western Reserve University School of Medicine.

Western blotting

HEK293 cells were purchased from American Type Culture Collection (Bethesda, MD) and were cultured in DMEM supplemented with 10% fetal bovine serum and 1% Pen/Strep. Cells were transfected with Lipofectamine 2000 (Invitrogen) according to manufacturer's instructions. HEK293 cells were transfected with 1 µg mouse PAR4 or human PAR4. After 48hrs, the cells were lysed in RIPA buffer (1% NP-40, 0.5% Deoxycholate, 0.1% SDS) on ice. Following lysis, the lysate was collected and quantitated using the Biorad DC protein assay. 100µg of total protein was loaded and resolved by SDS-PAGE and transferred onto nitrocellulose. The membranes were incubated with primary goat antibody to CAN12. To determine equal protein loading, the membrane was probed with rabbit antibody to α-actinin (1, 1000; Santa Cruz Biotechnology Inc.). The membrane was developed using the Odyssey Infrared Imaging System. The optical densities of proteins in the blot were quantified using software provided with the imaging system (Application Software version 3.0).

For examining the CAN12 binding region of PAR4, HEK293 cells were transfected with 4.0 µg human PAR4 or human PAR4-AAAA (D57A, D59A, E62A, D65A) [165]. The lysis and blotting procedure was the same as above.

Cleavage assays

HEK293 cells were transfected with HA-PAR1 (human) (4.0 µg) and V5-PAR4 (human) (0.1 µg) for 48 hours (described previously [185]). Aliquots containing $1x10^6$ cells were treated with PBS, IgG (2 µg/ml), or CAN12 (2 µg/ml) for 10 min and were activated with thrombin (100 nM) for 0, 2, or 30 min. The cells were then pelleted and lysed in RIPA buffer on ice. Following lysis, the entire sample was resolved by SDS-PAGE and

transferred onto nitrocellulose for Western blotting with anti-V5-tag (1, 10,000; AbD Serotec.) and anti-α-actinin (1, 1000; Santa Cruz Biotechnology Inc.) as described above.

PRP, Gel Filtered Platelets, and Washed Platelets Preparation

Human platelets were obtained from healthy donors. These studies were approved by the Case Western Reserve University Institutional Review Board and informed consent was obtained from all donors. Whole blood was collected into the anticoagulant acid citrate dextrose (ACD) (2.5% sodium citrate, 71.4 mM citric acid, 2% D-glucose) and centrifuged at 200xg for 10 minutes at room temperature. The platelet rich plasma (PRP) was used for aggregation experiments within 3 hours or used to generate gel filtered platelets as previously described [238]. Briefly, platelets were separated from plasma proteins using a sepharose 2B column in HEPES-Tyrode buffer pH 7.4 (10 mM HEPES, 12 mM $NaHCO_3$, 130 mM NaCl, 5 mM KCl, 0.4 mM Na_2HPO_4, 1 mM $MgCl_2$, 5 mM glucose, 0.1% bovine serum albumin). The number of platelets was quantitated using a Hemavet 950FS (Drew Scientific Inc, Waterbury, CT, USA).

Mice were anesthetized by intraperitoneal injection of pentobarbital (62 mg/kg). Blood was collected by heparinized capillary puncture of the retro-orbital venous sinus and immediately combined with ACD (1/5). The whole blood was centrifuged at 2300xg for 20 sec at room temperature to isolate the PRP. To pellet the platelets, the PRP was centrifuged at 2200xg for 3 minutes at room temperature. The platelets were resuspended in HEPES-Tyrode buffer pH 7.4 (10 mM HEPES, 12 mM $NaHCO_3$, 130 mM NaCl, 5 mM KCl, 0.4 mM Na_2HPO_4, 1 mM $MgCl_2$, 5 mM glucose, 0.33% human serum

albumin). The number of platelets was quantitated using a Hemavet 950FS (Drew Scientific Inc, Waterbury, CT, USA).

Aggregation

Aggregation was measured using a lumi-aggregometer (Model 700, Chrono-log Corporation). The sample was stirred constantly at 1200 RPM at 37°C. Dense granule secretion was detected by ATP luminescence using CHROMO-LUME. For all experiments, PRP, gel filtered platelets, or washed platelets were treated with HEPES-Tyrode buffer, IgG (goat), or CAN12 for 10 minutes prior to activation with thrombin, AYPGKF, SFLLRN, ADP, collagen, or convulxin. Aggrolink8 version 1.3.98 was used for data acquisition. The IC_{50} was determined using GraphPad Prism.

Mouse Arterial Thrombosis Studies

The arterial thrombosis experiments were performed using the Rose Bengal carotid artery thrombosis model, as previously described [239]. Saline, IgG (2 mg/kg), or CAN12 (1, 0.5, 0.25, 0.125 mg/kg) was injected by tail vein into C57BL/6 mice 10 minutes before initiation of injury. Alternatively, injury was initiated first and 15 minutes later IgG (2 µg/ml) or CAN12 (0.5 mg/kg) was injected via tail vein. The experiment was terminated at 90 min. After the experiment, blood was collected from the retro-orbital venous sinus and immediately combined with (1/5) volume of ACD as an anticoagulant. The platelets were counted using a Hemavet 950FS.

Mouse Tail Bleeding Assay

C57BL/6 mice were retro-orbitaly injected with IgG (2 mg/kg) or CAN12 (2 mg/kg); untreated PAR4$^{-/-}$ mice were used as a control. Ten minutes following injection, tail bleeding times were measured by clipping 3 mm from the tip of the tail of anesthetized mice. The tail was placed in prewarmed saline at 37°C, and the time to cessation of bleeding was measured or the experiment was terminated at 10 min. The quantity of blood loss was determined by lysing the red blood cells in red blood cell lysing buffer, measuring the absorbance of hemoglobin at 550 nm, and comparing to a standard curve.

Mouse Saphenous Vein Bleeding Assay

The method was modified from the previously described protocol by Buyue *et al.* [240]. Mice were treated as described for tail bleeding assay. The saphenous vein was exposed in the right hind limb and pierced with a 23-G needle. Blood was removed around the site of injury using a Kimwipe. After the formation of a clot (~1.5 min), a 1 mm longitudinal incision was made using the initial site of injury for entry into the vessel. Bleeding was observed for 20 min and each time a subsequent clot formed it was disrupted by stroking a needle across the site of injury in the direction of blood flow. The average bleeding time was calculated by dividing the total bleeding time by the number of clots formed. In addition, the number of clots formed was recorded.

3.4 Results

CAN12 reduces the rate of PAR4 cleavage

The interaction between PAR4 and thrombin is mediated by two sites, the cleavage site (L^{43}PAPR) and an anionic region (D^{57}-D^{65}) [164, 165]. The anionic region has a single

amino acid change between human and mouse PAR4 (CANDSDTLELPD vs. CANDSDTLELPA) suggesting a conserved function. Therefore, we developed a goat polyclonal PAR4 antibody (CAN12) that targets the anionic cluster of PAR4 (Fig. 3.1A) [164]. CAN12 interacted with both human (hPAR4) and mouse PAR4 (mPAR4) in transfected HEK293 cells (Fig. 3.1B, C). To determine if CAN12 was specifically interacting with the anionic region of PAR4, we transfected 293 cells with hPAR4 or hPAR4-AAAA; a construct in which each of the residues in the anionic region is mutated to alanine (D57A, D59A, E62A, D65A). CAN12 did not interact with the mutated anionic region (Fig. 3.1 D). We next determined if CAN12 was able to inhibit PAR4 cleavage by α-thrombin. To mirror the expression profile of PARs in human platelets, HEK293 cells were cotransfected with HA-PAR1 and V5-PAR4 and the cleavage of PAR4 was measured by the disappearance of the N-terminal V5-tag. CAN12 (2 μg/ml) treatment completely inhibited PAR4 cleavage by α-thrombin at 2 min compared to 44.5 ± 6.9% cleavage for the IgG control (2 μg/ml). Thirty minutes after CAN12 treatment, PAR4 cleavage was reduced to 39.4 ± 12.5% compared to 64.5 ± 15.4% for the IgG control (Fig. 3.1E, F). All together these results demonstrate that CAN12 interacts with mPAR4 and hPAR4 at the anionic region and is able to slow the rate of PAR4 cleavage.

The effect of CAN12 treatment on human platelet aggregation and secretion

We next sought to determine if CAN12 is able to inhibit thrombin induced platelet aggregation and secretion. Gel filtered platelets were pretreated with buffer, IgG (2 μg/ml), or CAN12 (0.2 ng/ml-2 μg/ml) for 10 min at 37°C. Platelets were stimulated with a threshold-dose of α-thrombin (0.5 nM) and the percent aggregation was measured.

CAN12 inhibited thrombin induced aggregation in a dose dependent manner with an IC_{50} of 10 ng/ml (2-49 ng/ml, 95% CI) (Fig. 3.2A, B). In contrast, IgG did not influence aggregation at a 200 fold higher concentration. CAN12 also inhibited dense granule secretion as measured by ATP release in a dose dependent manner similar to aggregation (Fig. 3.2C).

We next examined the influence of CAN12 on platelet aggregation and secretion initiated by other agonists (AYPGKF, SFLLRN, ADP, and collagen). PRP was isolated from normal healthy donors and treated with buffer, IgG (2 µg/ml), or CAN12 (0.2 ng/ml-2 µg/ml) for 10 min at 37°C. High doses of CAN12 (0.02-2 µg/ml) inhibited aggregation by the PAR4 agonist peptide, AYPGKF (500 µM), but when the dose was decreased to 2 ng/ml the percent aggregation returned to 100% (Fig. 3.3A). This is likely due to the large antibody molecule sterically blocking access of AYPGKF to the proposed binding site in extracellular loop 2. In contrast, CAN12 had no effect on aggregation of platelets activated with SFLLRN (25 µM) (Fig. 3.3B). CAN12 dose dependently inhibited ADP (5 µM) induced aggregation (Fig. 3.3C). For collagen (1 µg/ml) activated platelets, CAN12 inhibited in a dose dependent manner (Fig. 3.3D). This could be due to PAR4 having a synergistic effect on collagen activation of GPVI [241]. Interestingly, CAN12 had no effect on convulxin induced aggregation of platelets (Fig. 3.3E). Similar to aggregation, CAN12 inhibited dense granule secretion from platelets activated with AYPGKF (500 µM), ADP (5 µM), and collagen (1 µg/ml) (Fig. 3.4 A, C, D). However, CAN12 had no effect on secretion induced by SFLLRN (25 µM) and convulxin (5 nM) (Fig. 3.4 B, E).

CAN12 inhibits aggregation through PAR4

PAR4 and P2Y12 are known to heterodimerize and these interactions influence the function of each receptor [172, 189, 190]. Therefore, we examined if CAN12's influence on ADP-induced aggregation was dependent on PAR4 using platelets isolated from PAR4$^{-/-}$ mice. Washed platelets isolated from wild-type or PAR4$^{-/-}$ mice were pretreated with IgG (2 μg/ml) or CAN12 (2 μg/ml) for 10 min at 37°C. In wild-type mice, AYPGKF-induced (500 μM) platelet aggregation of CAN12 treated platelets was reduced to 9.3% from 37% for the IgG control (Fig. 3.5A). As expected, platelets from PAR4$^{-/-}$ mice did not respond to AYPGKF (Fig. 3.5B). Similarly, CAN12 reduced ADP-induced aggregation of platelets from wild-type mice from 21% to 8.3%. Importantly, ADP-induced aggregation was not influenced in platelets from PAR4$^{-/-}$ mice. CAN12 also appeared to have a slight effect on collagen aggregation; however, the results did not reach statistical significance (Fig. 3.5A). These data are in agreement with data from human platelets in which CAN12 reduced ADP-induced aggregation. Further, these data demonstrate that inhibitory effects of the antibody are dependent on the presence of PAR4.

CAN12 inhibits arterial thrombosis

Since CAN12 is able to interact with murine PAR4 (Fig. 3.1B) and affect mouse platelet activation (Fig. 3.5), our studies determined the ability of CAN12 to affect arterial thrombosis *in vivo* in the Rose Bengal model. The time to thrombosis was delayed to more than 90 minutes when CAN12, 1.0 mg/kg (~14 μg/ml plasma concentration), was

injected 10 minutes prior to injury (Fig. 3.6A). We next wanted to determine the minimal dose of CAN12 required to influence the time to thrombosis. The intermediate doses of 0.5 mg/kg and 0.25 mg/kg had a time to thrombosis of 82 minutes and 60 min, respectively. At 0.125 mg/kg CAN12, the time to occlusion was 37 minutes; the same time as the controls (saline and IgG) (Fig 3.6A). We verified that the delay in thrombosis was not due to a decrease in the platelet number (Fig. 3.6B). Next we investigated whether CAN12 prolonged the time to thrombosis when administered after initiation of the injury. For these studies we used the lowest dose of CAN12 (0.5 mg/kg) that significantly prolonged the time to occlusion (see Fig. 3.6A). CAN12 delivered 15 minutes after injury was able to prolong the time to complete occlusion to 84 minutes (Fig. 3.6C). CAN12 also did not reduce platelet numbers when administered after the injury (Fig. 3.6D). Similarly, there was no difference in platelet number between IgG and CAN12 treatment when injury was not initiated ($425 \times 10^6 \pm 56$ platelets/ml vs. $462 \times 10^6 \pm 90$ platelets/ml, respectively). Overall, CAN12 treatment is able to delay arterial thrombosis when delivered either before or after injury.

CAN12 does not affect bleeding time

Finally, we wanted to examine if CAN12 treatment influences hemostasis using two assays. The first was the tail clip assay. C57BL/6 mice were injected with IgG (2 mg/kg) or a high dose of CAN12 (2 mg/kg) 10 minutes before the procedure. There was no difference in time to cessation of bleeding or total blood loss between IgG or CAN12 treated mice (Fig. 3.7A, B). $PAR4^{-/-}$ mice have a prolonged bleeding phenotype and were used as controls [242]. An alternative method for examining the effect of CAN12 on

hemostasis was the saphenous vein model. CAN12 (2 mg/kg) had no effect on the bleeding time or number of clot formations compared to the IgG (2 mg/kg) control (Fig. 3.7C, D). Similar to the tail clip model, PAR4$^{-/-}$ mice had a prolonged bleeding time and fewer clot formations. Using two independent methods, we demonstrated that CAN12 treatment does not delay hemostasis in mice.

3.5 Discussion

In the current study, we have identified the anionic region of PAR4 as a potential therapeutic target using an inhibitory antibody. The antibody is directed toward the sequence C^{54}ANDSDTLELPD, which has been identified to be important for PAR4's interaction with thrombin using purified exodomains and cell lines [164, 165, 237]. This region is conserved between murine and human PAR4. A co-crystal with a murine PAR4 derived peptide and murine thrombin shows that the anionic region of PAR4 makes direct contact with thrombin's autolysis loop [163]. The antibody CAN12 exploits these interactions to slow the rate of PAR4 cleavage (Fig. 3.1E and F) resulting in a decrease in PAR4 activation. These data are consistent with published results that demonstrate the importance of the anionic region for PAR4 activation by thrombin [164, 165]. By interfering with PAR4 activation, CAN12 inhibits thrombin-induced human platelet aggregation and thrombosis in the Rose Bengal thrombosis mouse model (Fig. 3.2 and 3.6). Importantly, CAN12 does not delay hemostasis in two mouse models. The studies in the current report demonstrate the feasibility of targeting PAR4 in general and, in particular, the anionic region of PAR4's exodomain.

Human platelets express two subtypes of protease activated receptors, PAR1 and PAR4, which mediate thrombin-induced platelet activation [55, 66, 67]. The interaction and subsequent activation of PAR1 and PAR4 by thrombin is mechanistically different. PAR1 contains a hirudin-like sequence that binds exosite I of thrombin, which likely allosterically induces thrombin into the protease conformation [186]. The net effect is efficient activation of PAR1 by low concentrations of thrombin [204, 237]. In contrast, PAR4 relies on an anionic cluster (D^{57}, D^{59}, E^{62}, D^{65}), which slows the rate of thrombin dissociation and prolongs the interaction time between PAR4 and thrombin [164, 165]. However, this region does not interact with thrombin's exosite I and likely does not contribute to thrombin allostery, which leads to inefficient PAR4 activation [66, 67]. However the rate of PAR4 activation is enhanced when it is coexpressed with PAR1 [165, 184, 185]. We have recently demonstrated that PAR1-mediated enhancement of PAR4 cleavage is dependent on PAR1-PAR4 heterodimerization [185]. We have previously shown that the anionic cluster contributes to PAR4's interaction with thrombin both in the presence and absence of PAR1 [165]. Therefore, we targeted this region for developing a PAR4 antagonist. The inhibitory antibody, CAN12, was able to block thrombin-induced human platelet aggregation in a dose-dependent manner (Fig. 3.2). Since PAR1 and PAR4 form homodimers and heterodimers, the antibody, CAN12, is likely blocking PAR1 activation due to the interactions of PAR1 and PAR4 on the platelet surface as CAN12 does not influence PAR1 activation [183-185, 243].

The primary focus of thrombin signaling has been directed at PAR1, which has led to the development of two PAR1 antagonists that have undergone clinical trials with mixed

results. The most recent clinical trial for a PAR1 antagonist, the vorapaxar TRA-CER trial, had to be terminated due to intracranial hemorrhage [136]. PAR4 has received much less attention than PAR1. However, there have been two PAR4 antagonists developed, the small molecule YD-3 and the peptide P4pal-10 [244-247]. CAN12 differs from these antagonists in two ways. First, it targets the extracellular anionic region of PAR4. Second, it does not delay hemostasis in mouse models. This effect is likely due to the fact that CAN12 slows the rate of PAR4 activation rather than completely inhibiting it. In the arterial thrombosis model in which there is a high flow rate in the vessel, the platelets with CAN12 bound will be rapidly cleared from the site of injury containing high thrombin concentrations, thus, reducing PAR4 mediated platelet activation at the site of injury. In contrast, in the tail clip and saphenous vein models both have a lower flow rate. This may allow the platelets with CAN12 bound to remain in proximity of higher thrombin concentrations at the site of injury for a prolonged length of time allowing for PAR4 to be cleaved by thrombin and enable platelet activation. This also explains why the bleeding times of the $PAR4^{-/-}$ mice (with zero PAR4 expression) are significantly prolonged in both hemostasis assays and the CAN12 treated mice are unaffected (Fig. 3.7).

The antibody, CAN12, also affects ADP and collagen-induced human platelet aggregation. The inhibition of ADP induced aggregation is likely through PAR4's direct and indirect interactions with the ADP receptor, P2Y12. PAR4 and P2Y12 physically interact in heterodimeric complexes that directly influence their signaling activities [189, 190]. In addition, the signaling from the two receptors indirectly influences the activity

of one another [172]. CAN12 was able to interfere with collagen-induced aggregation, but did not affect a different GPVI agonist, convulxin (Fig. 3.3). One theory is that CAN12 is indirectly affecting collagen-induced aggregation through inhibition of P2Y12 as previously demonstrated with the P2Y12 antagonist AR-C69931MX, which decreased platelet activation by collagen [248]. A second explanation is that CAN12 may be sterically interfering with the $\alpha_2\beta_1$ integrin since collagen activates both $\alpha_2\beta_1$ integrin and GPVI, whereas convulxin specifically activates GPVI [41, 48, 249, 250]. A third option is the size discrepancy between collagen and convulxin. CAN12 could be blocking the larger collagen molecule (300 KDa) from interacting with its receptor, but the smaller convulxin (72 KDa) can still reach its receptor. While each of these theories is possible, the net effect is that targeting the extracellular domain of PAR4 inhibits human platelet aggregation *ex vivo* and thrombosis *in vivo* in mice. Importantly, our experiments with $PAR4^{-/-}$ platelets demonstrate the inhibition of ADP induced aggregation is dependent upon the presence of PAR4. Finally, targeting multiple pathways with a single agent can be beneficial. For example, the FDA approved antiplatelet therapy Ticagralor, a non-competitive P2Y12 antagonist, also influences multiple pathways, which likely contributes to its overall effectiveness [251, 252].

The current study demonstrates that targeting the thrombin-binding site away from the cleavage site on PAR4 is a viable strategy for antiplatelet therapy. These studies provide justification for developing a humanized monoclonal CAN12 antibody, which is currently underway. The current study also justifies targeting PAR4 for antiplatelet therapies in general. To date, PAR4 has been considered a back-up receptor for PAR1

signaling and has been studied less. However, a recent study has shown that black populations have higher levels of microRNA's that are associated with increased PAR4 reactivity; PAR1 was unaffected [192]. In this light, PAR4 may be an attractive target for specific populations. Our studies that identify a novel target region on PAR4 provide insight toward developing future PAR antagonists based on the mechanism of thrombin binding to PAR4.

3.6 Addendum

M. M. Mumaw and M. T. Nieman conceived and designed the experiments. M. M. Mumaw, D. N. Noble, and M. de la Fuente performed the experiments. M. M. Mumaw and M. T. Nieman analyzed the data. M. M. Mumaw and M. T. Nieman wrote the manuscript.

3.7 Acknowledgements

The authors would like to thank Drs. Matthew Bilodeau and Lalitha Nayak for helpful discussions. We also thank Dr. Alvin Schmaier for use of the thrombosis equipment. The work was supported by grants from the American Heart Association (AHA Beginning Grant In Aid, 0865441D) and (AHA Scientist Development Grant, 10SDG2600021), American Society for Hematology (ASH Scholar Award) and the NIH (HL098217) to M.T. Nieman, the Cardiovascular Training Grant 5T32HL105338 (M.M. Mumaw), and CWRU/UH Center for AIDS Research (NIH P30 AI036219).

Figure 3.1: CAN12 reduces the rate of PAR4 cleavage. (A) The N-terminus of PAR4 with C^{54}ANDSDTLELPD (CAN12) and the thrombin cleavage site (*) indicated. **(B)** HEK293 cells (293) or cells transfected with mouse PAR4 (1.0 µg) or human PAR4 (1.0 µg) blotted with CAN12 (1:100) and actinin (1:1000). **(C)** Full gel for CAN12 interacting with hPAR4 expressed in HEK293 cells. **(D)** HEK293 cells (293) or cells transfected with hPAR4 (4.0 µg) or hPAR4-AAAA (D57A, D59A, E62A, D65A) (4.0 µg) blotted with CAN12, PAR4 (C-10), and actinin. **(E)** HEK293 cells transfected with HA-hPAR1 (4.0 µg) and V5-hPAR4 (0.1 µg) pretreated with buffer (PAR1PAR4), IgG (2 µg/ml), or CAN12 (2 µg/ml) for 10 min at room temperature. The cells were then activated with thrombin (100nM) for 0, 2, or 30 min at 37°C. Cleavage of PAR4 was measured by loss of the N-terminal V5 epitope. **(F)** Quantitation of percent of uncleaved PAR4 compared to 0 min as 100%. n=4 **p<0.01 vs. time zero

Figure 3.1: CAN12 reduces the rate of PAR4 cleavage.

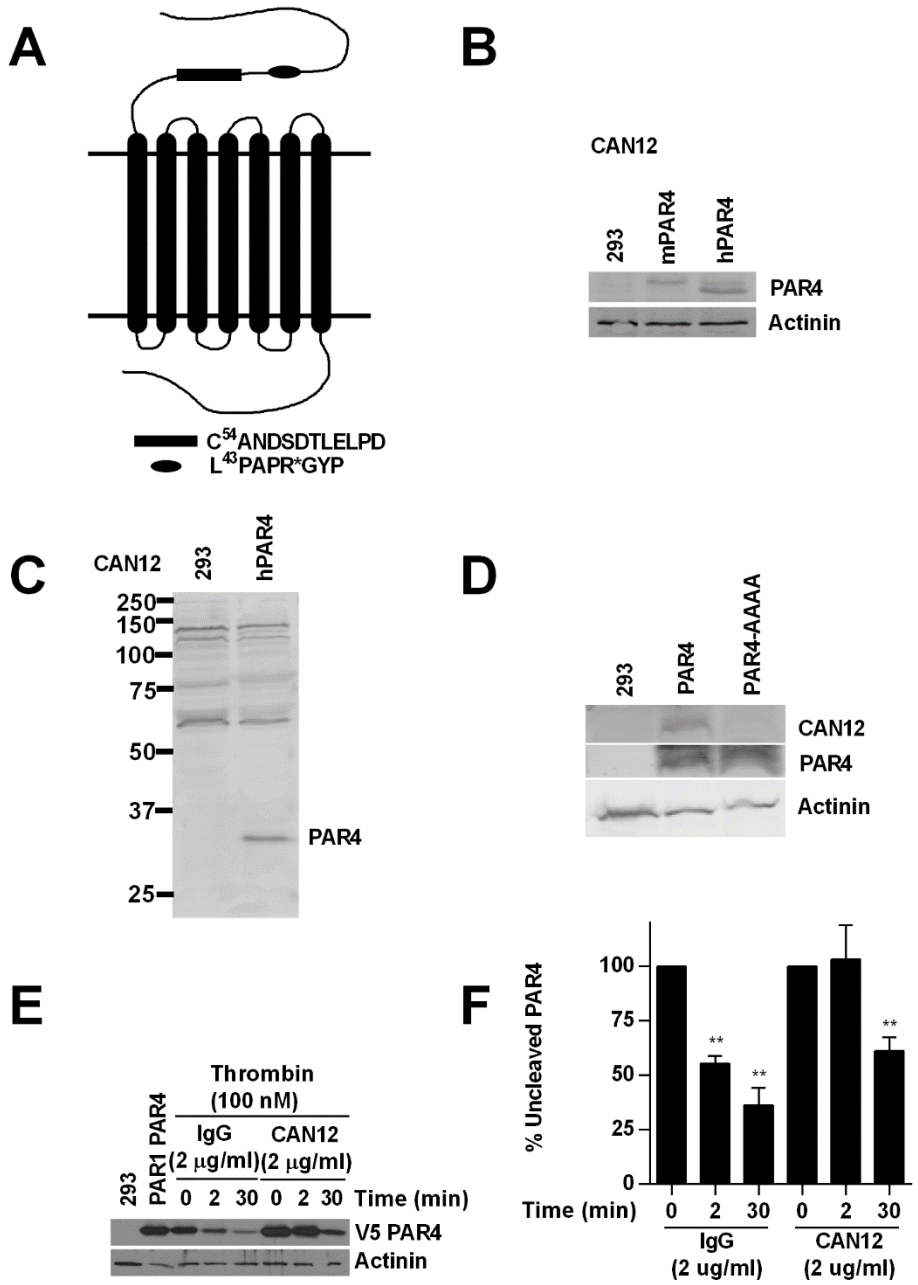

Figure 3.2: CAN12 inhibits thrombin induced aggregation and dense granule secretion. (A) Gel filtered platelets were isolated from healthy donors. Following treatment with goat IgG (2.0 µg/ml) or CAN12 (0.2 ng/ml – 2.0 µg/ml) for 10 min at 37°C, percent aggregation was determined for thrombin (0.5 nM). Representative curves shown. **(B)** Dose response curve for CAN12 inhibition of thrombin induced aggregation (0.5 nM). IC_{50}=10 ng/ml (2-49 ng/ml, 95% CI) **(C)** Dense granule secretion as determined by ATP (nM). *p<0.05 vs. IgG, NS=not significant

Figure 3.2: CAN12 inhibits thrombin induced aggregation and dense granule secretion.

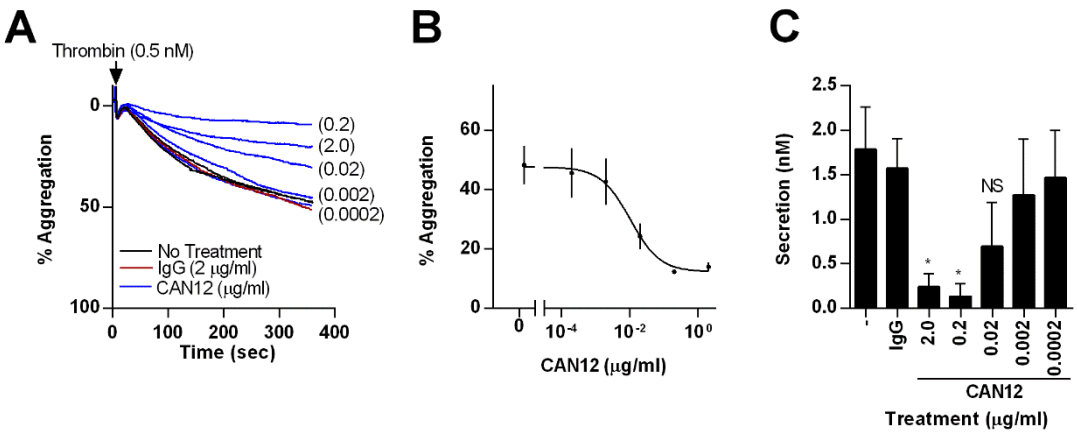

Figure 3.3: CAN12 specificity on aggregation. PRP was isolated from healthy donors. Following treatment with goat IgG (2.0 µg/ml) or CAN12 (dose response) for 10 min at 37°C, percent aggregation was determined for **(A)** AYPGKF (500 µM), **(B)** SFLLRN (25 µM), **(C)** ADP (5 µM), **(D)** collagen (1 µg/ml), **(E)** convulxin (5 nM). Representative curves and average percent aggregation shown. *$p<0.05$ vs. IgG, **$p<0.01$ vs. IgG, NS=not significant

Figure 3.3: CAN12 specificity on aggregation.

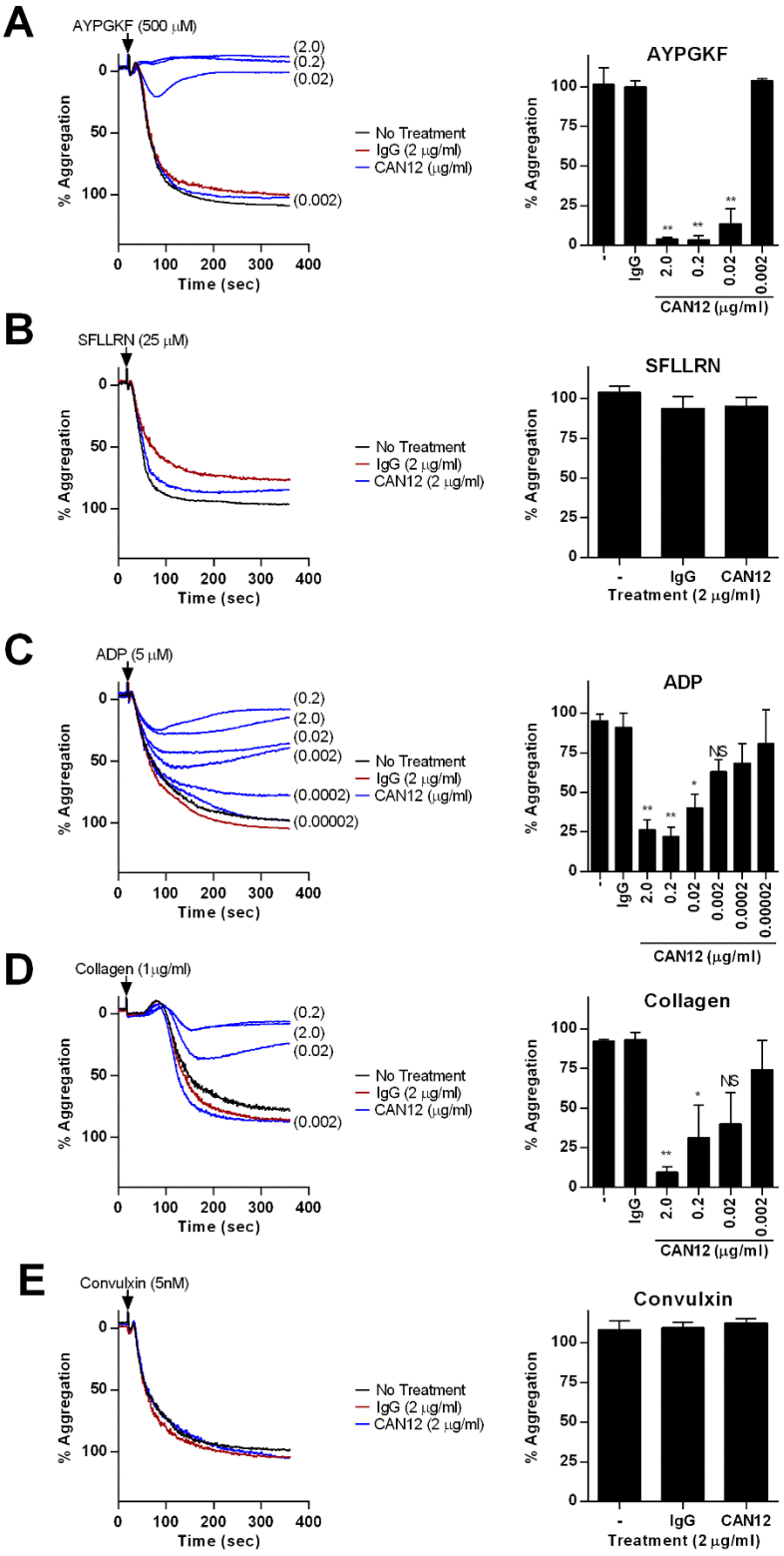

Figure 3.4: CAN12 specificity on dense granule secretion. PRP was isolated from healthy donors. Following treatment with goat IgG (2.0 µg/ml) or CAN12 (dose response) for 10 min at 37°C, secretion was determined for **(A)** AYPGKF (500 µM), **(B)** SFLLRN (25 µM), **(C)** ADP (5 µM), **(D)** collagen (1 µg/ml), **(E)** convulxin (5 nM). *p<0.05 vs. IgG, **p<0.01 vs. IgG, NS=not significant

Figure 3.4: CAN12 specificity on dense granule secretion.

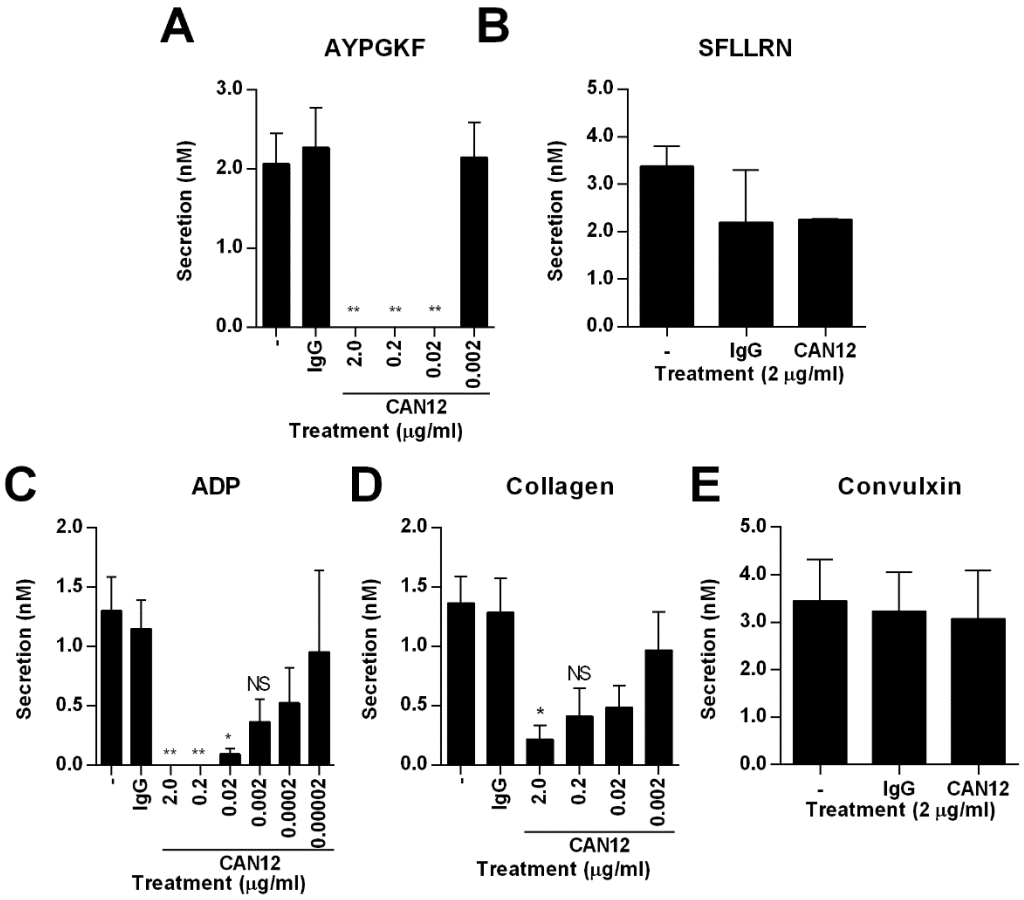

Figure 3.5: CAN12 inhibits aggregation through PAR4. Washed platelets were isolated from wild-type and PAR4$^{-/-}$ mice. Following treatment with goat IgG (2.0 µg/ml) or CAN12(2.0 µg/ml) for 10 min at 37°C percent aggregation was evaluated for **(A)** wild-type and **(B)** PAR4$^{-/-}$ platelets activated with AYPGFK (500 µM), ADP (5 µM) supplemented with 1 mg/ml fibrinogen, or collagen (1 µg/ml). **p<0.01 vs. IgG

Figure 3.5: CAN12 inhibits aggregation through PAR4.

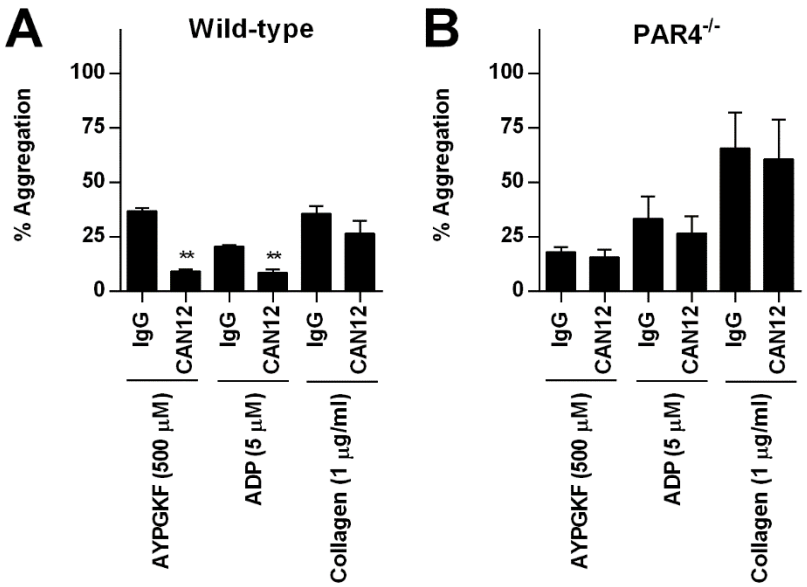

Figure 3.6: CAN12 inhibits arterial thrombosis. (A) C57BL/6 mice were pretreated with saline, goat IgG (2 mg/kg), or CAN12 (1, 0.5, 0.25, 0.125 mg/kg) for 10 min and then subjected to the Rose Bengal carotid artery thrombosis model. Time to complete occlusion is indicated or the experiment was terminated at 90 min. **(B)** The concentration of platelets in the blood at termination of the experiment was determined. **(C)** 15 minutes after the initiation of carotid artery thrombosis, C57BL/6 mice were injected with goat IgG (2 mg/kg) or CAN12 (0.5 mg/kg) and the time to complete arterial occlusion was determined. The experiment was terminated at 90 min. **(D)** The concentration of platelets in the blood at termination of the experiment was determined. **$p<0.01$

Figure 3.6: CAN12 inhibits arterial thrombosis.

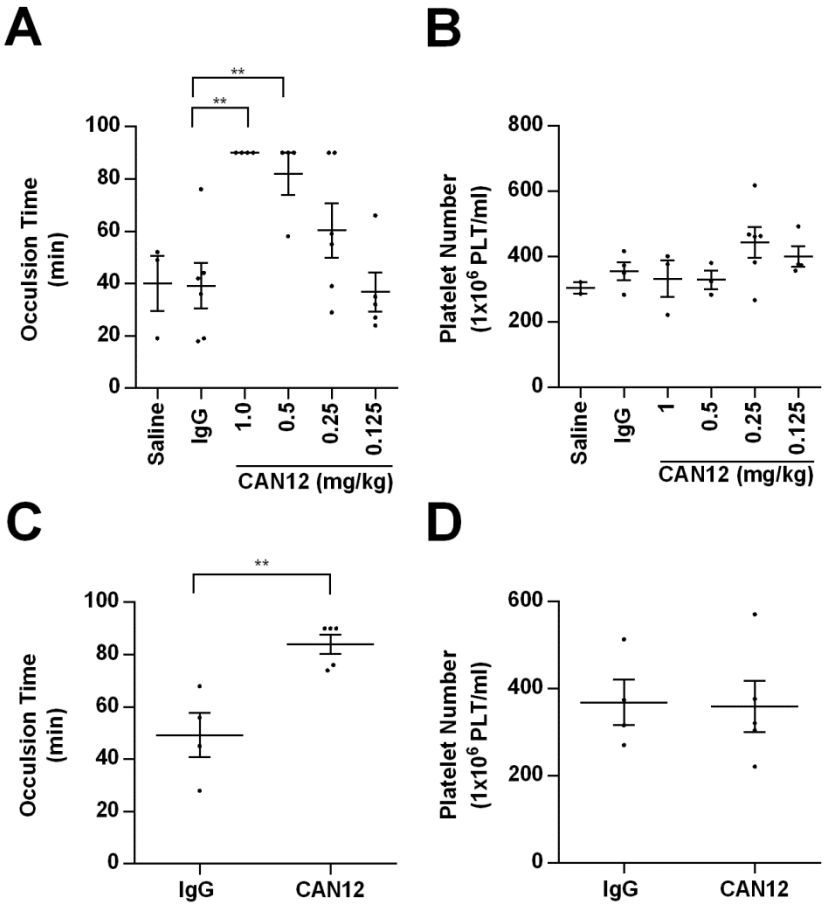

Figure 3.7: CAN12 does not affect bleeding time. (A) C57BL/6 mice or PAR4$^{-/-}$ mice were anesthetized and 3 mm of the tail was cut. The time to cessation of bleeding was determined or the experiment was terminated at 10 min. **(B)** The total amount of blood loss was determined by reading the absorbance of hemoglobin from lysed red blood cells and was compared to a standard curve. **(C)** C57BL/6 mice or PAR4$^{-/-}$ mice were anesthetized and the saphenous vein was exposed and pierced. Once, bleeding ceased, the clot was disrupted. The procedure was repeated for 20 min. The average time of bleeding and **(D)** the number of clot formations were determined. **$p<0.01$, NS=not significant

Figure 3.7: CAN12 does not affect bleeding time.

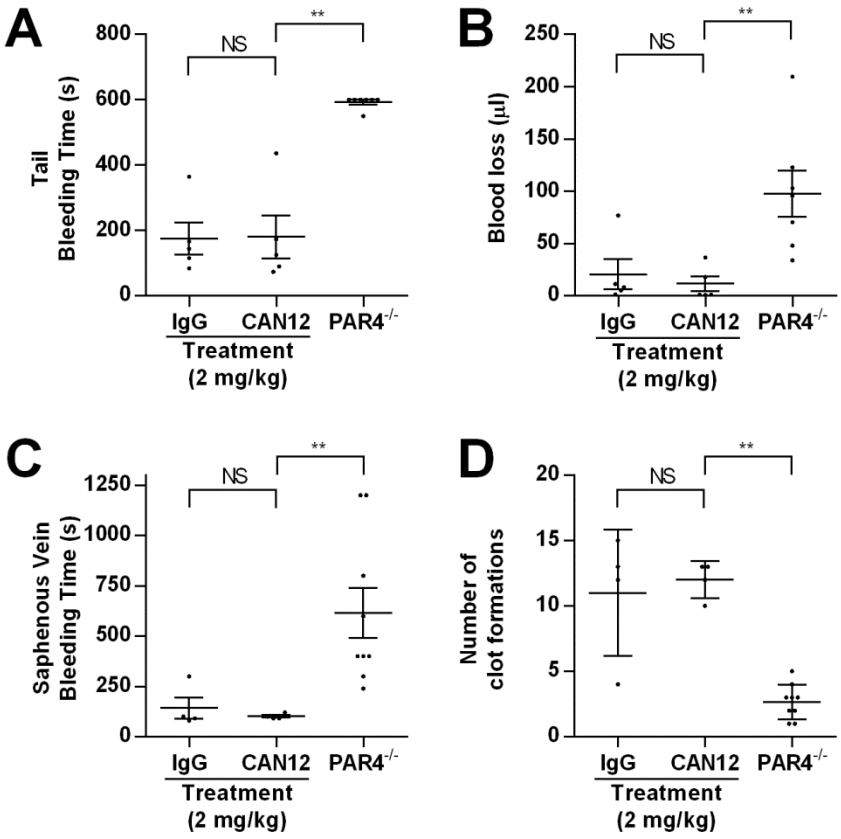

Chapter 4 [§]

Development and Characterization of Monoclonal Antibodies Against Protease Activated Receptor 4

4.1 Abstract

Background: Protease activated receptor 4 (PAR4) is a G protein coupled receptor (GPCR) which is activated by proteolytic cleavage of its N-terminal exodomain. This generates a tethered ligand that activates the receptor and triggers downstream signaling events. With the current focus in the development of antiplatelet therapies shifted towards PARs, new reagents are needed for expanding the field's knowledge on PAR4. Currently, there are no PAR4 reagents which are able to detect activation of the receptor.

Methods: Monoclonal PAR4 antibodies were purified from hybridomas producing antibody that were generated by fusing splenocytes with NS-1 cells. Immunoblotting, immunofluorescence, and flow cytometry were utilized to detect the epitope for each antibody and to evaluate the interaction of the antibodies with cells.

Results: Here, we report the successful generation of three monoclonal antibodies to the N-terminal extracellular domain of PAR4: 14H6, 5F10, and 2D6. We mapped the epitope on PAR4 of 14H6, 5F10, and 2D6 antibodies to residues (48-53), (41-47), and (73-78), respectively. Two of the antibodies (14H6 and 5F10) interacted close to the thrombin cleavage and were sensitive to α-thrombin cleavage of PAR4. In addition, 5F10 was able to partially inhibit the cleavage of PAR4 expressed in HEK293 cells by α-thrombin.

[§] A version of this chapter was accepted for publication in the June 2015 issue of *Thrombosis Research*.

Conclusions: These new antibodies provide a means to monitor endogenous PAR4 expression and activation by proteases on cells. Further, 5F10 will enable experiments that specifically block PAR4 activation.

4.2 Introduction

Protease activated receptors (PARs) are a unique family of seven transmembrane receptors, G-Protein Coupled Receptors (GPCRs), that are activated by proteolysis of their N-terminus [225]. Once cleaved, the newly exposed N-terminus serves as a tethered ligand that activates the receptor by binding extracellular loop 2 [54, 143, 227]. There are four members of the PAR family (PAR1-4), which are widely expressed and activated by multiple proteases [225, 226]. PARs are capable of initiating signaling through G_i, G_q, and $G_{12/13}$ depending on the activating protease and cellular context [228-232]. PAR1 and PAR2 have been the most thoroughly studied, however recent advances have renewed interest in PAR4.

The functional roles of PAR4 have primarily been elucidated on platelets. PAR4 is traditionally thought of as a low-affinity thrombin receptor that serves as a redundant, back up receptor to PAR1. This view is fueled by the overlapping signaling functions of PAR1 and PAR4. However, several recent studies demonstrate that PAR4 has distinct signaling properties [172, 203, 253]. A key feature that distinguishes PAR4 is its ability to form hetero-oligomers with both PAR1 and the ADP receptor P2Y12, which allows PAR4 to influence both thrombin and ADP initiated signaling [184, 189, 254, 255]. For example, the rate of PAR4 cleavage is significantly enhanced by coexpression of PAR1

and PAR4 through hetero-oligomerization [164, 165, 204, 255]. Although it remains to be determined if PAR1-PAR4 hetero-oligomers initiate distinct signaling pathways. In contrast, the interaction between PAR4 and P2Y12 is directly linked to arrestin-2 recruitment and AKT signaling [189, 254]. The lateral associations of PAR4 with PAR1 and P2Y12 place PAR4 at the center of platelet signaling. These interactions take on clinical significance in the context of current antiplatelet therapies that target PAR1, P2Y12, or both in which case thrombin signaling will be funneled exclusively through PAR4 [256].

It is well known that there are multiple genetic risk factors for cardiovascular disease. Among these is a heritable inter-individual variation in platelet reactivity, which is greater in black than white individuals [257]. Recent studies directly link these differences to PAR4 [191-193]. Edelstein and colleagues provide direct genetic evidence for PAR4 by identifying polymorphisms that change amino acids in PAR4 at positions 120 (Ala/Thr) and 296 (Phe/Val) [191]. The polymorphism at 120 is common and is distributed by race. PAR4-120A exhibited a lower reactivity and was found primarily in white individuals, whereas, PAR4-120T was hyper reactive to agonists, resistant to a PAR4 antagonist, and found primarily in black individuals. The precise mechanism by which these PAR4 mutants effect PAR4 activation still needs to be examined.

Although PAR4 has been primarily studied in platelets, it has physiologic roles in other tissues and disease states. PAR4 inhibition has cardioprotective effects against myocardial ischemia/reperfusion injury [166]. In rodents, PAR4 has been shown to play a

role in joint pain and inflammation [167-169]. In addition, PAR4 expression is enhanced in high glucose stimulated human vascular smooth muscle cells [170]. And most recently, Pavic and colleagues demonstrated that PAR4 expression was upregulated in diabetes and plays a role in diabetic vasculopathy [171]. The sum of these studies demonstrates that PAR4 has emerging roles beyond platelets that need to be explored.

Currently, there is a paucity of good reagents for studying PAR4. Here, we report the successful generation of three monoclonal antibodies to the extracellular N-terminus of PAR4: 14H6, 5F10, and 2D6. We have mapped the epitope of these antibodies and each interacts with a unique region on PAR4. Two of the antibodies (14H6 and 5F10) interact near the thrombin cleavage site and are sensitive to α-thrombin cleavage of PAR4. Further, 5F10 partially blocks thrombin cleavage of PAR4. This new panel of PAR4 antibodies will allow experiments that monitor the expression and activation of PAR4 on cells without the use of exogenous epitope tags. These antibodies provide the field with essential tools to determine the roles of PAR4 in greater detail.

4.3 Materials and Methods

Reagents and Antibodies

Human α-thrombin was purchased from Haematological Technologies (specific activity 3200-3400 U/mg) (Essex Junction, VT). The secondary antibody IRDYE 800CW donkey anti-mouse IgG was purchased from LI-COR Biosciences (Lincoln, NE). HA-Tag (6E2) mouse mAB (Alexa Fluor® 647 Conjugate) was purchased from Cell Signaling Technology (Beverly, MA). Poly-L-Lysine and fibrinogen were purchased from Sigma-

Aldrich (St. Louis, MO). VECTASHIELD mounting medium was purchased from Vector Laboratories, Inc. (Burlingame, CA). All cell culture reagents, zeocin, hygromycin B, and secondary antibodies Alexa Fluor® 647 donkey anti-mouse IgG and Alexa Fluor® 488 goat anti-mouse IgG were purchased from Invitrogen.

Cell Culture

NS-1 cells and J7774A.1 cells were grown in HY media (DMEM, NCTC, insulin, oxalacetic acid, and pyruvic acid) supplemented with 20% FBS and 1% Penicillin-Streptomycin. Flp-In™ T-REx™ 293 cells were purchased from Invitrogen and were cultured in DMEM supplemented with 10% fetal bovine serum, 1% Pen/Strep, and Zeocin. To generate Flp-In™ T-REx™ 293 cells expressing PAR4, cells were transfected with pOG44 vector and pcDNA5/FRT containing PAR4 using Lipofectamine 2000 (Invitrogen) according to manufacturer's instructions. Cells stably expressing PAR4 were selected with Hygromycin B (200 μg/ml). PAR4 expression was induced with tetracycline (1 μg/ml) for 36 hr.

Production and Purification of Recombinant Proteins

The full-length cDNA for human PAR4 was purchased from UMR cDNA resource center. Maltose binding protein-PAR4 fusion proteins (MBP-PAR4(18-78), MBP-PAR4(41-66), MBP-PAR4(48-72), and MBP-PAR4(54-66) (see Figure 4.1) were generated by amplifying the region of interest with PCR and subcloning into pMAL-c2 as an EcoRI-HinDIII fragment. The specific primer sequences are available upon request. The MBP-PAR4 fusion proteins were expressed in BL-21 *E. coli* and were purified by

affinity chromatography on an amylose column. Briefly, the lysate was loaded onto an amylose column pre-equilibrated with column buffer (20 mM Tris-HCl pH 7.4, 0.2M NaCl, 1mM EDTA) at 4°C. The column was washed with 12 column volumes of column buffer, and the protein was eluted in 1 ml fractions with elution buffer (20 mM Tris-HCl pH 7.4, 0.2M NaCl, 1mM EDTA, 10 mM maltose). The concentration of purified protein was determined using BioRad protein assay kit.

Animals

F2RL3$^{-/-}$ mice (referred to as PAR4$^{-/-}$) were obtained from the Mutant Mouse Regional Resource Center (MMRRC) (Chapel Hill, NC). All animal studies were approved by the Institutional Animal Care and Use Committee at Case Western Reserve University School of Medicine.

Mouse Immunization and Antibody Production

The method was modified from the previously described protocol by James K. Wahl, III [258]. Five week old C57BL/6 F2RL3$^{-/-}$ mice were subcutaneously injected with 150 µg of antigen (MBP-hPAR4(18-78)) in complete Freud's adjuvant. The mice were administered 150 µg of antigen via intraperitoneal injections every 2 weeks for 6 weeks. Two weeks after the final injection, additional boosts were given daily for three days prior to harvesting the splenoctyes. Mouse primary splenocytes were isolated and fused with the myeloma cell line NS-1 using polyethylene glycol. The fusion was plated into 96 well plates and treated the following day with aminopterin to remove unfused NS-1 cells. The hybridoma supernatants were screened by immunoblotting against maltose binding

protein (MBP) and MBP-PAR4 antigen. Positive hybridomas were selected by limiting dilution and maintained in HY media.

Antibody Purification

The antibody supernatant was isolated from hybridoma cells by centrifugation (200×*g* for 5 min). The supernatant was clarified by centrifuging at 14000×*g* for 10 min at 4°C. The supernatant was loaded onto a Protein A column pre-equilibrated with 20 mM sodium phosphate buffer pH 7.0. The column was then washed with 20 mM sodium phosphate buffer pH 7.0. The antibody was eluted from the column with 0.1 M Gylcine-HCl pH 2.5 and the pH was immediately raised to 8.0 with 1 M Tris pH 9.0. The purified antibody was placed in dialysis buffer (0.1 M $NaHCO_3$ pH 8.5, 0.5 M NaCl) overnight. The antibody concentration was quantitated using a NanoDrop ND-1000 spectrophotometer (molar extinction coefficient 210,000 M^{-1} cm^{-1}).

Monoclonal Antibody Isotype

The purified antibodies were diluted (100 ng/ml) and loaded on to isotyping cassettes (Thermo Scientific Pierce Rapid Mouse Antibody Isotyping Kit). The isotype for each antibody was determined (14H6: IgG2b, kappa; 5F10: IgG2b, lambda; 2D6: IgG1, kappa).

Western Blot Analysis

Immunoblotting was used to determine the epitope for each antibody. MBP, MBP-PAR4(18-78), MBP- PAR4(41-66), MBP- PAR4(48-72), and MBP-PAR4(54-66) (5 µg)

were loaded and resolved by SDS-PAGE and transferred onto nitrocellulose. The membranes were incubated with purified primary monoclonal antibody (anti-MBP, 14H6, 5F10, or 2D6) for 1 hr. Followed by incubation with secondary antibody IRDYE 800CW donkey anti-mouse IgG for 1 hr. The membranes were developed using the Odyssey Infrared Imaging System.

For HEK293 cells expressing PAR4 and human platelets, the cells were lysed in RIPA buffer (1% NP-40, 0.5% Deoxycholate, 0.1% SDS) on ice. Following lysis, the lysate was collected and quantitated using the Biorad DC protein assay. 100µg of total protein was loaded and resolved by SDS-PAGE and transferred onto nitrocellulose. The membranes were incubated with 50 µg primary antibody (anti-MBP, 14H6, 5F10, or 2D6) for 1 hr, secondary antibody IRDYE 800CW donkey anti-mouse IgG for 1 hr, and developed using the Odyssey Infrared Imaging System.

Flow Cytometry Analysis

Flp-In™ T-REx™ 293 cells were treated with 1 µg/ml tetracycline for 36 hrs to induce expression of HA-PAR4. Cells (2×10^5) were washed in suspension twice with PBS; some cells were treated with α-thrombin (100 nM) for 5 min at 37°C prior to staining. For staining, the cells were incubated in PBS containing 2% BSA and treated with 2 µg of primary antibody (14F6, 5F10, 2D6) for 1hr, washed with PBS twice, treated with anti-mouse 647 secondary antibody (10 µg/ml) in PBS with 2% BSA for 30 min, and washed twice with PBS. The cells were analyzed using the BD LSRFortessa cell analyzer.

For measuring the effect of 14H6 and 5F10 on PAR4 cleavage, the experiment was carried out the same as described above except the cells were pretreated with 14H6 or 5F10 (2-50 μg) for 10 minutes and then activated with 100 nM α-thrombin for 5 min at 37°C. Following activation the cells were labeled with anti-HA-Tag Alexa Fluor 647 (2.5 μg/ml, clone 6E2, Cell Signaling). Data are expressed as percent cleavage, which was calculated by subtracting the mean fluorescence intensity from uninduced cells and setting it to 0%. Induced cells without thrombin were set to 100%.

Human Platelet Isolation

Human platelets were obtained from healthy donors. These studies were approved by the Case Western Reserve University Institutional Review Board and informed consent was obtained from all donors. Whole blood was collected into the anticoagulant acid citrate dextrose (ACD) (2.5% sodium citrate, 71.4 mM citric acid, 2% D-glucose) and centrifuged at 200×*g* for 10 minutes at room temperature. The top PRP layer was removed and centrifuged at 400xg for 10 minutes at room temperature to pellet the platelets. The platelet pellet was resuspended in HEPES-Tyrode buffer pH 7.4 (10 mM HEPES, 12 mM $NaHCO_3$, 130 mM NaCl, 5 mM KCl, 0.4 mM Na_2HPO_4, 1 mM $MgCl_2$, and 5 mM glucose). The number of platelets was quantitated using a Hemavet 950FS (Drew Scientific Inc, Waterbury, CT, USA).

Immunofluorescence Microscopy

Flp-In™ T-REx™ 293 cells adherent to coverslips coated with Poly-L-Lysine were treated with 1 μg/ml tetracycline for 36 hrs to induce expression of PAR4. The cells were

fixed using 4% formaldehyde, blocked (1% BSA and 40 µg/ml non-immune human IgG in PBS), incubated with 20 µg primary monoclonal antibody (14H6, 2D6, 5F10), and labeled with secondary antibody (Alexa Fluor® 488 goat anti-mouse IgG). The coverslips were mounted on standard glass slides using VECTASHIELD mounting medium. For human platelets, washed coverslips were coated with fibrinogen and subsequently blocked with 5% BSA in PBS. 0.5 ml of washed human platelets (1 $x10^7$ platelets/ml) in Medium 199 was added to the coverslips and let adhere for 30 min at 37°C. The platelets were activated with thrombin (1 nM) for 2 hrs at 37°C. The platelets were then treated the same as HEK293 cells described above.

4.4 Results and Discussion

Generation of PAR4 Monoclonal Antibodies

Protease activated receptors are activated by cleavage of their N-terminus and antibodies targeted to this region have to potential to monitor receptor cleavage and internalization on primary cells. In this study we aimed to generate monoclonal antibodies against the N-terminal extracellular domain of PAR4. We used the entire mature exodomain of human PAR4 fused to maltose binding protein (MBP) as an antigen (MBP-PAR4(18-78)) (Figure 4.1). To maximize the immune response from the MBP-PAR4 fusion protein, we used $PAR4^{-/-}$ mice as the host for antibody production. The hybridomas resulting from the splenocyte/NS-1 fusion were screened by immunoblotting for MBP and MBP-PAR4(18-78) simultaneously. The antibodies that recognized both recombinant proteins were discarded as they were directed toward the MBP region of the fusion protein.

Identification of the Antibody Epitopes on PAR4

The initial screening and epitope mapping resulted in antibodies that fell into 3 classes; the respective hybridomas were selected by serial dilution and further analyzed. Our preliminary screen against a panel of MBP-PAR4 fusion proteins identified three classes of antibodies. One antibody from each class (14H6, 5F10, and 2D6) were chosen to map the epitope on PAR4 in greater detail (Figure 4.1). Equal loading on the gel was verified by blotting with MBP antibody (Figure 4.2A). 14H6 interacted with MBP-PAR4(18-78), MBP-PAR4(41-66), and MBP-PAR4(48-72), but not MBP-PAR4(54-66) indicating that the PAR4 antibody 14H6 recognizes residues 48-53 of PAR4 (Figure 4.1, Figure 4.2B). 5F10 interacted with MBP-PAR4(18-78) and MBP-PAR4(41-66), but not MBP-PAR4(48-72) or MBP-PAR4(54-66) indicating that the PAR4 antibody 5F10 interacts with amino acids 41-47 of PAR4 (Figure 4.1, Figure 4.2C). 2D6 only recognized MBP-PAR4(18-78) (Figure 4.2D) indicating the epitope is at either end of the PAR4 exodomain (amino acids 18-40 or 73-78). The epitope was ultimately mapped to amino acids 73-78 (see below and Figure 4.3).

Detection of PAR4 Cleavage

Two of the antibodies (14H6 and 5F10) mapped epitopes near the thrombin cleavage site. Antibodies sensitive to PAR4 cleavage by thrombin would be useful reagents to monitor endogenous PAR4 activation on cells. To test if 14H6 and 5F10 recognized cleaved PAR4, MBP-PAR4(18-78) was proteolyzed with α-thrombin (100 nM) and the resulting MBP-PAR4(18-47) fragment was resolved by SDS PAGE. Neither 14H6 nor 5F10 recognized the thrombin cleaved PAR4 indicating that the epitope was disrupted

following proteolysis (Figure 4.3). Our preliminary characterization of 2D6 mapped the epitope to either the N-or C-terminus of the PAR4 exodomain (Figure 4.2). The epitope was further mapped using thrombin cleaved MBP-PAR4(18-78). Following proteolysis, the 2D6 epitope was lost indicating that 2D6 binds C-terminal to the cleavage site; the 30 amino acid fragment (48-78) is too small to be detected on the gel (Figure 4.3). The combined mapping experiments determined the 2D6 epitope to be amino acids 73-78, the extreme C-terminus of the PAR4 exodomain.

In this study we focused on α-thrombin activation of PAR4. However, numerous other proteases (trypsin, plasmin, cathepsin) also activate PAR4 and therefore, cause platelet activation [55, 259, 260]. Plasmin, trypsin, and α-thrombin all cleave PAR4 at Arg^{47}. Therefore, 14H6 and 5F10 will be able to detect PAR4 activation by all of the PAR4 activating proteases in endogenous cells.

Recognition of PAR4 on Cells

To determine if the antibodies are able to detect PAR4 expressed on cells, we used Flp-In™ 293 cells engineered to express PAR4 or HA-tagged PAR4 (HA-PAR4) when treated with tetracycline (1 μg/ml). 14H6, 5F10, and 2D6 were able to detect PAR4 expressed on HEK293 cells by immunofluorescence (Figure 4.4A). HA-tag and secondary antibody were used as positive and negative controls, respectively. By immunoblotting, 14H6 and 5F10 were able to detect PAR4 in HEK293 expressing PAR4 cells; however, 2D6 was not able to recognize PAR4 (Figure 4.4B). Our mapping studies with recombinant proteins show that 14H6 and 5F10 bind near the thrombin cleavage

site. We next determined if these antibodies are able to detect the cleavage of PAR4 on cells with flow cytometry. The interaction of 14H6 and 5F10 with PAR4 was disrupted following activation by α-thrombin (Figure 4.4C). Consistent with previous studies, the maximum cleavage of PAR4 was ~50% [255, 261]. Expression of HA-PAR4 was confirmed by flow cytometry using a HA-tag antibody.

Recognition of PAR4 on Platelets

For a more physiological readout we examined if 14H6 and 5F10 were able to detect endogenous PAR4 expressed on human platelets. 14H6 and 5F10 both interacted with PAR4 expressed in unstimulated human platelets (Figure 4.5A). Following activation by α-thrombin (1, 10, 100 nM), 14H6 and 5F10 were able to detect a decreased level of uncleaved PAR4 as a result of the epitope for 14H6 and 5F10 being cleaved from the receptor. This effect was dependent on the concentration of α-thrombin used to activate the human platelets. A similar effect was observed when examining PAR4 expression on the surface of human platelets. Using immunofluorescence, 14H6 was able to detect PAR4 expressed on the surface of human platelets and following activation with thrombin, there was a decrease in the interaction between PAR4 and 14H6 (Figure 4.5B). This indicates that on human platelets, 14H6 and 5F10 only interact with unactivated and uncleaved PAR4.

Inhibition of PAR4 Cleavage

Based on the location of the PAR4 interaction site of 14H6 and 5F10, we investigated if the antibodies were able to inhibit PAR4 cleavage. Flp-In™ 293 cells induced to express

HA-tagged PAR4 were pretreated with 14H6 or 5F10 (2-50 μg) and activated with α-thrombin (100 nM) for 10 min; loss of the N-terminal HA-tag was used as the readout for detecting PAR4 cleavage. To quantify the amount of PAR4 cleavage, background staining from uninduced cells was subtracted from all samples (Figure 4.6). The antibody 14H6 did not interfere with thrombin cleavage up to 50 μg total antibody. However, 5F10 was able to partially inhibit PAR4 cleavage at 50 μg total antibody. These data are consistent with our mapping studies in which 5F10 mapped to the P7-P1 residues (nomenclature of Schecter and Berger [205]) corresponding to Ser^{41} to Arg^{47} that are important for thrombin recognition of its substrates [188, 262]. In contrast, 14H6 maps to P1'-P7' residues (Gly^{48}-Val^{53}). We have previously described an antibody to PAR4 that blocks platelet thrombin-induced activation of human platelets and delays thrombosis in mouse models *in vivo* [261]. Therefore we tested the ability of 14H6 and 5F10 to block human platelet activation. Neither 14H6 nor 5F10 were able to block thrombin-induced aggregation at concentrations up to 10 μg/ml. The most plausible explanations for these results are that 14H6 and 5F10 bind with an affinity that is too low to overcome PAR1 activation, which is also present on the platelet surface.

4.5 Conclusions

In the current study, we generated three classes of monoclonal antibodies that recognize unique regions on human PAR4. Two of the antibodies (14H6, 5F10) were able to detect PAR4 expression in HEK293 cells by immunoblotting, immunofluorescence, and flow cytometry and were found to be sensitive to PAR4 activation. In addition, 5F10 could partially inhibit PAR4 cleavage by α-thrombin. Importantly, 14H6 and 5F10 were able to

detect endogenous PAR4 expression in human platelets. The third antibody, 2D6, was able to detect PAR4 expressed on cells by immunofluorescence microscopy. The studies described in this current report demonstrate the development of three useful tools for advancing our understanding of PAR4 in platelets and less well studied tissues.

In studies moving forward examining genetic variations of PAR4 in human platelets and the role of PAR4 in other tissues, these antibodies provide novel tools, which provide the invaluable ability to detect PAR4 in endogenous tissues/cells and to measure the initial step in PAR4 activation, PAR4 cleavage. These antibodies fill a gap in the currently available reagents for examining PAR4 and enable further advances in understanding the function and role of PAR4 in newly appreciated tissues and disease conditions.

4.6 Addendum

M. M. Mumaw and M. T. Nieman conceived and designed the experiments. M. M. Mumaw, M. de la Fuente, A. Arachiche, and J. K. Wahl III performed the experiments. M. M. Mumaw and M. T. Nieman analyzed the data. M. M. Mumaw and M. T. Nieman wrote the manuscript.

4.7 Acknowledgements

The authors would like to thank Dr. Vera Moiseenkova-Bell and Kevin Huynh for technical assistance with purifying the antibodies. This study was funded by grants from the National Institutes of Health (HL098217) to M.T.N., the Cardiovascular Training

Grant T32HL105338 (M.M.M.), and CWRU/UH Center for AIDS Research (NIH P30 AI036219).

Figure 4.1: Schematic of PAR4 extracellular constructs fused to MBP. PAR4 extracellular fragments were subcloned into pMAL-C2 to generate MBP-PAR4(18-78), MBP-PAR4(41-66), MBP-PAR4(48-72), and MBP-PAR4(54-66), which were used for generating and screening PAR4 monoclonal antibodies. The interaction for each antibody is illustrated.

Figure 4.1: Schematic of PAR4 extracellular constructs fused to MBP.

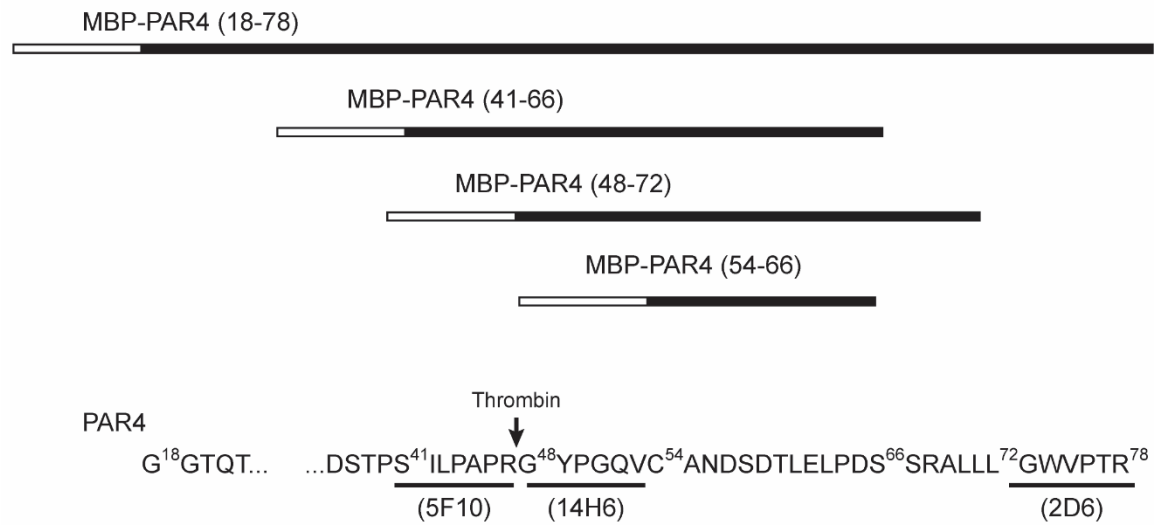

Figure 4.2: Characterization of extracellular PAR4 interaction sites. *E. coli* were transformed, cultured, lysed, and the fusion proteins (MBP, MBP-PAR4(18-78), MBP-PAR4(41-66), MBP-PAR4(48-72), and MBP-PAR4(54-66)) were purified by affinity chromatography. The epitopes for each PAR4 monoclonal antibody were determined by immunoblotting. **(A)** Control blot with MBP to show that all of the recombinant PAR4 sections were purified and are present on the gel. **(B)** 14H6 interacted with MBP-PAR4(18-78), MBP-PAR4(41-66), and MBP-PAR4(48-72) protein fragments. **(C)** 5F10 recognized MBP-PAR4(18-78) and MBP-PAR4(41-66). **(D)** 2D6 interacted with only the complete extracellular section, MBP-PAR4(18-78).

Figure 4.2: Characterization of extracellular PAR4 interaction sites.

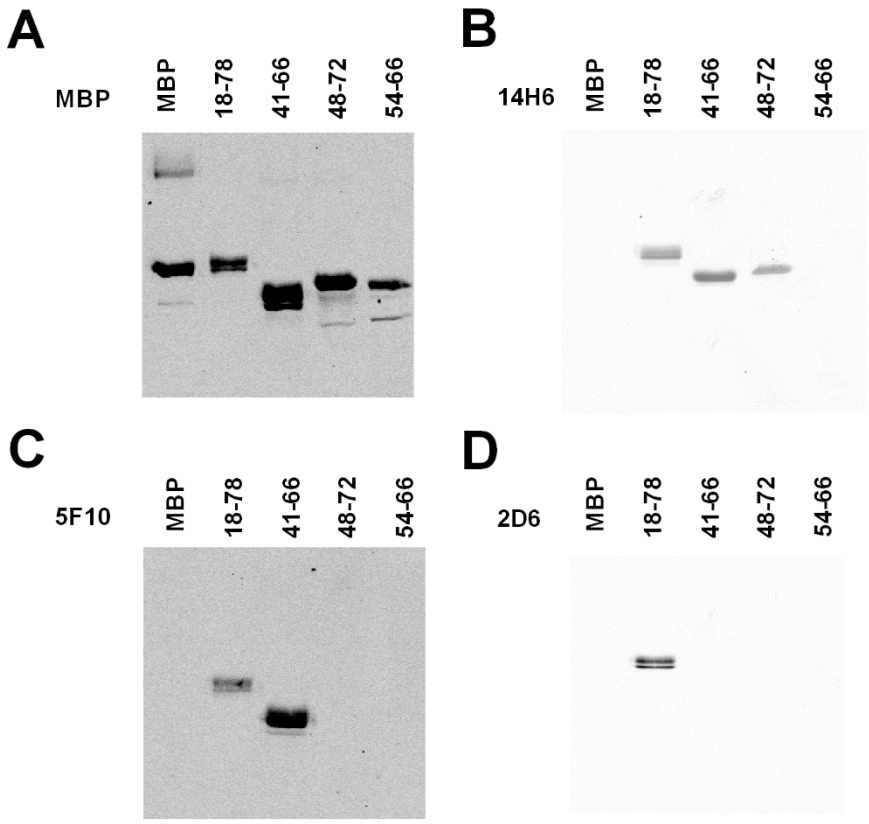

Figure 4.3: Monoclonal antibodies detect PAR4 cleavage by thrombin. The full exodomain of PAR4 (MBP-PAR4(18-78)) was cleaved with 100 nM α-thrombin (IIa) for 5 min and immunoblotted with 14H6 or 5F10 to determine if they recognize cleaved PAR4. The cleaved PAR4 exodomain was used to further map the 2D6 epitope to residues 73-78.

Figure 4.3: Monoclonal antibodies detect PAR4 cleavage by thrombin.

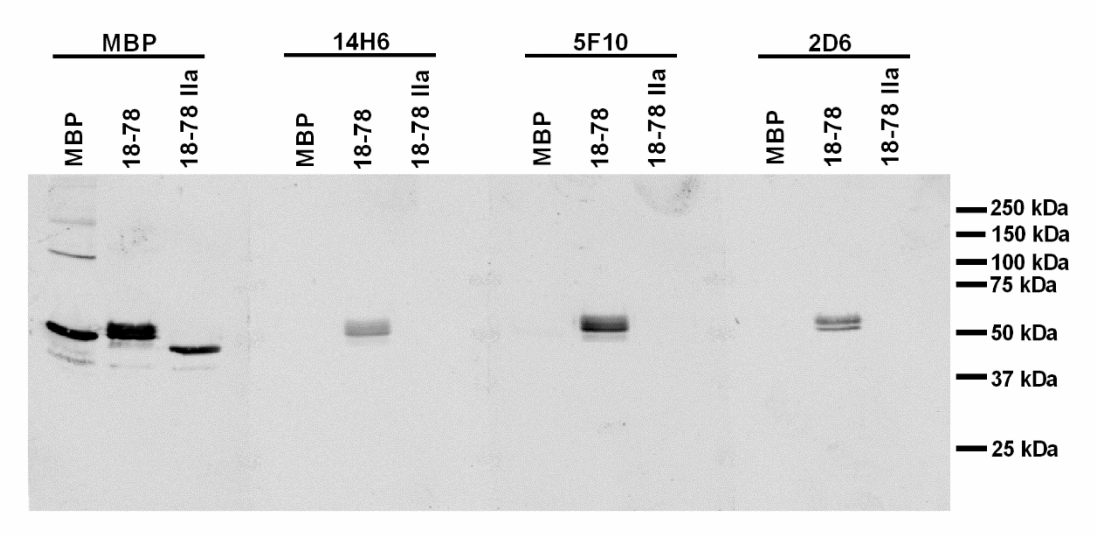

Figure 4.4: Detection of PAR4 on HEK293 cells. Following induction of Flp-In™ T-REx™ 293 cells with tetracycline (1 µg/ml) for 36 hrs, **(A)** immunofluorescence and **(B)** immunoblotting were used to determine the ability of 14H6, 5F10, or 2D6 to interact with PAR4 on cells. HA was used as a positive control. Secondary antibody was used a negative control. **(C)** Flow cytometry was used to evaluate the ability of 14H6, 5F10, and 2D6 to interact with uncleaved HA-PAR4 and cleaved HA-PAR4 (100 nM α-thrombin (IIa)) on cells. HA-PAR4 induction was determined using a HA-tag specific antibody. Mouse IgG was used as a negative control.

Figure 4.4: Detection of PAR4 on HEK293 cells.

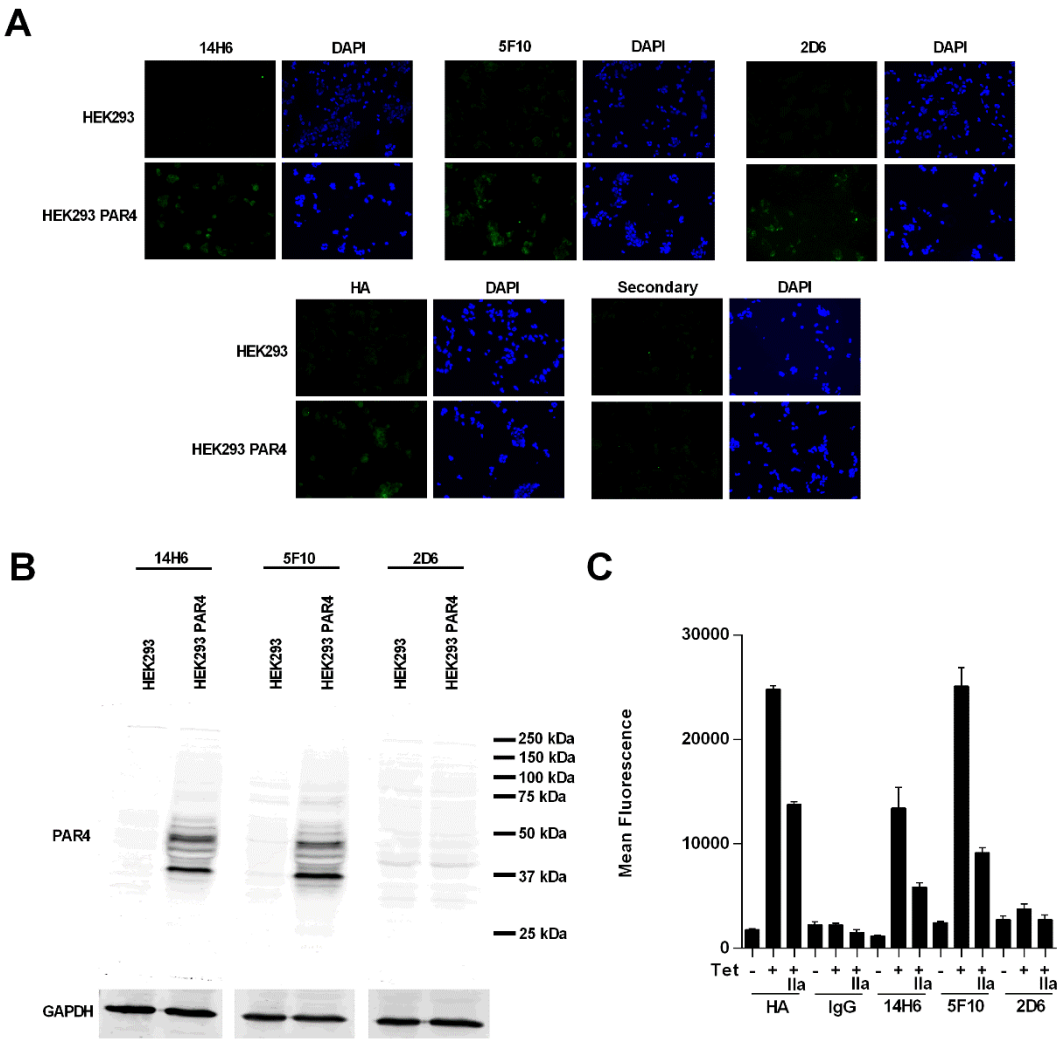

Figure 4.5: Detection of PAR4 on platelets. (A) Human platelets (hPLT) were activated with α-thrombin (0, 1, 10, 100 nM) for 5 min at 37°C, lysed, and immunoblotted with 14H6 and 5F10 (50 µg). HEK293 cells were used as a negative control. **(B)** Immunofluorescence examining the interaction of 14H6 (20 µg) with unstimulated and α-thrombin (1 nM) stimulated human platelets.

Figure 4.5: Detection of PAR4 on platelets.

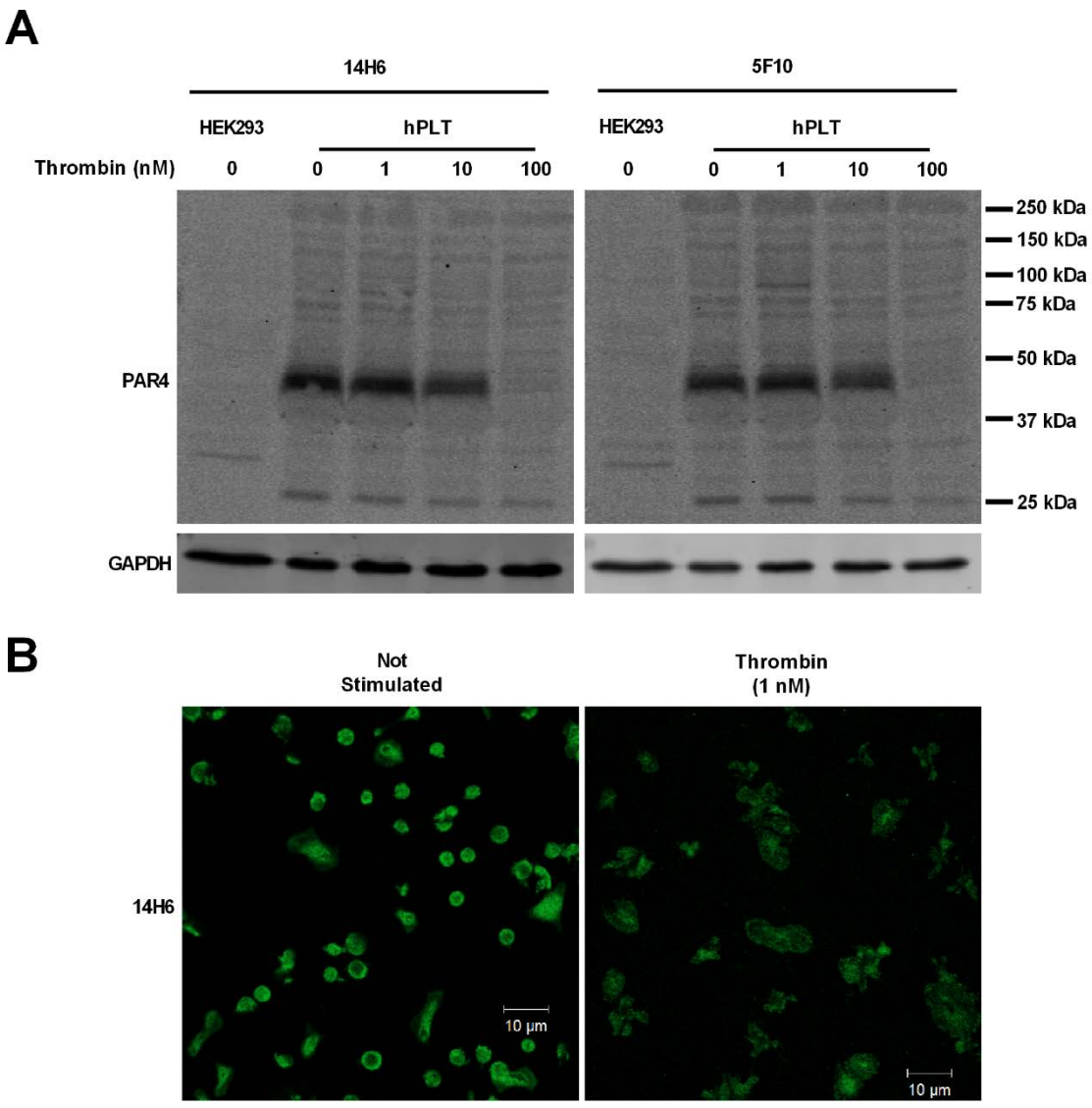

Figure 4.6: Inhibition of PAR4 cleavage. Flp-In™ T-REx™ 293 cells were induced with tetracycline (1 mg/ml) for 36 hrs to express HA-PAR4. Following induction cells were treated with buffer, 14H6, or 5F10 (2-50 μg) for 10 min and activated with α-thrombin (100 nM) for 5 min at 37°C. Cleavage of PAR4 was measured by loss of an N-terminal HA-tag. % uncleaved PAR4 was normalized to not induced, not activated, and buffer pretreatment (0%) and induced, not activated, and buffer pretreatment (100%). **$p<0.01$

Figure 4.6: Inhibition of PAR4 cleavage.

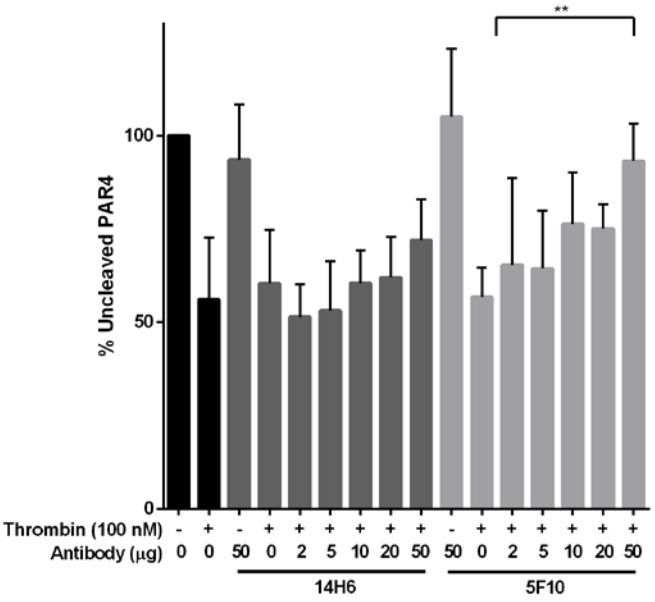

Chapter 5 : Discussion and Future Directions

Together the studies described in this body of work provide the framework to further understand how PAR1 and PAR4 interact and influence the function of one another. Through three independent studies it was shown that PAR1 and PAR4 form a α-thrombin dependent heterodimer that affects PAR4 activation, that the anionic cluster on PAR4 could be a new viable target to antiplatelet therapy, and that three PAR4 monoclonal antibodies that interact with unique regions on the receptor were developed. Each study is discussed in detail below and future experiments are proposed.

Chapter 5.1: PAR1-PAR4 Heterodimerization

In Chapter 2 we report our findings on the formation of PAR1-PAR4 heterodimers. This study determined that the formation of a heterodimer composed of PAR1 and PAR4 is dependent on cleavage of both receptors by α-thrombin. The heterodimer interface was mapped to four resides in transmembrane helix 4 from both PAR1 and PAR4. Finally, it was determined that PAR1 assisted PAR4 cleavage is disrupted when heterodimer formation is inhibited. Overall, these studies have characterized PAR1-PAR4 heterodimer formation and show the functional significance of heterodimer formation.

Bioluminescence resonance energy transfer (BRET) was utilized to examine heterodimer formation on living cells with minimal expression levels to avoid overexpression artifacts. Using HEK293 cells it was shown that only following cleavage by α-thrombin

would PAR1-PAR4 heterodimers form. Coimmunoprecipitiation was used to show that PAR1 and PAR4 form heterodimers which agrees with previously published studies by Leger et al [184]. For the current CO-IP experiments and past CO-IP experiments, activation with α-thrombin was not necessary for dimer formation. However, these experiments were performed in a different cell culture model (COS-7 cells) and required high expression levels of PAR1 and PAR4 (10-fold higher than BRET studies). Based on previous studies demonstrating that PAR1 and PAR4 coimmunopreciptiate in human platelets following stimulation with α-thrombin and the current studies, α-thrombin stimulation is necessary for PAR1-PAR4 heterodimerization [184].

While in this study it was determined that PAR1-PAR4 heterodimer formation is specific to activation with α-thrombin, it has previously been determined that PAR1 and PAR4 also form constitutive homodimers [182, 183]. In addition, these studies show that the same residues are necessary for both PAR4 homodimer formation and PAR1-PAR4 heterodimer formation. This suggests a balance between monomers, homodimers, and heterodimers. PAR1 and PAR4 monomers, homodimers, and heterodimers may play a specific role in regulating different signaling events. In the case of the PAR activation peptides which do not induce heterodimerization, they could be activating different signaling events compared to cleavage by α-thrombin. A current study is underway examining differences in the phosphoproteome of human platelets stimulated with PAR activation peptides versus α-thrombin.

It has previously been determined that localization of PAR1 in the plasma membrane in endothelial cells is determined by the protease activating the receptor [154-156]. Currently, limited data is available about the location of PAR1 and PAR4 in platelet membranes and the role that lipids play in PAR activation and signaling. Preliminary data suggests that PAR1 and PAR4 are excluded from limited rafts in platelets (data not shown). Future studies will have to examine in more detail if PARs are located in lipid rafts on platelets and if activation with different proteases and activation peptides influence their localization and signaling.

Overall, this study shows that PAR1 and PAR4 form heterodimers that are necessary for PAR1 assisted PAR4 cleavage. With the recent approval of vorapaxar, PAR1 antagonist, as an antiplatelet therapy, future studies will need to expand on what effect heterodimerization has on PAR activation and signaling and what effect vorapaxar has on heterodimerization. Also further studies examining the molecular arrangements on PARs on human platelets will aid in the development of further antiplatelet therapies.

Chapter 5.2: The N-terminus of PAR4 as an Antiplatelet Therapy Target

While many different approaches are available for treating and preventing acute coronary syndromes (ACS), there is currently an unmet need for antiplatelet therapies that inhibit thrombosis without significantly increasing bleeding risk. In Chapter 3, I discussed the findings that demonstrate that the anionic cluster (D^{57}, D^{59}, E^{62}, D^{65}) on the N-terminus of PAR4 is a new potential antiplatelet therapy target. A goat polyclonal antibody (CAN12)

was developed that specifically interacts with the anionic cluster allowing it to delay cleavage of PAR4. CAN12 was able to block thrombin-induced human platelet aggregation and secretion in a dose-dependent manner. In addition, when administered before or after injury CAN12 was able to prevent carotid artery thrombosis in mice. Importantly, CAN12 treatment did not influence hemostasis in two independent mouse models.

PAR1 and PAR4 are both expressed on human platelets and are responsible for regulating thrombin induced platelet activation [55]. PAR1 is activated by lower concentrations of thrombin while PAR4 requires higher concentrations of thrombin to be activated [66, 164, 165]. However, the rate of PAR4 activation is enhanced in the presence of PAR1, and heterodimerization of the two receptors is necessary for PAR1-mediated enhancement of PAR4 cleavage [185]. Additionally, PAR1 and PAR4 have been previously shown to form homodimers [182, 183]. Since CAN12 was shown to specifically interact with the anionic cluster on PAR4 and dose-dependently inhibit thrombin-induced human platelet aggregation, and not inhibit PAR1 activation by SFLLRN, CAN12 must be inhibiting both PAR1 and PAR4 activation through the interactions of the receptors on the platelet surface. However, the exact mechanism of inhibition and the arrangement of PAR1, PAR4, thrombin, and CAN12 need to be examined in future studies. While it was beyond the scope of the current study different approaches to examine exact mechanism of inhibition could be (1) examining if PAR1 and PAR4 inhibition is dimer dependent on platelets, (2) what type of complex is formed

in the presence of purified PAR1, PAR4, thrombin, and CAN12, and (3) does inhibition/activation affect localization of the receptors on platelets (i.e. lipid rafts).

In addition to affecting thrombin induced platelet aggregation and secretion, CAN12 also affected ADP-induced human platelet aggregation. Since CAN12's effect on ADP induced aggregation was PAR4 dependent, CAN12 was mostly likely able to inhibit ADP induced aggregation through PAR4's direct and indirect interactions with the ADP receptor, P2Y12 [172, 189, 190]. This is of note since the current standard of care for ACS includes a P2Y12 antagonist. If targeting the anionic cluster on PAR4 inhibits both ADP and thrombin induced aggregation, it could be used as an alternative to combination therapy.

For our *in vivo* studies we utilized mice as our animal model. Mice have a different expression profile of PARs on their platelets compared to humans [55, 67, 162]. On human platelets, both PAR1 and PAR4 are responsible for signaling and inducing platelet aggregation by thrombin, but on mouse platelets PAR4 cleavage is necessary for platelet activation by thrombin. PAR3 does not signal. While it is important to consider species differences in PAR expression on platelets, the effect of CAN12 on thrombosis and hemostasis in human platelets is likely to be similar to murine platelets. This is due to the fact that CAN12 was able to inhibit thrombin induced aggregation of human platelets through PAR1 and PAR4 and aggregation of murine platelets mediated by PAR4.

It should be noted that inhibition with CAN12 had differing effects on hemostasis compared to knocking-out PAR4 in mice ($PAR4^{-/-}$). $PAR4^{-/-}$ mice have a prolonged time to thrombosis and have significantly increased bleeding times. By comparison, inhibiting PAR4 prolonged thrombosis but did not affect the time to hemostasis. This is likely due to the fact that CAN12 slows the rate of PAR4 activation rather than completely inhibiting it. One hypothesis for this phenomenon is that in the case of arterial thrombosis where there is a high flow rate in the vessel, the platelets with CAN12 bound will be rapidly cleared from the site of injury containing high thrombin concentrations, allowing reduced PAR4 mediated platelet activation at the site of injury. In contrast, in a venous blood vessel there is a lower flow rate that would allow the platelets with CAN12 bound to remain in proximity of higher thrombin concentrations at the site of injury for a prolonged length of time. PAR4 would then be able to be cleaved by thrombin and induce platelet activation. Future studies using flow chambers could be utilized to elucidate the effect of flow rate on CAN12 mediated inhibition of platelet activation.

Overall, the current study demonstrates the feasibility of targeting the anionic cluster on PAR4 as an antiplatelet therapy strategy and provides justification to generate a monoclonal antibody targeting the anionic cluster on PAR4. After confirming that a monoclonal antibody has similar specificity and effect on aggregation, thrombosis, and hemostasis, it could then be humanized. Ideally, the antibody could be humanized with little effect on its affinity for the anionic cluster on PAR4. The development of Fab fragments and single-chain antibodies would be an alternate approach to decrease the immune response; however, this would sacrifice half-life since they have a lower

molecular mass and tissue permeability is not an issue since we are targeting cells in circulation, platelets. Thus while our studies provide the framework for the development of a PAR4 inhibitory antibody that inhibits thrombosis without affecting hemostasis, it will require greater in depth efforts to expand targeting PAR4 as an antiplatelet therapy.

Current studies by other labs with different approaches for targeting PAR4 (indole derived PAR4 antagonists such as ML354, the small molecule YD-3, and the peptide P4pal-10) are in progress [244-247, 263, 264]. In contrast to other labs' approaches, I hypothesize that using a monoclonal antibody as a therapy is ideal for our target. Because PAR4 is expressed on the surface of platelets in circulation, a monoclonal antibody will enable us to target PAR4 on platelets while preventing off target effects on other tissues since monoclonal antibodies have limited tissue permeability. In addition, monoclonal antibodies have less variability in the plasma concentration at a given dose between patients. This can be compared to metabolism of small molecules that can vary more on an individual patient basis. Finally, the half-life of monoclonal antibodies is longer than those of small molecule agents. Ideally, this will enable weekly dosing of antibody therapy compared to daily dosing of small molecule treatment.

Chapter 5.3: PAR4 Monoclonal Antibodies

To expand upon the studies in Chapter 3, three monoclonal antibodies (14H6, 5F10, 2D6) which interact with PAR4 were developed. Using purified sections of PAR4, the epitope for each antibody was mapped and all three interacted with a unique region on

the N-terminus of PAR4. 2D6 was found to interact with both cleaved and uncleaved PAR4. 14H6 and 5F10 were determined to only interact with uncleaved PAR4 since their epitope is close to the thrombin cleavage site on the receptor. 14H6 and 5F10 were able to detect endogenous PAR4 expression in human platelets. In addition 5F10 was found to be able to partially inhibit PAR4 cleavage, but only using a large quantity (500 μg/ml) of antibody. The third antibody, 2D6, was able to detect PAR4 expressed on cells by immunofluorescence microscopy. These studies lead to the development of three novel tools to advance the field's understanding of PAR4 in platelets and other endogenous cells and tissues.

The ultimate goal when this project began was to develop a monoclonal antibody that interacted with the anionic cluster (C^{54}ANDSDTLELPD) on the N-terminus of PAR4. Through a myriad of approaches using different immunogens (MBP-PAR4(18-78), MBP-PAR4(48-72), MBP-PAR4(54-66), IgG-PAR4(54-66), KLH-PAR4(54-66)) I was unsuccessful in generating a monoclonal PAR4 antibody that interacted with the anionic cluster on PAR4. However, these studies provide the ability to understand in more detail the importance of targeting the anionic cluster versus other locations on the N-terminus of PAR4 to inhibit platelet activation. Since 14H6 and 5F10 both target close to the thrombin cleavage site on the N-terminus but not the anionic cluster, these antibodies were utilized to examine the effect of targeting close to the thrombin cleavage site on human platelet aggregation. Neither 14H6 nor 5F10 were able to block thrombin-induced aggregation at concentrations up to 10 μg/ml (data not shown). CAN12 was able to completely inhibit thrombin induced aggregation of human platelets at a concentration of

0.2 μg/ml. These results suggest that targeting the anionic cluster on PAR4 provides a unique effect of inhibiting platelet aggregation by thrombin through inhibiting both PAR1 and PAR4. Without inhibiting PAR1, human platelets are able to be activated by thrombin and PAR1 can still enhance PAR4 cleavage. It is also possible that targeting the PAR4 cleavage site is not a viable option because thrombin has a higher affinity for the cleavage site than 14H6 and 5F10. Another option is 14H6 and 5F10 have significantly lower affinity for PAR4 versus CAN12. With current studies underway to purify recombinant human PAR4, we will be able to examine the affinity that each antibody has for the purified receptor. The antibody affinity can be compared to the affinity of thrombin for purified PAR4. As a starting point, the affinity of thrombin for purified PAR4 can be compared to the previously published affinity of thrombin for purified PAR4 exodomain (61 μM).

The incidence and severity of cardiovascular disease is dictated by numerous factors including medical adherence, environmental exposures, and genetic polymorphisms [265]. When looking at the genetic component, black individuals develop cardiovascular disease at a younger age and have a higher incidence of mortality from the disease. This correlates with a heritable interindividual variation in platelet reactivity observed to be higher in self-identified black individuals than white individuals [194-196]. Recent studies were able to directly link the differences in platelet reactivity to PAR4, specifically polymorphisms at positions 120 (Ala/Thr) and 296 (Phe/Val) [191-193]. While these polymorphisms have been found to correlate with PAR4 reactivity, the exact mechanism of how they affect PAR4 needs to be examined. The newly developed

antibodies will aid in studies investigating the influence of the polymorphisms on PAR4 activation. Specifically, they will enable detection of varying expression levels of PAR4 in platelets from individuals with different polymorphisms, measuring the effect that different polymorphisms have on the rate of PAR4 activation (cleavage), and examining what effect current antiplatelet therapies (ADP antagonist, PAR1 antagonist) have on PAR4 activation in relation to the different polymorphisms.

Human platelets express two thrombin receptors, PAR1 and PAR4, and the two receptors have distinct signaling properties [172, 203, 253]. A key feature that distinguishes PAR4 is its ability to influence both thrombin and ADP initiated signaling through the formation of hetero-oligomers with both PAR1 and the ADP receptor P2Y12 [184, 189, 190]. Because current antiplatelet therapies inhibit both PAR1 and P2Y12 signaling, PAR4 takes on a central role in both influencing the effectiveness of therapy and becoming the primary mediator of thrombin signaling. With the current antiplatelet therapies funneling platelet activation through PAR4 the field needs to expand the limited understanding of PAR4. The newly developed antibodies will help enable these studies.

Even though PAR4 has been primarily studied in platelets, it also plays a role in other tissues and disease states. PAR4 inhibition has been previously shown to have cardioprotective effects against myocardial ischemia/reperfusion injury [166]. PAR4 has also been shown to play a role in joint pain, inflammation, and diabetic vasculopathy [167-169, 171]. In addition, PAR4 expression is increased in high glucose stimulated

human vascular smooth muscle cells [170]. These antibodies will enable further expansion of these studies in endogenous cells and tissue and will enable examining PAR4 activation directly.

References

1 Versteeg HH, Heemskerk JW, Levi M, Reitsma PH. New fundamentals in hemostasis. *Physiol Rev*. 2013; **93**: 327-58.

2 Davie EW, Ratnoff OD. Waterfall Sequence for Intrinsic Blood Clotting. *Science*. 1964; **145**: 1310-2.

3 Macfarlane RG. An Enzyme Cascade in the Blood Clotting Mechanism, and Its Function as a Biochemical Amplifier. *Nature*. 1964; **202**: 498-9.

4 Gailani D, Renne T. Intrinsic pathway of coagulation and arterial thrombosis. *Arterioscler Thromb Vasc Biol*. 2007; **27**: 2507-13.

5 Mackman N. The role of tissue factor and factor VIIa in hemostasis. *Anesth Analg*. 2009; **108**: 1447-52.

6 Ariens RA, Lai TS, Weisel JW, Greenberg CS, Grant PJ. Role of factor XIII in fibrin clot formation and effects of genetic polymorphisms. *Blood*. 2002; **100**: 743-54.

7 Chapin JC, Hajjar KA. Fibrinolysis and the control of blood coagulation. *Blood Rev*. 2015; **29**: 17-24.

8 Orkin SH, Nathan DG. *Nathan and Oski's hematology of infancy and childhood*. Philadelphia: Saunders/Elsevier, 2009.

9 Cesarman-Maus G, Hajjar KA. Molecular mechanisms of fibrinolysis. *Br J Haematol*. 2005; **129**: 307-21.

10 Khalafallah A, Jarvis C, Morse M, Albarzan AM, Stewart P, Bates G, Hayes R, Robertson I, Seaton D, Brain T. Evaluation of the innovance d-dimer assay for the diagnosis of disseminated intravascular coagulopathy in different clinical settings. *Clin Appl Thromb Hemost*. 2014; **20**: 91-7.

11 van der Hulle T, den Exter PL, Erkens PG, van Es J, Mos IC, ten Cate H, Kamphuisen PW, Hovens MM, Buller HR, Klok FA, Huisman MV. Variable D-dimer thresholds for diagnosis of clinically suspected acute pulmonary embolism. *J Thromb Haemost*. 2013; **11**: 1986-92.

12 Gomes M, Khorana AA. Risk assessment for thrombosis in cancer. *Semin Thromb Hemost*. 2014; **40**: 319-24.

13 van der Hulle T, Tan M, den Exter PL, Mol GC, Iglesias del Sol A, van de Ree MA, Huisman MV, Klok FA. Selective D-dimer testing for the diagnosis of acute deep vein thrombosis: a validation study. *J Thromb Haemost*. 2013; **11**: 2184-6.

14 Michelson AD. *Platelets*. San Diego ; London: Academic Press, 2002.

15 Gresele P. *Antiplatelet agents*. Heidelberg ; New York: Springer Verlag, 2012.

16 White JG. Interaction of membrane systems in blood platelets. *Am J Pathol*. 1972; **66**: 295-312.

17 Brass LF. Ca2+ homeostasis in unstimulated platelets. *J Biol Chem*. 1984; **259**: 12563-70.

18 Ware JA, Johnson PC, Smith M, Salzman EW. Effect of common agonists on cytoplasmic ionized calcium concentration in platelets. Measurement with 2-methyl-6-methoxy 8-nitroquinoline (quin2) and aequorin. *J Clin Invest*. 1986; **77**: 878-86.

19 Hartwig JH, DeSisto M. The cytoskeleton of the resting human blood platelet: structure of the membrane skeleton and its attachment to actin filaments. *J Cell Biol*. 1991; **112**: 407-25.

20 Safer D, Nachmias VT. Beta thymosins as actin binding peptides. *Bioessays*. 1994; **16**: 473-9.
21 Rosenberg S, Stracher A, Lucas RC. Isolation and characterization of actin and actin-binding protein from human platelets. *J Cell Biol*. 1981; **91**: 201-11.
22 White JG. Effects of colchicine and Vinca alkaloids on human platelets. I. Influence on platelet microtubules and contractile function. *Am J Pathol*. 1968; **53**: 281-91.
23 White JG. The dense bodies of human platelets: inherent electron opacity of the serotonin storage particles. *Blood*. 1969; **33**: 598-606.
24 Israels SJ, McNicol A, Robertson C, Gerrard JM. Platelet storage pool deficiency: diagnosis in patients with prolonged bleeding times and normal platelet aggregation. *Br J Haematol*. 1990; **75**: 118-21.
25 Holmsen H, Weiss HJ. Secretable storage pools in platelets. *Annu Rev Med*. 1979; **30**: 119-34.
26 Blair P, Flaumenhaft R. Platelet alpha-granules: basic biology and clinical correlates. *Blood Rev*. 2009; **23**: 177-89.
27 Flaumenhaft R. Molecular basis of platelet granule secretion. *Arterioscler Thromb Vasc Biol*. 2003; **23**: 1152-60.
28 Maynard DM, Heijnen HF, Horne MK, White JG, Gahl WA. Proteomic analysis of platelet alpha-granules using mass spectrometry. *J Thromb Haemost*. 2007; **5**: 1945-55.
29 Niiya K, Hodson E, Bader R, Byers-Ward V, Koziol JA, Plow EF, Ruggeri ZM. Increased surface expression of the membrane glycoprotein IIb/IIIa complex induced by platelet activation. Relationship to the binding of fibrinogen and platelet aggregation. *Blood*. 1987; **70**: 475-83.
30 Berger G, Caen JP, Berndt MC, Cramer EM. Ultrastructural demonstration of CD36 in the alpha-granule membrane of human platelets and megakaryocytes. *Blood*. 1993; **82**: 3034-44.
31 Nurden P, Jandrot-Perrus M, Combrie R, Winckler J, Arocas V, Lecut C, Pasquet JM, Kunicki TJ, Nurden AT. Severe deficiency of glycoprotein VI in a patient with gray platelet syndrome. *Blood*. 2004; **104**: 107-14.
32 Suzuki H, Murasaki K, Kodama K, Takayama H. Intracellular localization of glycoprotein VI in human platelets and its surface expression upon activation. *Br J Haematol*. 2003; **121**: 904-12.
33 Cramer EM, Breton-Gorius J, Beesley JE, Martin JF. Ultrastructural demonstration of tubular inclusions coinciding with von Willebrand factor in pig megakaryocytes. *Blood*. 1988; **71**: 1533-8.
34 Gralnick HR, Williams SB, McKeown LP, Krizek DM, Shafer BC, Rick ME. Platelet von Willebrand factor: comparison with plasma von Willebrand factor. *Thromb Res*. 1985; **38**: 623-33.
35 Rendu F, Brohard-Bohn B. The platelet release reaction: granules' constituents, secretion and functions. *Platelets*. 2001; **12**: 261-73.
36 Ruggeri ZM, Ware J. von Willebrand factor. *FASEB J*. 1993; **7**: 308-16.
37 Tschopp TB, Weiss HJ, Baumgartner HR. Decreased adhesion of platelets to subendothelium in von Willebrand's disease. *J Lab Clin Med*. 1974; **83**: 296-300.

38 Weiss HJ, Turitto VT, Baumgartner HR. Effect of shear rate on platelet interaction with subendothelium in citrated and native blood. I. Shear rate--dependent decrease of adhesion in von Willebrand's disease and the Bernard-Soulier syndrome. *J Lab Clin Med*. 1978; **92**: 750-64.
39 Moroi M, Jung SM, Okuma M, Shinmyozu K. A Patient with Platelets Deficient in Glycoprotein-Vi That Lack Both Collagen-Induced Aggregation and Adhesion. *Journal of Clinical Investigation*. 1989; **84**: 1440-5.
40 Massberg S, Gawaz M, Gruner S, Schulte V, Konrad I, Zohlnhofer D, Heinzmann U, Nieswandt B. A crucial role of glycoprotein VI for platelet recruitment to the injured arterial wall in vivo. *Journal of Experimental Medicine*. 2003; **197**: 41-9.
41 Nieswandt B, Brakebusch C, Bergmeier W, Schulte V, Bouvard D, Mokhtari-Nejad R, Lindhout T, Heemskerk JW, Zirngibl H, Fassler R. Glycoprotein VI but not alpha2beta1 integrin is essential for platelet interaction with collagen. *EMBO J*. 2001; **20**: 2120-30.
42 Watson S, Berlanga O, Best D, Frampton J. Update on collagen receptor interactions in platelets: is the two-state model still valid? *Platelets*. 2000; **11**: 252-8.
43 Savage B, Saldivar E, Ruggeri ZM. Initiation of platelet adhesion by arrest onto fibrinogen or translocation on von Willebrand factor. *Cell*. 1996; **84**: 289-97.
44 Lopez JA, Dong JF. Structure and function of the glycoprotein Ib-IX-V complex. *Curr Opin Hematol*. 1997; **4**: 323-9.
45 Du X. Signaling and regulation of the platelet glycoprotein Ib-IX-V complex. *Curr Opin Hematol*. 2007; **14**: 262-9.
46 Mazzucato M, Pradella P, Cozzi MR, De Marco L, Ruggeri ZM. Sequential cytoplasmic calcium signals in a 2-stage platelet activation process induced by the glycoprotein Ibalpha mechanoreceptor. *Blood*. 2002; **100**: 2793-800.
47 Watson SP, Auger JM, McCarty OJ, Pearce AC. GPVI and integrin alphaIIb beta3 signaling in platelets. *J Thromb Haemost*. 2005; **3**: 1752-62.
48 Nieswandt B, Watson SP. Platelet-collagen interaction: is GPVI the central receptor? *Blood*. 2003; **102**: 449-61.
49 Eidt JF, Allison P, Noble S, Ashton J, Golino P, McNatt J, Buja LM, Willerson JT. Thrombin is an important mediator of platelet aggregation in stenosed canine coronary arteries with endothelial injury. *J Clin Invest*. 1989; **84**: 18-27.
50 Fitzgerald DJ, Fitzgerald GA. Role of thrombin and thromboxane A2 in reocclusion following coronary thrombolysis with tissue-type plasminogen activator. *Proc Natl Acad Sci U S A*. 1989; **86**: 7585-9.
51 Hanson SR, Harker LA. Interruption of acute platelet-dependent thrombosis by the synthetic antithrombin D-phenylalanyl-L-prolyl-L-arginyl chloromethyl ketone. *Proc Natl Acad Sci U S A*. 1988; **85**: 3184-8.
52 Heras M, Chesebro JH, Penny WJ, Bailey KR, Badimon L, Fuster V. Effects of thrombin inhibition on the development of acute platelet-thrombus deposition during angioplasty in pigs. Heparin versus recombinant hirudin, a specific thrombin inhibitor. *Circulation*. 1989; **79**: 657-65.
53 Jang IK, Gold HK, Ziskind AA, Leinbach RC, Fallon JT, Collen D. Prevention of platelet-rich arterial thrombosis by selective thrombin inhibition. *Circulation*. 1990; **81**: 219-25.

54 Vu TK, Hung DT, Wheaton VI, Coughlin SR. Molecular cloning of a functional thrombin receptor reveals a novel proteolytic mechanism of receptor activation. *Cell*. 1991; **64**: 1057-68.
55 Xu WF, Andersen H, Whitmore TE, Presnell SR, Yee DP, Ching A, Gilbert T, Davie EW, Foster DC. Cloning and characterization of human protease-activated receptor 4. *Proc Natl Acad Sci U S A*. 1998; **95**: 6642-6.
56 Hirata M, Hayashi Y, Ushikubi F, Yokota Y, Kageyama R, Nakanishi S, Narumiya S. Cloning and expression of cDNA for a human thromboxane A2 receptor. *Nature*. 1991; **349**: 617-20.
57 Ayyanathan K, Webbs TE, Sandhu AK, Athwal RS, Barnard EA, Kunapuli SP. Cloning and chromosomal localization of the human P2Y1 purinoceptor. *Biochem Biophys Res Commun*. 1996; **218**: 783-8.
58 Jin J, Kunapuli SP. Coactivation of two different G protein-coupled receptors is essential for ADP-induced platelet aggregation. *Proc Natl Acad Sci U S A*. 1998; **95**: 8070-4.
59 Janssens R, Communi D, Pirotton S, Samson M, Parmentier M, Boeynaems JM. Cloning and tissue distribution of the human P2Y1 receptor. *Biochem Biophys Res Commun*. 1996; **221**: 588-93.
60 Wilde JI, Retzer M, Siess W, Watson SP. ADP-induced platelet shape change: an investigation of the signalling pathways involved and their dependence on the method of platelet preparation. *Platelets*. 2000; **11**: 286-95.
61 Oury C, Sticker E, Cornelissen H, De Vos R, Vermylen J, Hoylaerts MF. ATP augments von Willebrand factor-dependent shear-induced platelet aggregation through Ca2+-calmodulin and myosin light chain kinase activation. *J Biol Chem*. 2004; **279**: 26266-73.
62 Clifford EE, Parker K, Humphreys BD, Kertesy SB, Dubyak GR. The P2X1 receptor, an adenosine triphosphate-gated cation channel, is expressed in human platelets but not in human blood leukocytes. *Blood*. 1998; **91**: 3172-81.
63 Kagaya A, Mikuni M, Yamamoto H, Muraoka S, Yamawaki S, Takahashi K. Heterologous supersensitization between serotonin2 and alpha 2-adrenergic receptor-mediated intracellular calcium mobilization in human platelets. *J Neural Transm Gen Sect*. 1992; **88**: 25-36.
64 Parise LV. Integrin alpha(IIb)beta(3) signaling in platelet adhesion and aggregation. *Curr Opin Cell Biol*. 1999; **11**: 597-601.
65 Shattil SJ, Kashiwagi H, Pampori N. Integrin signaling: the platelet paradigm. *Blood*. 1998; **91**: 2645-57.
66 Kahn ML, Nakanishi-Matsui M, Shapiro MJ, Ishihara H, Coughlin SR. Protease-activated receptors 1 and 4 mediate activation of human platelets by thrombin. *J Clin Invest*. 1999; **103**: 879-87.
67 Kahn ML, Zheng YW, Huang W, Bigornia V, Zeng D, Moff S, Farese RV, Jr., Tam C, Coughlin SR. A dual thrombin receptor system for platelet activation. *Nature*. 1998; **394**: 690-4.
68 Faull RJ, Ginsberg MH. Inside-out signaling through integrins. *J Am Soc Nephrol*. 1996; **7**: 1091-7.
69 Plow EF, D'Souza SE, Ginsberg MH. Ligand binding to GPIIb-IIIa: a status report. *Semin Thromb Hemost*. 1992; **18**: 324-32.

70 Ginsberg MH, O'Toole TE, Loftus JC, Plow EF. Ligand binding to integrins: dynamic regulation and common mechanisms. *Cold Spring Harb Symp Quant Biol*. 1992; **57**: 221-31.
71 Weisel JW, Nagaswami C, Vilaire G, Bennett JS. Examination of the platelet membrane glycoprotein IIb-IIIa complex and its interaction with fibrinogen and other ligands by electron microscopy. *J Biol Chem*. 1992; **267**: 16637-43.
72 Ruggeri ZM, Dent JA, Saldivar E. Contribution of distinct adhesive interactions to platelet aggregation in flowing blood. *Blood*. 1999; **94**: 172-8.
73 Ni H, Denis CV, Subbarao S, Degen JL, Sato TN, Hynes RO, Wagner DD. Persistence of platelet thrombus formation in arterioles of mice lacking both von Willebrand factor and fibrinogen. *J Clin Invest*. 2000; **106**: 385-92.
74 Ni H, Yuen PS, Papalia JM, Trevithick JE, Sakai T, Fassler R, Hynes RO, Wagner DD. Plasma fibronectin promotes thrombus growth and stability in injured arterioles. *Proc Natl Acad Sci U S A*. 2003; **100**: 2415-9.
75 Hantgan RR, Paumi C, Rocco M, Weisel JW. Effects of ligand-mimetic peptides Arg-Gly-Asp-X (X = Phe, Trp, Ser) on alphaIIbbeta3 integrin conformation and oligomerization. *Biochemistry*. 1999; **38**: 14461-74.
76 Miyamoto S, Akiyama SK, Yamada KM. Synergistic roles for receptor occupancy and aggregation in integrin transmembrane function. *Science*. 1995; **267**: 883-5.
77 Miyamoto S, Teramoto H, Coso OA, Gutkind JS, Burbelo PD, Akiyama SK, Yamada KM. Integrin function: molecular hierarchies of cytoskeletal and signaling molecules. *J Cell Biol*. 1995; **131**: 791-805.
78 Hato T, Pampori N, Shattil SJ. Complementary roles for receptor clustering and conformational change in the adhesive and signaling functions of integrin alphaIIb beta3. *J Cell Biol*. 1998; **141**: 1685-95.
79 Reverter JC, Beguin S, Kessels H, Kumar R, Hemker HC, Coller BS. Inhibition of platelet-mediated, tissue factor-induced thrombin generation by the mouse/human chimeric 7E3 antibody. Potential implications for the effect of c7E3 Fab treatment on acute thrombosis and "clinical restenosis". *J Clin Invest*. 1996; **98**: 863-74.
80 Law DA, Nannizzi-Alaimo L, Ministri K, Hughes PE, Forsyth J, Turner M, Shattil SJ, Ginsberg MH, Tybulewicz VL, Phillips DR. Genetic and pharmacological analyses of Syk function in alphaIIbbeta3 signaling in platelets. *Blood*. 1999; **93**: 2645-52.
81 Shattil SJ. Signaling through platelet integrin alpha IIb beta 3: inside-out, outside-in, and sideways. *Thromb Haemost*. 1999; **82**: 318-25.
82 Miranti CK, Leng L, Maschberger P, Brugge JS, Shattil SJ. Identification of a novel integrin signaling pathway involving the kinase Syk and the guanine nucleotide exchange factor Vav1. *Curr Biol*. 1998; **8**: 1289-99.
83 Law DA, DeGuzman FR, Heiser P, Ministri-Madrid K, Killeen N, Phillips DR. Integrin cytoplasmic tyrosine motif is required for outside-in alphaIIbbeta3 signalling and platelet function. *Nature*. 1999; **401**: 808-11.
84 Wakefield TW, Myers DD, Henke PK. Mechanisms of venous thrombosis and resolution. *Arterioscler Thromb Vasc Biol*. 2008; **28**: 387-91.
85 Ross R. Atherosclerosis--an inflammatory disease. *N Engl J Med*. 1999; **340**: 115-26.

86 Hansson GK, Libby P, Schonbeck U, Yan ZQ. Innate and adaptive immunity in the pathogenesis of atherosclerosis. *Circ Res*. 2002; **91**: 281-91.
87 Lundberg AM, Hansson GK. Innate immune signals in atherosclerosis. *Clin Immunol*. 2010; **134**: 5-24.
88 Andersson J, Libby P, Hansson GK. Adaptive immunity and atherosclerosis. *Clin Immunol*. 2010; **134**: 33-46.
89 Badimon L, Vilahur G. Thrombosis formation on atherosclerotic lesions and plaque rupture. *J Intern Med*. 2014; **276**: 618-32.
90 Virmani R, Kolodgie FD, Burke AP, Finn AV, Gold HK, Tulenko TN, Wrenn SP, Narula J. Atherosclerotic plaque progression and vulnerability to rupture: angiogenesis as a source of intraplaque hemorrhage. *Arterioscler Thromb Vasc Biol*. 2005; **25**: 2054-61.
91 Lippi G, Franchini M, Targher G. Arterial thrombus formation in cardiovascular disease. *Nat Rev Cardiol*. 2011; **8**: 502-12.
92 Kesieme E, Kesieme C, Jebbin N, Irekpita E, Dongo A. Deep vein thrombosis: a clinical review. *J Blood Med*. 2011; **2**: 59-69.
93 Hirsh J, Fuster V, Ansell J, Halperin JL. American Heart Association/American College of Cardiology Foundation guide to warfarin therapy. *Circulation*. 2003; **107**: 1692-711.
94 Ageno W, Gallus AS, Wittkowsky A, Crowther M, Hylek EM, Palareti G. Oral anticoagulant therapy: Antithrombotic Therapy and Prevention of Thrombosis, 9th ed: American College of Chest Physicians Evidence-Based Clinical Practice Guidelines. *Chest*. 2012; **141**: e44S-88S.
95 Chuang YJ, Swanson R, Raja SM, Olson ST. Heparin enhances the specificity of antithrombin for thrombin and factor Xa independent of the reactive center loop sequence. Evidence for an exosite determinant of factor Xa specificity in heparin-activated antithrombin. *J Biol Chem*. 2001; **276**: 14961-71.
96 Kelton JG, Smith JW, Warkentin TE, Hayward CP, Denomme GA, Horsewood P. Immunoglobulin G from patients with heparin-induced thrombocytopenia binds to a complex of heparin and platelet factor 4. *Blood*. 1994; **83**: 3232-9.
97 Cabral KP, Ansell J. Oral direct factor Xa inhibitors for stroke prevention in atrial fibrillation. *Nat Rev Cardiol*. 2012; **9**: 385-91.
98 Wisler JW, Becker RC. Oral factor Xa inhibitors for the long-term management of ACS. *Nat Rev Cardiol*. 2012; **9**: 392-401.
99 Harter K, Levine M, Henderson SO. Anticoagulation drug therapy: a review. *West J Emerg Med*. 2015; **16**: 11-7.
100 Arsenault KA, Hirsh J, Whitlock RP, Eikelboom JW. Direct thrombin inhibitors in cardiovascular disease. *Nat Rev Cardiol*. 2012; **9**: 402-14.
101 Hamm CW, Bassand JP, Agewall S, Bax J, Boersma E, Bueno H, Caso P, Dudek D, Gielen S, Huber K, Ohman M, Petrie MC, Sonntag F, Uva MS, Storey RF, Wijns W, Zahger D. ESC Guidelines for the management of acute coronary syndromes in patients presenting without persistent ST-segment elevation: The Task Force for the management of acute coronary syndromes (ACS) in patients presenting without persistent ST-segment elevation of the European Society of Cardiology (ESC). *Eur Heart J*. 2011; **32**: 2999-3054.

102 Koutouzis M, Lagerqvist B, Oldgren J, Akerblom A, Wahlin M, Karlsson T, Albertsson P, Matejka G, Grip L. Long-term results following switch from abciximab to eptifibatide during percutaneous coronary intervention. *Clin Cardiol*. 2010; **33**: 686-92.
103 Roth GJ, Majerus PW. The mechanism of the effect of aspirin on human platelets. I. Acetylation of a particulate fraction protein. *J Clin Invest*. 1975; **56**: 624-32.
104 Smith WL, Garavito RM, DeWitt DL. Prostaglandin endoperoxide H synthases (cyclooxygenases)-1 and -2. *J Biol Chem*. 1996; **271**: 33157-60.
105 Loll PJ, Picot D, Garavito RM. The structural basis of aspirin activity inferred from the crystal structure of inactivated prostaglandin H2 synthase. *Nat Struct Biol*. 1995; **2**: 637-43.
106 Roth GJ, Stanford N, Majerus PW. Acetylation of prostaglandin synthase by aspirin. *Proc Natl Acad Sci U S A*. 1975; **72**: 3073-6.
107 Smith WL, DeWitt DL. Biochemistry of prostaglandin endoperoxide H synthase-1 and synthase-2 and their differential susceptibility to nonsteroidal anti-inflammatory drugs. *Semin Nephrol*. 1995; **15**: 179-94.
108 Smith WL, Dewitt DL. Prostaglandin endoperoxide H synthases-1 and -2. *Adv Immunol*. 1996; **62**: 167-215.
109 FitzGerald GA. Mechanisms of platelet activation: thromboxane A2 as an amplifying signal for other agonists. *Am J Cardiol*. 1991; **68**: 11B-5B.
110 Morita I, Schindler M, Regier MK, Otto JC, Hori T, DeWitt DL, Smith WL. Different intracellular locations for prostaglandin endoperoxide H synthase-1 and -2. *J Biol Chem*. 1995; **270**: 10902-8.
111 Weber AA, Zimmermann KC, Meyer-Kirchrath J, Schror K. Cyclooxygenase-2 in human platelets as a possible factor in aspirin resistance. *Lancet*. 1999; **353**: 900.
112 McAdam BF, Catella-Lawson F, Mardini IA, Kapoor S, Lawson JA, FitzGerald GA. Systemic biosynthesis of prostacyclin by cyclooxygenase (COX)-2: the human pharmacology of a selective inhibitor of COX-2. *Proc Natl Acad Sci U S A*. 1999; **96**: 272-7.
113 Vane JR, Bakhle YS, Botting RM. Cyclooxygenases 1 and 2. *Annu Rev Pharmacol Toxicol*. 1998; **38**: 97-120.
114 Jaffe EA, Weksler BB. Recovery of endothelial cell prostacyclin production after inhibition by low doses of aspirin. *J Clin Invest*. 1979; **63**: 532-5.
115 Patrono C, Coller B, Dalen JE, FitzGerald GA, Fuster V, Gent M, Hirsh J, Roth G. Platelet-active drugs : the relationships among dose, effectiveness, and side effects. *Chest*. 2001; **119**: 39S-63S.
116 Burch JW, Majerus PW. The role of prostaglandins in platelet function. *Semin Hematol*. 1979; **16**: 196-207.
117 Berger PB, Bell MR, Rihal CS, Ting H, Barsness G, Garratt K, Bellot V, Mathew V, Melby S, Hammes L, Grill D, Holmes DR, Jr. Clopidogrel versus ticlopidine after intracoronary stent placement. *J Am Coll Cardiol*. 1999; **34**: 1891-4.
118 Muller C, Buttner HJ, Petersen J, Roskamm H. A randomized comparison of clopidogrel and aspirin versus ticlopidine and aspirin after the placement of coronary-artery stents. *Circulation*. 2000; **101**: 590-3.
119 Quinn MJ, Fitzgerald DJ. Ticlopidine and clopidogrel. *Circulation*. 1999; **100**: 1667-72.

120 Bassand JP, Hamm CW, Ardissino D, Boersma E, Budaj A, Fernandez-Aviles F, Fox KA, Hasdai D, Ohman EM, Wallentin L, Wijns W. Guidelines for the diagnosis and treatment of non-ST-segment elevation acute coronary syndromes. *Eur Heart J*. 2007; **28**: 1598-660.
121 Anderson JL, Adams CD, Antman EM, Bridges CR, Califf RM, Casey DE, Jr., Chavey WE, 2nd, Fesmire FM, Hochman JS, Levin TN, Lincoff AM, Peterson ED, Theroux P, Wenger NK, Wright RS, Smith SC, Jr., Jacobs AK, Halperin JL, Hunt SA, Krumholz HM, Kushner FG, Lytle BW, Nishimura R, Ornato JP, Page RL, Riegel B. ACC/AHA 2007 guidelines for the management of patients with unstable angina/non ST-elevation myocardial infarction: a report of the American College of Cardiology/American Heart Association Task Force on Practice Guidelines (Writing Committee to Revise the 2002 Guidelines for the Management of Patients With Unstable Angina/Non ST-Elevation Myocardial Infarction): developed in collaboration with the American College of Emergency Physicians, the Society for Cardiovascular Angiography and Interventions, and the Society of Thoracic Surgeons: endorsed by the American Association of Cardiovascular and Pulmonary Rehabilitation and the Society for Academic Emergency Medicine. *Circulation*. 2007; **116**: e148-304.
122 Kazui M, Nishiya Y, Ishizuka T, Hagihara K, Farid NA, Okazaki O, Ikeda T, Kurihara A. Identification of the human cytochrome P450 enzymes involved in the two oxidative steps in the bioactivation of clopidogrel to its pharmacologically active metabolite. *Drug Metab Dispos*. 2010; **38**: 92-9.
123 Beitelshees AL, Voora D, Lewis JP. Personalized antiplatelet and anticoagulation therapy: applications and significance of pharmacogenomics. *Pharmgenomics Pers Med*. 2015; **8**: 43-61.
124 Payne CD, Li YG, Small DS, Ernest CS, 2nd, Farid NA, Jakubowski JA, Brandt JT, Salazar DE, Winters KJ. Increased active metabolite formation explains the greater platelet inhibition with prasugrel compared to high-dose clopidogrel. *J Cardiovasc Pharmacol*. 2007; **50**: 555-62.
125 Brandt JT, Close SL, Iturria SJ, Payne CD, Farid NA, Ernest CS, 2nd, Lachno DR, Salazar D, Winters KJ. Common polymorphisms of CYP2C19 and CYP2C9 affect the pharmacokinetic and pharmacodynamic response to clopidogrel but not prasugrel. *J Thromb Haemost*. 2007; **5**: 2429-36.
126 Cattaneo M. New P2Y(12) inhibitors. *Circulation*. 2010; **121**: 171-9.
127 Zhou D, Andersson TB, Grimm SW. In vitro evaluation of potential drug-drug interactions with ticagrelor: cytochrome P450 reaction phenotyping, inhibition, induction, and differential kinetics. *Drug Metab Dispos*. 2011; **39**: 703-10.
128 Coller BS, Peerschke EI, Scudder LE, Sullivan CA. A murine monoclonal antibody that completely blocks the binding of fibrinogen to platelets produces a thrombasthenic-like state in normal platelets and binds to glycoproteins IIb and/or IIIa. *J Clin Invest*. 1983; **72**: 325-38.
129 Knight DM, Wagner C, Jordan R, McAleer MF, DeRita R, Fass DN, Coller BS, Weisman HF, Ghrayeb J. The immunogenicity of the 7E3 murine monoclonal Fab antibody fragment variable region is dramatically reduced in humans by substitution of human for murine constant regions. *Mol Immunol*. 1995; **32**: 1271-81.
130 Egbertson MS, Chang CT, Duggan ME, Gould RJ, Halczenko W, Hartman GD, Laswell WL, Lynch JJ, Jr., Lynch RJ, Manno PD, et al. Non-peptide fibrinogen receptor

antagonists. 2. Optimization of a tyrosine template as a mimic for Arg-Gly-Asp. *J Med Chem*. 1994; **37**: 2537-51.
131 Scarborough RM, Naughton MA, Teng W, Rose JW, Phillips DR, Nannizzi L, Arfsten A, Campbell AM, Charo IF. Design of potent and specific integrin antagonists. Peptide antagonists with high specificity for glycoprotein IIb-IIIa. *J Biol Chem*. 1993; **268**: 1066-73.
132 Chackalamannil S, Wang Y, Greenlee WJ, Hu Z, Xia Y, Ahn HS, Boykow G, Hsieh Y, Palamanda J, Agans-Fantuzzi J, Kurowski S, Graziano M, Chintala M. Discovery of a novel, orally active himbacine-based thrombin receptor antagonist (SCH 530348) with potent antiplatelet activity. *J Med Chem*. 2008; **51**: 3061-4.
133 Doller D, Chackalamannil S, Czarniecki M, McQuade R, Ruperto V. Design, synthesis, and structure-activity relationship studies of himbacine derived muscarinic receptor antagonists. *Bioorg Med Chem Lett*. 1999; **9**: 901-6.
134 Zhang C, Srinivasan Y, Arlow DH, Fung JJ, Palmer D, Zheng Y, Green HF, Pandey A, Dror RO, Shaw DE, Weis WI, Coughlin SR, Kobilka BK. High-resolution crystal structure of human protease-activated receptor 1. *Nature*. 2012; **492**: 387-92.
135 Becker RC, Moliterno DJ, Jennings LK, Pieper KS, Pei J, Niederman A, Ziada KM, Berman G, Strony J, Joseph D, Mahaffey KW, Van de Werf F, Veltri E, Harrington RA. Safety and tolerability of SCH 530348 in patients undergoing non-urgent percutaneous coronary intervention: a randomised, double-blind, placebo-controlled phase II study. *Lancet*. 2009; **373**: 919-28.
136 Tricoci P, Huang Z, Held C, Moliterno DJ, Armstrong PW, Van de Werf F, White HD, Aylward PE, Wallentin L, Chen E, Lokhnygina Y, Pei J, Leonardi S, Rorick TL, Kilian AM, Jennings LH, Ambrosio G, Bode C, Cequier A, Cornel JH, Diaz R, Erkan A, Huber K, Hudson MP, Jiang L, Jukema JW, Lewis BS, Lincoff AM, Montalescot G, Nicolau JC, Ogawa H, Pfisterer M, Prieto JC, Ruzyllo W, Sinnaeve PR, Storey RF, Valgimigli M, Whellan DJ, Widimsky P, Strony J, Harrington RA, Mahaffey KW. Thrombin-receptor antagonist vorapaxar in acute coronary syndromes. *N Engl J Med*. 2012; **366**: 20-33.
137 Morrow DA, Braunwald E, Bonaca MP, Ameriso SF, Dalby AJ, Fish MP, Fox KA, Lipka LJ, Liu X, Nicolau JC, Ophuis AJ, Paolasso E, Scirica BM, Spinar J, Theroux P, Wiviott SD, Strony J, Murphy SA. Vorapaxar in the secondary prevention of atherothrombotic events. *N Engl J Med*. 2012; **366**: 1404-13.
138 Morrow DA, Alberts MJ, Mohr JP, Ameriso SF, Bonaca MP, Goto S, Hankey GJ, Murphy SA, Scirica BM, Braunwald E. Efficacy and safety of vorapaxar in patients with prior ischemic stroke. *Stroke*. 2013; **44**: 691-8.
139 O'Donoghue ML, Bhatt DL, Wiviott SD, Goodman SG, Fitzgerald DJ, Angiolillo DJ, Goto S, Montalescot G, Zeymer U, Aylward PE, Guetta V, Dudek D, Ziecina R, Contant CF, Flather MD. Safety and tolerability of atopaxar in the treatment of patients with acute coronary syndromes: the lessons from antagonizing the cellular effects of Thrombin-Acute Coronary Syndromes Trial. *Circulation*. 2011; **123**: 1843-53.
140 White HD. Oral antiplatelet therapy for atherothrombotic disease: current evidence and new directions. *Am Heart J*. 2011; **161**: 450-61.
141 Serebruany VL, Kogushi M, Dastros-Pitei D, Flather M, Bhatt DL. The in-vitro effects of E5555, a protease-activated receptor (PAR)-1 antagonist, on platelet

biomarkers in healthy volunteers and patients with coronary artery disease. *Thromb Haemost*. 2009; **102**: 111-9.
142 Goto S, Ogawa H, Takeuchi M, Flather MD, Bhatt DL. Double-blind, placebo-controlled Phase II studies of the protease-activated receptor 1 antagonist E5555 (atopaxar) in Japanese patients with acute coronary syndrome or high-risk coronary artery disease. *Eur Heart J*. 2010; **31**: 2601-13.
143 Coughlin SR. How the protease thrombin talks to cells. *Proc Natl Acad Sci U S A*. 1999; **96**: 11023-7.
144 Coughlin SR. Protease-activated receptors in hemostasis, thrombosis and vascular biology. *J Thromb Haemost*. 2005; **3**: 1800-14.
145 Ramachandran R, Noorbakhsh F, Defea K, Hollenberg MD. Targeting proteinase-activated receptors: therapeutic potential and challenges. *Nat Rev Drug Discov*. 2012; **11**: 69-86.
146 Canto I, Soh UJ, Trejo J. Allosteric modulation of protease-activated receptor signaling. *Mini Rev Med Chem*. 2012; **12**: 804-11.
147 Hung DT, Vu TK, Wheaton VI, Ishii K, Coughlin SR. Cloned platelet thrombin receptor is necessary for thrombin-induced platelet activation. *J Clin Invest*. 1992; **89**: 1350-3.
148 Ngaiza JR, Jaffe EA. A 14 amino acid peptide derived from the amino terminus of the cleaved thrombin receptor elevates intracellular calcium and stimulates prostacyclin production in human endothelial cells. *Biochem Biophys Res Commun*. 1991; **179**: 1656-61.
149 Vu TK, Wheaton VI, Hung DT, Charo I, Coughlin SR. Domains specifying thrombin-receptor interaction. *Nature*. 1991; **353**: 674-7.
150 Rydel TJ, Ravichandran KG, Tulinsky A, Bode W, Huber R, Roitsch C, Fenton JW, 2nd. The structure of a complex of recombinant hirudin and human alpha-thrombin. *Science*. 1990; **249**: 277-80.
151 Liu LW, Vu TK, Esmon CT, Coughlin SR. The region of the thrombin receptor resembling hirudin binds to thrombin and alters enzyme specificity. *J Biol Chem*. 1991; **266**: 16977-80.
152 Soh UJ, Dores MR, Chen B, Trejo J. Signal transduction by protease-activated receptors. *Br J Pharmacol*. 2010; **160**: 191-203.
153 Ludeman MJ, Kataoka H, Srinivasan Y, Esmon NL, Esmon CT, Coughlin SR. PAR1 cleavage and signaling in response to activated protein C and thrombin. *J Biol Chem*. 2005; **280**: 13122-8.
154 Russo A, Soh UJ, Paing MM, Arora P, Trejo J. Caveolae are required for protease-selective signaling by protease-activated receptor-1. *Proc Natl Acad Sci U S A*. 2009; **106**: 6393-7.
155 Bae JS, Yang L, Manithody C, Rezaie AR. The ligand occupancy of endothelial protein C receptor switches the protease-activated receptor 1-dependent signaling specificity of thrombin from a permeability-enhancing to a barrier-protective response in endothelial cells. *Blood*. 2007; **110**: 3909-16.
156 Feistritzer C, Riewald M. Endothelial barrier protection by activated protein C through PAR1-dependent sphingosine 1-phosphate receptor-1 crossactivation. *Blood*. 2005; **105**: 3178-84.

157 Nystedt S, Emilsson K, Larsson AK, Strombeck B, Sundelin J. Molecular cloning and functional expression of the gene encoding the human proteinase-activated receptor 2. *Eur J Biochem*. 1995; **232**: 84-9.
158 O'Brien PJ, Molino M, Kahn M, Brass LF. Protease activated receptors: theme and variations. *Oncogene*. 2001; **20**: 1570-81.
159 Ishihara H, Connolly AJ, Zeng D, Kahn ML, Zheng YW, Timmons C, Tram T, Coughlin SR. Protease-activated receptor 3 is a second thrombin receptor in humans. *Nature*. 1997; **386**: 502-6.
160 Madhusudhan T, Wang H, Straub BK, Grone E, Zhou Q, Shahzad K, Muller-Krebs S, Schwenger V, Gerlitz B, Grinnell BW, Griffin JH, Reiser J, Grone HJ, Esmon CT, Nawroth PP, Isermann B. Cytoprotective signaling by activated protein C requires protease-activated receptor-3 in podocytes. *Blood*. 2012; **119**: 874-83.
161 Burnier L, Mosnier LO. Novel mechanisms for activated protein C cytoprotective activities involving noncanonical activation of protease-activated receptor 3. *Blood*. 2013; **122**: 807-16.
162 Nakanishi-Matsui M, Zheng YW, Sulciner DJ, Weiss EJ, Ludeman MJ, Coughlin SR. PAR3 is a cofactor for PAR4 activation by thrombin. *Nature*. 2000; **404**: 609-13.
163 Bah A, Chen Z, Bush-Pelc LA, Mathews FS, Di Cera E. Crystal structures of murine thrombin in complex with the extracellular fragments of murine protease-activated receptors PAR3 and PAR4. *Proc Natl Acad Sci U S A*. 2007; **104**: 11603-8.
164 Jacques SL, Kuliopulos A. Protease-activated receptor-4 uses dual prolines and an anionic retention motif for thrombin recognition and cleavage. *Biochem J*. 2003; **376**: 733-40.
165 Nieman MT. Protease-activated receptor 4 uses anionic residues to interact with alpha-thrombin in the absence or presence of protease-activated receptor 1. *Biochemistry*. 2008; **47**: 13279-86.
166 Strande JL, Hsu A, Su J, Fu X, Gross GJ, Baker JE. Inhibiting protease-activated receptor 4 limits myocardial ischemia/reperfusion injury in rat hearts by unmasking adenosine signaling. *J Pharmacol Exp Ther*. 2008; **324**: 1045-54.
167 McDougall JJ, Zhang C, Cellars L, Joubert E, Dixon CM, Vergnolle N. Triggering of proteinase-activated receptor 4 leads to joint pain and inflammation in mice. *Arthritis Rheum*. 2009; **60**: 728-37.
168 Russell FA, Veldhoen VE, Tchitchkan D, McDougall JJ. Proteinase-activated receptor-4 (PAR4) activation leads to sensitization of rat joint primary afferents via a bradykinin B2 receptor-dependent mechanism. *J Neurophysiol*. 2010; **103**: 155-63.
169 Russell FA, Zhan S, Dumas A, Lagarde S, Pouliot M, McDougall JJ. The pronociceptive effect of proteinase-activated receptor-4 stimulation in rat knee joints is dependent on mast cell activation. *Pain*. 2011; **152**: 354-60.
170 Dangwal S, Rauch BH, Gensch T, Dai L, Bretschneider E, Vogelaar CF, Schror K, Rosenkranz AC. High glucose enhances thrombin responses via protease-activated receptor-4 in human vascular smooth muscle cells. *Arterioscler Thromb Vasc Biol*. 2011; **31**: 624-33.
171 Pavic G, Grandoch M, Dangwal S, Jobi K, Rauch BH, Doller A, Oberhuber A, Akhyari P, Schror K, Fischer JW, Fender AC. Thrombin receptor protease-activated receptor 4 is a key regulator of exaggerated intimal thickening in diabetes mellitus. *Circulation*. 2014; **130**: 1700-11.

172 Holinstat M, Voss B, Bilodeau ML, McLaughlin JN, Cleator J, Hamm HE. PAR4, but not PAR1, signals human platelet aggregation via Ca2+ mobilization and synergistic P2Y12 receptor activation. *J Biol Chem*. 2006; **281**: 26665-74.
173 Offermanns S, Toombs CF, Hu YH, Simon MI. Defective platelet activation in G alpha(q)-deficient mice. *Nature*. 1997; **389**: 183-6.
174 Offermanns S, Laugwitz KL, Spicher K, Schultz G. G proteins of the G12 family are activated via thromboxane A2 and thrombin receptors in human platelets. *Proc Natl Acad Sci U S A*. 1994; **91**: 504-8.
175 Kozasa T, Jiang X, Hart MJ, Sternweis PM, Singer WD, Gilman AG, Bollag G, Sternweis PC. p115 RhoGEF, a GTPase activating protein for Galpha12 and Galpha13. *Science*. 1998; **280**: 2109-11.
176 Klages B, Brandt U, Simon MI, Schultz G, Offermanns S. Activation of G12/G13 results in shape change and Rho/Rho-kinase-mediated myosin light chain phosphorylation in mouse platelets. *J Cell Biol*. 1999; **144**: 745-54.
177 Jin J, Mao Y, Thomas D, Kim S, Daniel JL, Kunapuli SP. RhoA downstream of G(q) and G(12/13) pathways regulates protease-activated receptor-mediated dense granule release in platelets. *Biochem Pharmacol*. 2009; **77**: 835-44.
178 Covic L, Gresser AL, Kuliopulos A. Biphasic kinetics of activation and signaling for PAR1 and PAR4 thrombin receptors in platelets. *Biochemistry*. 2000; **39**: 5458-67.
179 Covic L, Singh C, Smith H, Kuliopulos A. Role of the PAR4 thrombin receptor in stabilizing platelet-platelet aggregates as revealed by a patient with Hermansky-Pudlak syndrome. *Thromb Haemost*. 2002; **87**: 722-7.
180 Mazharian A, Roger S, Berrou E, Adam F, Kauskot A, Nurden P, Jandrot-Perrus M, Bryckaert M. Protease-activating receptor-4 induces full platelet spreading on a fibrinogen matrix: involvement of ERK2 and p38 and Ca2+ mobilization. *J Biol Chem*. 2007; **282**: 5478-87.
181 Chen J, Ishii M, Wang L, Ishii K, Coughlin SR. Thrombin receptor activation. Confirmation of the intramolecular tethered liganding hypothesis and discovery of an alternative intermolecular liganding mode. *J Biol Chem*. 1994; **269**: 16041-5.
182 McLaughlin JN, Patterson MM, Malik AB. Protease-activated receptor-3 (PAR3) regulates PAR1 signaling by receptor dimerization. *Proc Natl Acad Sci U S A*. 2007; **104**: 5662-7.
183 de la Fuente M, Noble DN, Verma S, Nieman MT. Mapping human protease-activated receptor 4 (PAR4) homodimer interface to transmembrane helix 4. *J Biol Chem*. 2012; **287**: 10414-23.
184 Leger AJ, Jacques SL, Badar J, Kaneider NC, Derian CK, Andrade-Gordon P, Covic L, Kuliopulos A. Blocking the protease-activated receptor 1-4 heterodimer in platelet-mediated thrombosis. *Circulation*. 2006; **113**: 1244-54.
185 Arachiche A, Mumaw MM, de la Fuente M, Nieman MT. Protease-activated Receptor 1 (PAR1) and PAR4 Heterodimers Are Required for PAR1-enhanced Cleavage of PAR4 by alpha-Thrombin. *J Biol Chem*. 2013; **288**: 32553-62.
186 Kamath P, Huntington JA, Krishnaswamy S. Ligand binding shuttles thrombin along a continuum of zymogen- and proteinase-like states. *J Biol Chem*. 2010; **285**: 28651-8.
187 Huntington JA. Thrombin plasticity. *Biochim Biophys Acta*. 2012; **1824**: 246-52.

188 Nieman MT, Schmaier AH. Interaction of thrombin with PAR1 and PAR4 at the thrombin cleavage site. *Biochemistry*. 2007; **46**: 8603-10.
189 Li D, D'Angelo L, Chavez M, Woulfe DS. Arrestin-2 differentially regulates PAR4 and ADP receptor signaling in platelets. *J Biol Chem*. 2011; **286**: 3805-14.
190 Khan A, Li D, Ibrahim S, Smyth E, Woulfe DS. The Physical Association of the P2Y12 Receptor with PAR4 Regulates Arrestin-mediated Akt Activation. *Mol Pharmacol*. 2014.
191 Edelstein LC, Simon LM, Lindsay CR, Kong X, Montoya RT, Tourdot BE, Chen ES, Ma L, Coughlin S, Nieman M, Holinstat M, Shaw C, Bray PF. Common variants in the human platelet PAR4 thrombin receptor alter platelet function and differ by race. *Blood*. 2014; **in press**.
192 Edelstein LC, Simon LM, Montoya RT, Holinstat M, Chen ES, Bergeron A, Kong X, Nagalla S, Mohandas N, Cohen DE, Dong JF, Shaw C, Bray PF. Racial differences in human platelet PAR4 reactivity reflect expression of PCTP and miR-376c. *Nat Med*. 2013; **19**: 1609-16.
193 Tourdot BE, Conaway S, Niisuke K, Edelstein LC, Bray PF, Holinstat M. Mechanism of Race-Dependent Platelet Activation Through the Protease-Activated Receptor-4 and Gq Signaling Axis. *Arterioscler Thromb Vasc Biol*. 2014.
194 Thomas KL, Honeycutt E, Shaw LK, Peterson ED. Racial differences in long-term survival among patients with coronary artery disease. *Am Heart J*. 2010; **160**: 744-51.
195 Berry JD, Liu K, Folsom AR, Lewis CE, Carr JJ, Polak JF, Shea S, Sidney S, O'Leary DH, Chan C, Lloyd-Jones DM. Prevalence and progression of subclinical atherosclerosis in younger adults with low short-term but high lifetime estimated risk for cardiovascular disease: the coronary artery risk development in young adults study and multi-ethnic study of atherosclerosis. *Circulation*. 2009; **119**: 382-9.
196 Howard G, Cushman M, Howard VJ, Kissela BM, Kleindorfer DO, Moy CS, Switzer J, Woo D. Risk factors for intracerebral hemorrhage: the REasons for geographic and racial differences in stroke (REGARDS) study. *Stroke*. 2013; **44**: 1282-7.
197 Ishihara H, Zeng D, Connolly AJ, Tam C, Coughlin SR. Antibodies to protease-activated receptor 3 inhibit activation of mouse platelets by thrombin. *Blood*. 1998; **91**: 4152-7.
198 Weiss EJ, Hamilton JR, Lease KE, Coughlin SR. Protection against thrombosis in mice lacking PAR3. *Blood*. 2002; **100**: 3240-4.
199 Arachiche A, de la Fuente M, Nieman MT. Calcium mobilization and protein kinase C activation downstream of protease activated receptor 4 (PAR4) is negatively regulated by PAR3 in mouse platelets. *PLoS One*. 2013; **8**: e55740.
200 Leger AJ, Covic L, Kuliopulos A. Protease-activated receptors in cardiovascular diseases. *Circulation*. 2006; **114**: 1070-7.
201 Riewald M, Ruf W. Protease-activated receptor-1 signaling by activated protein C in cytokine-perturbed endothelial cells is distinct from thrombin signaling. *J Biol Chem*. 2005; **280**: 19808-14.
202 Soh UJ, Trejo J. Activated protein C promotes protease-activated receptor-1 cytoprotective signaling through beta-arrestin and dishevelled-2 scaffolds. *Proc Natl Acad Sci U S A*. 2011; **108**: E1372-80.

203 Voss B, McLaughlin JN, Holinstat M, Zent R, Hamm HE. PAR1, but not PAR4, activates human platelets through a Gi/o/phosphoinositide-3 kinase signaling axis. *Mol Pharmacol*. 2007; **71**: 1399-406.
204 Jacques SL, LeMasurier M, Sheridan PJ, Seeley SK, Kuliopulos A. Substrate-assisted catalysis of the PAR1 thrombin receptor. Enhancement of macromolecular association and cleavage. *J Biol Chem*. 2000; **275**: 40671-8.
205 Schechter I, Berger A. On the size of the active site in proteases. I. Papain. *Biochem Biophys Res Commun*. 1967; **27**: 157-62.
206 Grynkiewicz G, Poenie M, Tsien RY. A new generation of Ca2+ indicators with greatly improved fluorescence properties. *J Biol Chem*. 1985; **260**: 3440-50.
207 Schwede T, Kopp J, Guex N, Peitsch MC. SWISS-MODEL: An automated protein homology-modeling server. *Nucleic Acids Res*. 2003; **31**: 3381-5.
208 Arnold K, Bordoli L, Kopp J, Schwede T. The SWISS-MODEL workspace: a web-based environment for protein structure homology modelling. *Bioinformatics*. 2006; **22**: 195-201.
209 Bordoli L, Kiefer F, Arnold K, Benkert P, Battey J, Schwede T. Protein structure homology modeling using SWISS-MODEL workspace. *Nat Protoc*. 2009; **4**: 1-13.
210 Lopez-Gimenez JF, Canals M, Pediani JD, Milligan G. The alpha1b-adrenoceptor exists as a higher-order oligomer: effective oligomerization is required for receptor maturation, surface delivery, and function. *Mol Pharmacol*. 2007; **71**: 1015-29.
211 Guo W, Urizar E, Kralikova M, Mobarec JC, Shi L, Filizola M, Javitch JA. Dopamine D2 receptors form higher order oligomers at physiological expression levels. *EMBO J*. 2008; **27**: 2293-304.
212 Patowary S, Alvarez-Curto E, Xu TR, Holz JD, Oliver JA, Milligan G, Raicu V. The muscarinic M3 acetylcholine receptor exists as two differently sized complexes at the plasma membrane. *Biochem J*. 2013; **452**: 303-12.
213 Whorton MR, Bokoch MP, Rasmussen SG, Huang B, Zare RN, Kobilka B, Sunahara RK. A monomeric G protein-coupled receptor isolated in a high-density lipoprotein particle efficiently activates its G protein. *Proc Natl Acad Sci U S A*. 2007; **104**: 7682-7.
214 Whorton MR, Jastrzebska B, Park PS, Fotiadis D, Engel A, Palczewski K, Sunahara RK. Efficient coupling of transducin to monomeric rhodopsin in a phospholipid bilayer. *J Biol Chem*. 2008; **283**: 4387-94.
215 Park PS, Filipek S, Wells JW, Palczewski K. Oligomerization of G protein-coupled receptors: past, present, and future. *Biochemistry*. 2004; **43**: 15643-56.
216 Birdsall NJ. Class A GPCR heterodimers: evidence from binding studies. *Trends Pharmacol Sci*. 2010; **31**: 499-508.
217 Jastrzebska B, Ringler P, Lodowski DT, Moiseenkova-Bell V, Golczak M, Muller SA, Palczewski K, Engel A. Rhodopsin-transducin heteropentamer: three-dimensional structure and biochemical characterization. *J Struct Biol*. 2011; **176**: 387-94.
218 Jastrzebska B, Orban T, Golczak M, Engel A, Palczewski K. Asymmetry of the rhodopsin dimer in complex with transducin. *FASEB J*. 2013; **27**: 1572-84.
219 Lodowski DT, Salom D, Le Trong I, Teller DC, Ballesteros JA, Palczewski K, Stenkamp RE. Crystal packing analysis of Rhodopsin crystals. *J Struct Biol*. 2007; **158**: 455-62.

220 Huang J, Chen S, Zhang JJ, Huang XY. Crystal structure of oligomeric beta1-adrenergic G protein-coupled receptors in ligand-free basal state. *Nat Struct Mol Biol*. 2013; **20**: 419-25.
221 Kasai RS, Suzuki KG, Prossnitz ER, Koyama-Honda I, Nakada C, Fujiwara TK, Kusumi A. Full characterization of GPCR monomer-dimer dynamic equilibrium by single molecule imaging. *J Cell Biol*. 2011; **192**: 463-80.
222 Prinster SC, Hague C, Hall RA. Heterodimerization of g protein-coupled receptors: specificity and functional significance. *Pharmacol Rev*. 2005; **57**: 289-98.
223 Wang HX, Konopka JB. Identification of amino acids at two dimer interface regions of the alpha-factor receptor (Ste2). *Biochemistry*. 2009; **48**: 7132-9.
224 McMillin SM, Heusel M, Liu T, Costanzi S, Wess J. Structural basis of M3 muscarinic receptor dimer/oligomer formation. *J Biol Chem*. 2011; **286**: 28584-98.
225 Coughlin SR. Thrombin signalling and protease-activated receptors. *Nature*. 2000; **407**: 258-64.
226 Steinhoff M, Buddenkotte J, Shpacovitch V, Rattenholl A, Moormann C, Vergnolle N, Luger TA, Hollenberg MD. Proteinase-activated receptors: transducers of proteinase-mediated signaling in inflammation and immune response. *Endocr Rev*. 2005; **26**: 1-43.
227 Nanevicz T, Ishii M, Wang L, Chen M, Chen J, Turck CW, Cohen FE, Coughlin SR. Mechanisms of thrombin receptor agonist specificity. Chimeric receptors and complementary mutations identify an agonist recognition site. *J Biol Chem*. 1995; **270**: 21619-25.
228 Keularts IM, van Gorp RM, Feijge MA, Vuist WM, Heemskerk JW. alpha(2A)-adrenergic receptor stimulation potentiates calcium release in platelets by modulating cAMP levels. *J Biol Chem*. 2000; **275**: 1763-72.
229 Varga-Szabo D, Braun A, Nieswandt B. Calcium signaling in platelets. *J Thromb Haemost*. 2009; **7**: 1057-66.
230 Woulfe DS. Platelet G protein-coupled receptors in hemostasis and thrombosis. *J Thromb Haemost*. 2005; **3**: 2193-200.
231 Kim S, Foster C, Lecchi A, Quinton TM, Prosser DM, Jin J, Cattaneo M, Kunapuli SP. Protease-activated receptors 1 and 4 do not stimulate G(i) signaling pathways in the absence of secreted ADP and cause human platelet aggregation independently of G(i) signaling. *Blood*. 2002; **99**: 3629-36.
232 Kim S, Jin J, Kunapuli SP. Relative contribution of G-protein-coupled pathways to protease-activated receptor-mediated Akt phosphorylation in platelets. *Blood*. 2006; **107**: 947-54.
233 Angiolillo DJ, Guzman LA, Bass TA. Current antiplatelet therapies: benefits and limitations. *Am Heart J*. 2008; **156**: S3-9.
234 Angiolillo DJ, Ferreiro JL. Antiplatelet and anticoagulant therapy for atherothrombotic disease: the role of current and emerging agents. *Am J Cardiovasc Drugs*. 2013; **13**: 233-50.
235 Schwarz M, Meade G, Stoll P, Ylanne J, Bassler N, Chen YC, Hagemeyer CE, Ahrens I, Moran N, Kenny D, Fitzgerald D, Bode C, Peter K. Conformation-specific blockade of the integrin GPIIb/IIIa: a novel antiplatelet strategy that selectively targets activated platelets. *Circ Res*. 2006; **99**: 25-33.

236 Kastrati A, Neumann FJ, Schulz S, Massberg S, Byrne RA, Ferenc M, Laugwitz KL, Pache J, Ott I, Hausleiter J, Seyfarth M, Gick M, Antoniucci D, Schomig A, Berger PB, Mehilli J. Abciximab and heparin versus bivalirudin for non-ST-elevation myocardial infarction. *N Engl J Med*. 2011; **365**: 1980-9.
237 Mathews, II, Padmanabhan KP, Ganesh V, Tulinsky A, Ishii M, Chen J, Turck CW, Coughlin SR, Fenton JW, 2nd. Crystallographic structures of thrombin complexed with thrombin receptor peptides: existence of expected and novel binding modes. *Biochemistry*. 1994; **33**: 3266-79.
238 Tangen O, Berman HJ, Marfey P. Gel filtration. A new technique for separation of blood platelets from plasma. *Thromb Diath Haemorrh*. 1971; **25**: 268-78.
239 Nieman MT, Warnock M, Hasan AA, Mahdi F, Lucchesi BR, Brown NJ, Murphey LJ, Schmaier AH. The preparation and characterization of novel peptide antagonists to thrombin and factor VIIa and activation of protease-activated receptor 1. *J Pharmacol Exp Ther*. 2004; **311**: 492-501.
240 Buyue Y, Whinna HC, Sheehan JP. The heparin-binding exosite of factor IXa is a critical regulator of plasma thrombin generation and venous thrombosis. *Blood*. 2008; **112**: 3234-41.
241 Graff J, Klinkhardt U, Harder S. Pharmacodynamic profile of antiplatelet agents: marked differences between single versus costimulation with platelet activators. *Thromb Res*. 2004; **113**: 295-302.
242 Sambrano GR, Weiss EJ, Zheng YW, Huang W, Coughlin SR. Role of thrombin signalling in platelets in haemostasis and thrombosis. *Nature*. 2001; **413**: 74-8.
243 Lin H, Liu AP, Smith TH, Trejo J. Cofactoring and dimerization of proteinase-activated receptors. *Pharmacol Rev*. 2013; **65**: 1198-213.
244 Wu CC, Huang SW, Hwang TL, Kuo SC, Lee FY, Teng CM. YD-3, a novel inhibitor of protease-induced platelet activation. *Br J Pharmacol*. 2000; **130**: 1289-96.
245 Wu CC, Hwang TL, Liao CH, Kuo SC, Lee FY, Lee CY, Teng CM. Selective inhibition of protease-activated receptor 4-dependent platelet activation by YD-3. *Thromb Haemost*. 2002; **87**: 1026-33.
246 Covic L, Gresser AL, Talavera J, Swift S, Kuliopulos A. Activation and inhibition of G protein-coupled receptors by cell-penetrating membrane-tethered peptides. *Proc Natl Acad Sci U S A*. 2002; **99**: 643-8.
247 Kuliopulos A, Covic L. Blocking receptors on the inside: pepducin-based intervention of PAR signaling and thrombosis. *Life Sci*. 2003; **74**: 255-62.
248 Storey RF, Sanderson HM, White AE, May JA, Cameron KE, Heptinstall S. The central role of the P(2T) receptor in amplification of human platelet activation, aggregation, secretion and procoagulant activity. *Br J Haematol*. 2000; **110**: 925-34.
249 Santoro SA, Walsh JJ, Staatz WD, Baranski KJ. Distinct determinants on collagen support alpha 2 beta 1 integrin-mediated platelet adhesion and platelet activation. *Cell Regul*. 1991; **2**: 905-13.
250 Polgar J, Clemetson JM, Kehrel BE, Wiedemann M, Magnenat EM, Wells TN, Clemetson KJ. Platelet activation and signal transduction by convulxin, a C-type lectin from Crotalus durissus terrificus (tropical rattlesnake) venom via the p62/GPVI collagen receptor. *J Biol Chem*. 1997; **272**: 13576-83.

251 Nylander S, Femia EA, Scavone M, Berntsson P, Asztely AK, Nelander K, Lofgren L, Nilsson RG, Cattaneo M. Ticagrelor inhibits human platelet aggregation via adenosine in addition to P2Y12 antagonism. *J Thromb Haemost*. 2013; **11**: 1867-76.
252 JJ VANG, Nilsson L, Berntsson P, Wissing BM, Giordanetto F, Tomlinson W, Greasley PJ. Ticagrelor binds to human P2Y(12) independently from ADP but antagonizes ADP-induced receptor signaling and platelet aggregation. *J Thromb Haemost*. 2009; **7**: 1556-65.
253 Holinstat M, Voss B, Bilodeau ML, Hamm HE. Protease-activated receptors differentially regulate human platelet activation through a phosphatidic acid-dependent pathway. *Mol Pharmacol*. 2007; **71**: 686-94.
254 Khan A, Li D, Ibrahim S, Smyth E, Woulfe DS. The physical association of the P2Y12 receptor with PAR4 regulates arrestin-mediated Akt activation. *Mol Pharmacol*. 2014; **86**: 1-11.
255 Arachiche A, Mumaw MM, de la Fuente M, Nieman MT. Protease-activated Receptor 1 (PAR1) and PAR4 Heterodimers Are Required for PAR1-enhanced Cleavage of PAR4 by α-Thrombin. *J Biol Chem*. 2013; **288**: 32553-62.
256 Mumaw MM, Nieman MT. Race differences in platelet reactivity: is protease activated receptor 4 a predictor of response to therapy? *Arterioscler Thromb Vasc Biol*. 2014; **34**: 2524-6.
257 Bray PF, Mathias RA, Faraday N, Yanek LR, Fallin MD, Herrera-Galeano JE, Wilson AF, Becker LC, Becker DM. Heritability of platelet function in families with premature coronary artery disease. *J Thromb Haemost*. 2007; **5**: 1617-23.
258 Wahl JK, 3rd. Generation of monoclonal antibodies specific for desmoglein family members. *Hybrid Hybridomics*. 2002; **21**: 37-44.
259 Sambrano GR, Huang W, Faruqi T, Mahrus S, Craik C, Coughlin SR. Cathepsin G activates protease-activated receptor-4 in human platelets. *J Biol Chem*. 2000; **275**: 6819-23.
260 Quinton TM, Kim S, Derian CK, Jin J, Kunapuli SP. Plasmin-mediated activation of platelets occurs by cleavage of protease-activated receptor 4. *J Biol Chem*. 2004; **279**: 18434-9.
261 Mumaw MM, de la Fuente M, Noble DN, Nieman MT. Targeting the anionic region of human protease-activated receptor 4 inhibits platelet aggregation and thrombosis without interfering with hemostasis. *J Thromb Haemost*. 2014; **12**: 1331-41.
262 Harris JL, Backes BJ, Leonetti F, Mahrus S, Ellman JA, Craik CS. Rapid and general profiling of protease specificity by using combinatorial fluorogenic substrate libraries. *Proc Natl Acad Sci U S A*. 2000; **97**: 7754-9.
263 Young SE, Duvernay MT, Schulte ML, Lindsley CW, Hamm HE. Synthesis of indole derived protease-activated receptor 4 antagonists and characterization in human platelets. *PLoS One*. 2013; **8**: e65528.
264 Young SE, Duvernay MT, Schulte ML, Nance KD, Melancon BJ, Engers J, Wood MR, Hamm HE, Lindsley CW. A Novel and Selective PAR4 Antagonist: ML354. *Probe Reports from the NIH Molecular Libraries Program*. Bethesda (MD), 2010.
265 O'Donnell CJ, Larson MG, Feng D, Sutherland PA, Lindpaintner K, Myers RH, D'Agostino RA, Levy D, Tofler GH. Genetic and environmental contributions to platelet aggregation: the Framingham heart study. *Circulation*. 2001; **103**: 3051-6.